Dottorato di Ricerca in Biologia Cellulare e Molecolare, Dipartimento di Biotecnologie e Scienze della Vita, Università degli Studi dell'Insubria

GALECTIN-1 IS A NEW POTENTIAL THERAPEUTIC TARGET IN MULTIPLE MYELOMA

Tesi di Dottorato di Ferri Valentina

Anno Accademico 2014/2015

Index

ABSTRACT

Galectin-1 (Gal-1) is a lectin, involved in several processes related to cancer, including immunosuppression, angiogenesis, hypoxia, and metastases. Currently, the role of Gal-1 in multiple myeloma (MM) pathophysiology and in MM-induced angiogenesis is unknown. Firstly, we found that Gal-1 was expressed by malignant plasma cells in the bone marrow microenvironment. Moreover, our data demonstrated that Gal-1 expression was up-regulated in MM cells by hypoxia treatment (1% of O_2).Furthermore, the stable knock-down of Hypoxia Inducible Factor-1α, the master regulator of oxygen homeostasis, in human myeloma cell lines (HMCLs) markedly down-regulated Gal-1 expression. Thereafter, we found that the stable inhibition of Gal-1 by lentiviral vector short hairpin RNA (shRNA) anti-Gal-1 did not affect the proliferation and survival of MM cells, but significantly modified their transcriptional profiles, both in normoxic and hypoxic conditions. Notably, Gal-1 inhibition in MM cells significantly down-regulated genes involved in promoting tumor angiogenesis such as *CCL2* and *MMP9*, and up-regulated some putative anti-angiogenic genes, including *SEMA3A* and *CXCL10*. In line with these observations, we found that Gal-1 suppression significantly decreased the pro-angiogenic proprieties of HMCLs, assessed by *in vitro* angiogenesis assay. Finally, we found that NOD-SCID mice, injected subcutaneously with HMCLs carrying a stable infection with lentiviral vector shRNA anti-Gal-1, showed a reduction in tumor volume and a significant reduction in the plasmacytomas microvascular density, compared to mice inoculated with HMCLs carrying a stable infection with the control vector. In a different set of experiments, a HMCL JJN3 infected with shRNA anti-Gal-1 and with control vector were injected in NIH-III SCID mice, an intratibial mouse model. We found that the anti-Gal-1 group developed tumors reduced in length, thickness, width and volume size and, in addition, developed fewer and smaller lytic lesions on x-ray compared to the control group.

Overall, our data indicate that Gal-1 exerts a role in MM pathophysiology and in MM-induced angiogenesis and its inhibition in MM cells significantly reduced tumor growth *in vivo*, suggesting that Gal-1 is a new potential therapeutic target in MM.

1. INTRODUCTION

1.1. Multiple Myeloma

Multiple Myeloma (MM) is a neoplastic disorder of terminally differentiated plasma cells (PCs) that accumulate in the bone marrow (BM) and secrete a monoclonal immunoglobulin (M-protein), usually IgG or IgA, detectable by serum protein electrophoresis, or only circulating k or λ-free light chains.[1,2]

MM is associated with hypercalcemia, renal impairment, immunodeficiency, anemia, and bone loss.[1] It occurs more frequently with increasing age, often around 70 years, and it is more common among men than women.[3] Despite recent advantages in the therapeutic approaches, including chemotherapy and hematopoietic stem cell transplantation, MM remains an incurable disease with a median survival of 3-5 years and accounting for 2% of all cancer death.[4,5]

In most, if not all, cases the intramedullary MM is preceded by a premalignant condition, known as monoclonal gammopathy of undetermined significance (MGUS), and/or by a smoldering multiple myeloma (SMM).[6] MGUS and SMM lack of clinical features attributable to the PCs disorder, but are characterized by the presence of M-protein and by some genetic features of symptomatic MM.[3,7] In MGUS the-M-protein level is less than 3 g/dL and the PCs comprise no more than 10% of the mononuclear cells (MNCs) in the BM, whereas SMM is characterized by the presence of the M-protein level of 3 g/dL or higher, a stable BM tumor content >10% and a highly probability of progressing to symptomatic MM.[4,5] Indeed, the potential risk of progression to MM is about 1% per year for MGUS vs 10-20% per year for SMM conditions.[7]

Rarely, clonal PCs proliferation can involve sites outside of the BM, such as skin, peripheral blood and kidney. This more aggressive condition, manifesting as extramedullary MM, includes primary or secondary plasmacytoma and primary or secondary plasma cell leukemia (PCL), depending if the BM is the first localization.[8]

1.2. Multiple Myeloma pathophysiology

In recent years, numerous studies have focused on the biology of MM to better understand the mechanisms involved in the disease and identify new therapeutic targets. Epidemiological data have showed associations between MM and particular employments such as miners, agricultural workers, workers exposed to wood dust and metal workers.[9] Fritschi *et al.*,[10] focusing their studies on families with two or more MM affected individuals, have demonstrated a possible genetic predisposition for the disease.

Nowadays, several lines of evidence suggest that in MM pathogenesis it is possible to distinguish two main phases: the first characterized by the acquisition of chromosomal and genetic aberrations by PCs, the second characterized by the modifications of the BM microenvironment that support an aberrant angiogenesis and an increased bone resorption.

1.2.1. Genetic alterations

Several genetic mutations, occurring in different pathways, collaborate to deregulate the biology of PCs and to support the pathogenesis and the progression of the disease.[1] Unlike most hematopoietic cancers, 30-50% of MM patients present complex chromosomal abnormalities involving both ploidy and structural rearrangement.[11] Kuel *et al*.[12] have proposed that primary translocations occur early in the pathogenesis, already at MGUS level, whereas secondary translocations are involved in the progression of the disease, supporting a multistep development of MM. In this context, Liu *et al.*[13] showed that activating mutations of NRAS or KRAS2 oncogenes distinguish MM from MGUS.

During the pathogenesis of MM, most primary translocations are simple reciprocal translocations that juxtapose an oncogene and one of the Ig enhancers. They are mediated mainly by errors in immunoglobulin heavy chain (IgH) switch recombination, but sometimes by errors in somatic hypermutation during PCs generation in germinal centres.[12] The incidence of heavy-chain translocations increases with the stage of tumorigenesis, from 50% in MGUS to 90% in Human Myeloma cell lines (HMCLs).[12] Light-chain translocations are less common: Igλ translocations are present in approximately 10% of MGUS and in 20% of advanced MM and HMCLs, whereas IGk translocations are rare (Fonseca R., Martelli M., unpublished data). Early primary translocations, involving the immunoglobulin switch region on chromosome 14 (q32.33), are a genetic trait of MM. As a consequence of these chromosomal translocations, the proto-oncogenes located on chromosome partners 14 (q32.33) are placed under the control of the strong enhancers of the Ig loci, leading to their deregulation.[14]

Most Ig translocations involve just four groups of genes:

- t(11;14)(q13;q32), occurs in 15–20% of MM patients and induces cyclin D1 (CCND1) overexpression;
- t(4;14)(p16.3;q32), deregulates the MM SET domain and leads the inhibition of fibroblast growth factor receptor 3 (FGFR3) inducing PCs differentiation and apoptosis;
- t(14;16)(q32;q23), occurs in 5–10% of MM patients and activates the oncogene MAF, a basic-leucine zipper transcription factor. Its persistent and uncontrolled activity

promotes MM cell proliferation and increases MM cell adhesion to bone marrow stromal cells (BMSCs);

- t(14;20)(q32;q11), in 5% of the cases affects MAFB, another member of the same family.

Rarely, in MM PCs occur multiple and independent Ig translocations involving two or three of the four groups.[15] Many studies have highlighted that chromosomal translocations represent an important prognostic value in MM.[11] The type, the frequency and the extent of the karyotypic abnormalities correlates with the stage, prognosis, and response to therapy. It is observed a poor prognosis in patients carrying t(14;16) and t(4;14), whereas t(11;14) is associated with a better prognosis. In this regards, approximately 20% of abnormalities are present in MM patients with stage I of the disease, 60% in patients with stage III, and > 80% in patients with extramedullary disease.[16] However, even if the genetic events seem to play the key role in the initiation and progression of the disease, significant changes also occur in the BM microenvironment and are crucial features of MM progression. **(Figure A)**

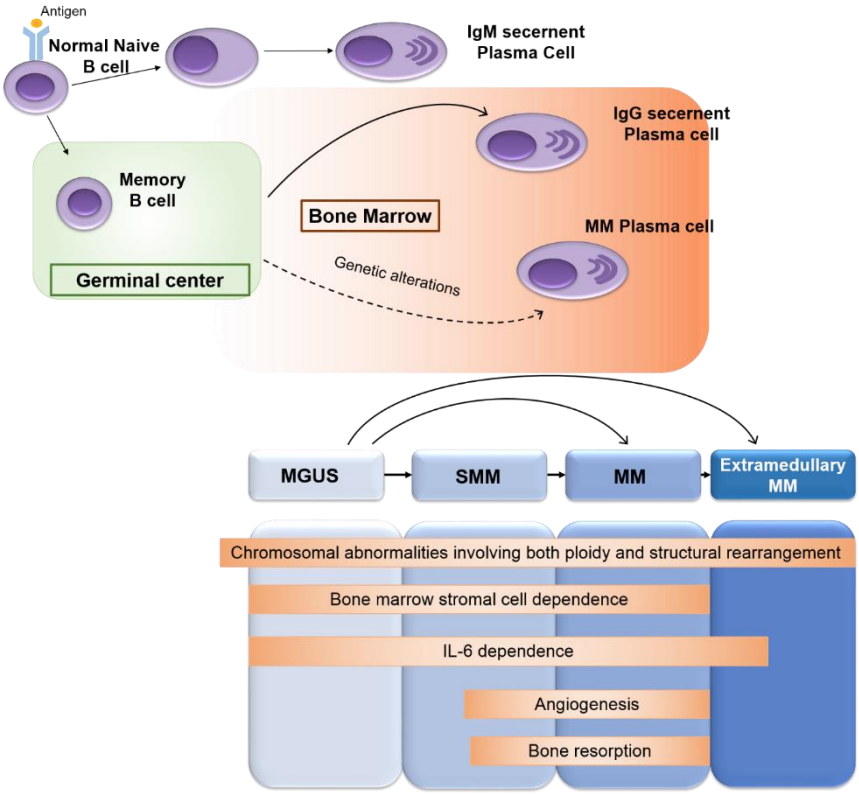

Figure A: Biological events involved in MM pathogenesis and progression. The genetic instability in normal PC can promote the transition to malignant PC, supporting a multistep development of the disease. At the same time, the mutual interaction of the BM cells and cancer cells causes changes in the microenvironment, which are responsible for the osteolytic lesions and the abnormal angiogenesis. (Modified from: Giuiani N et al. Ematologia Oncologica, Fondazione Matarelli. 2015.

1.2.2. Role and modifications of MM bone marrow microenvironment

BM microenvironment modifications play a key role in the pathogenesis of MM supporting the malignant PCs growth, survival, migration, acquisition of drug resistance and thus the progression of the disease. The BM microenvironment is organized in a complex three-dimensional architecture of sub-microenvironments, the niches. The niches consist of a cellular component and a non-cellular component:

- The cellular component includes hematopoietic stem cells (HSCs), erythroid cells, immune cells, as well as BMSC such as mesenchymal stem cells (MSCs), marrow adipocytes, fibroblasts, osteoblasts (OBs), osteoclasts (OCs) and endothelial cells (ECs);[17]
- The non-cellular component includes extracellular matrix components (ECM), such as fibrous proteins, proteoglycans and glycosaminoglycans,[17] and soluble factors such as cytokines, adhesion molecules and growth factors.[18]

In the BM microenvironment the interactions between MM cells and BMSCs occur through adhesion molecules or through soluble factors. The adhesion of MM cells to hematopoietic and stromal cells induces the secretion of cytokines and growth factors resulting in the activation of pleiotropic signaling pathways (one of the major is NF-κB pathway), inhibition of osteoblastogenesis, increase of osteoclastogenesis, angiogenesis and migration of MM cells. On the hand, NF-κB mediates the expression of many adhesion molecules expressed on both MM cells and BMSCs, on the other hand cell adhesion and cytokines activate NF-κB, augmenting the binding of MM cells to BMSC, which in turn induces interleukin-6 (IL-6) transcription and secretion by BMSC.
Cytokines more involved in these interactions, with both autocrine and paracrine mechanisms, are:

- IL-6
- Interleukin-1β (IL-1β)
- Insulin-like Growth Factor-1 (IGF-1)
- Fibroblast Growth Factor (FGF)
- Vascular Endothelial Growth Factor (VEGF)
- Transforming Growth Factor β (TGF-β)
- Hepatocyte Growth Factor (HGF)

The main adhesion molecules involved are:

- β1-integrins: VLA-1 (very late antigen-1), VLA-4, VLA-5
- β2-integrins: LFA-1 (lymphocyte function-associated antigen-1)
- Immunoglobulin superfamily: NCAM (neural cell adhesion molecule), VCAM-1 (vascular cell adhesion molecule), ICAM-1 (intercellular cell adhesion molecule-1), ICAM-2 and ICAM-3
- CD44
- Syndecan-1 (CD138)
- Collagen-1 binding protein
- CD21

In the last decade, the introduction in the therapeutic strategy of new classes of drug, that target the interactions between MM cells and BMSCs, have allowed a substantial improvements in the treatment of the disease. In particular, the immunomodulatory drugs (IMiDs) thalidomide, lenalidomide and pomalidomide and the proteasome inhibitors, such as bortezomib and carfilzomib, seem to have a pioneering role in the newer MM treatments in both the up-front and relapse-refractory settings.[19,20]

1.3. Osteolytic lesions

Up to 90% of MM patients develops osteolytic lesions resulting in pathologic fractures and severe bone pain.[21,22] MM bone lesions are more frequently localized at the spine, ribs, skull, and pelvis, even though any skeletal site can be involved.[23] This condition has a profound impact on the quality of life and consequently on the survival of MM patients. Osteolytic lesions result from a markedly increased activity of OCs and profound decreased osteoblastogenesis that occur in close proximity to MM cells,[24,25] stromal and BM cells.[26]

In normal conditions, the bone of adult individual is a rigid yet dynamic organ that is continuously remodelling for the proper maintenance of the homeostasis calcium/phosphate, for the control of bone volume in response to mechanical loading and eventual healing of the fractures. On a cellular level, key participants in bone homeostasis are OCs and OBs. OCs are a tissue-specific macrophage polykaryon originated by the differentiation of monocyte-macrophage progenitors and are appointed to the bone resorption, whereas OBs are of mesenchymal origin and mediate bone formation producing the organic matrix of bone tissue. Bone formation process is characterized by a sequence of events: partly by a mechanical

stimulus, which follows the stimulation of stromal cells, the osteoclastogenesis, the bone resorption and the osteoblastogenesis and partly by the formation of bone.

Histomorphometric studies have demonstrated that in MM patients with bone lesions there is uncoupled or severely imbalanced bone remodeling with increased bone resorption and decreased or absent bone formation. In contrast, MM patients without bone lesions display balanced bone remodeling with increased osteoclastogenesis and normal or increased bone formation rate.

Furthermore, histologic studies of bone biopsies from patients with MM showed that increased OCs activity occurs mainly adjacent to MM cells, suggesting that local factors rather than systemic mechanisms are involved in the pathogenesis of osteolytic lesions.[27,28]

1.3.1. Osteoclastogenesis and osteoblastogenesis in MM bone disease

MM cells stimulate OCs activity by several molecular mechanisms, involving differentiation of OCs and the production, by microenvironmental cells and MM cells, of osteoclast-survival factors.[27] The factors produced by MM cells include: receptor activator of nuclear factor-B ligand (RANKL), which is part of the tumor necrosis factor (TNF) gene family, macrophage inflammatory protein-1α (MIP-1α), interleukin-3 (IL-3) and IL-6.[26] OCs begin their maturation when receptor activator of nuclear factor-B (RANK) interacts with RANKL, produced by stromal cells, pre-osteoblasts and activated T lymphocytes. RANKL, together with macrophage colony-stimulating factor (M-CSF), directly induces osteoclastogenesis, through the activation of many intracellular signaling pathways (MAPK, NF-kB, JNK pathways, etc.). As a result of this activation, several osteoclastogenic transcription factors are mobilized leading to the expression of osteoclast-specific genes during differentiation, the activation of resorption by mature OCs, and the inhibition of osteoclast apoptosis.[26] The activity of RANKL is balanced by the presence of its decoy receptor, osteoprotegerin (OPG), which is a member of the TNF receptor family and contains four homologous binding domains for RANKL. When OPG binds RANKL impedes RANK-RANKL binding and in this way inhibits OCs maturation and bone resorption.[29] The MM BM microenvironment shows an imbalance between OPG and RANKL levels in favour of RANKL, and also promotes an upregulation of pro-osteoclastogenic cytokines, such as IL-1, IL-3, IL-6, TNFα, M-CSF and MIP-1α, produced by stromal cell, OBs and MM cells. Indeed, binding of MM cells through α4β1 integrin to VCAM-1 on BMSC decreases secretion of OPG and increases expression of RANKL, thereby promoting bone resorption and osteolysis.[30] Importantly, deregulation of the RANKL-OPG axis occurs in MM, but not in MGUS.[31] On the other hands OCs can promote PCs growth through an increased

production of IL-6 and osteopontin (OPN), mediated by their cellular contact, thus contributing to the maintenance of the vicious circle. In addition to increased OCS activity, OBs activity is markedly suppressed in MM; this is mainly due to the block of the osteogenic differentiation process of mesenchymal cells induced by MM cells.[21] Osteoblastic lineage cells, that mediate bone formation, originate from MSCs and are responsible for bone matrix synthesis. Runt-related transcription factor 2 (Runx2), also named Cbfa1 or AML3, is the major transcription factor regulating OBs commitment and osteogenic differentiation of mesenchymal cells.[32] Malignant PCs actively suppress osteoblastogenesis and down-regulate the expression of RUNX2, and on the other hand, inhibit the wingless interaction site (Wnt) signalling pathway, which is crucial for OBs differentiation.[33] (**Figure B**)

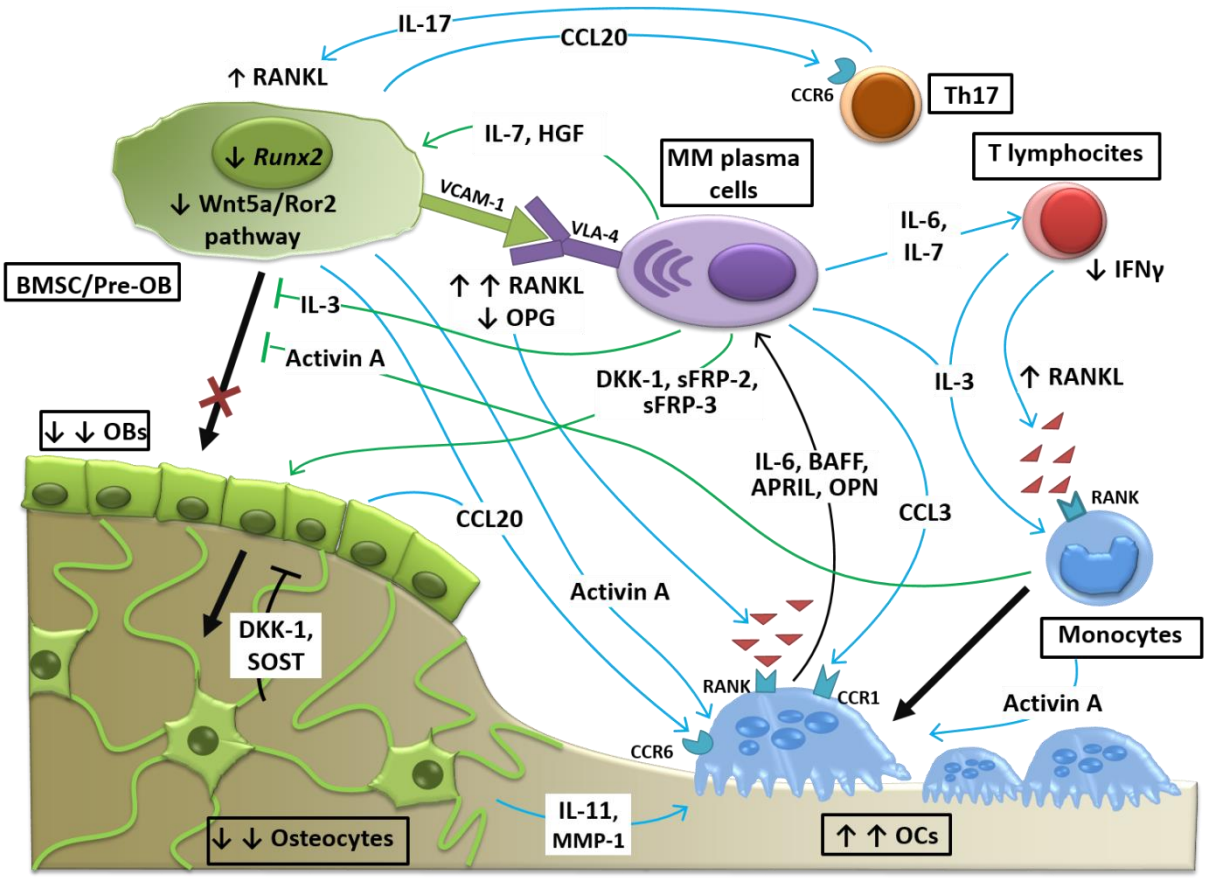

Figure B: Pathogenesis of MM-induced bone disease. Mechanisms involved in the increased activity of osteoclasts and in the profound decreased osteoblatogenesis that occur in close proximity to MM cells, stromal and BM cells.

1.4. Bone marrow angiogenesis in Multiple Myeloma

Angiogenesis is the sprouting of new blood vessels from an existing capillary network.[34] It is a multistep process consisting in a vasodilatation of existing vessels, increased permeability, degradation of surrounding matrix and activation, proliferation and migration of ECs to form the lumen of new vessels. Blood vessels form extensive networks that supply oxygen and nutrients in all tissues in the body and provide gateway for immune surveillance. In the adult, vessels are quiescent and rarely form new branches[35] and structural or functional abnormalities contribute to many diseases. Indeed, insufficient oxygen and nutrients maintenance or inadequate vessels growth cause myocardial infarction, stroke, or neurodegenerative disorders, whereas abnormal vascular growth promotes cancer, inflammatory disorders and eye disease.[34,36] In tumor-induced angiogenesis the key step is the angiogenic switch, a process characterized by an imbalance between pro- and anti-angiogenic molecules in favor of the first ones leading the formation of aberrant blood vessels. Already in 1971 Folkman have speculated the importance of pathological angiogenesis in the tumor microenvironment and proposed its manipulation as a therapeutic opportunity.[37] In this context, several studies have demonstrated an increased angiogenesis in the BM microenvironment in hematologic malignancies, including MM, suggesting a potential pathophysiological role for angiogenesis in MM.[38] Indeed, aberrant angiogenesis is a hallmark of MM progression and a prognostic factor for survival.[39] MM progression is characterized by an avacular phase and a subsequent vascular phase in which the imbalance between pro- and anti-angiogenic molecules results in perivascular detachment and vessels dilatation, in formation of new blood vessels and recruitment of other perivascular cells, allowing the exponential growth of the tumor.[38] Increased BM angiogenesis in MM patients was first demonstrated by Vacca *et al*.[40,41] They described increased *in vitro* pro-angiogenic activity of isolated PCs from patients with active MM as compared with PCs from inactive MM and MGUS patients. Other studies of the same group compared MM ECs with MGUS ECs or with human umbelican vein endothelial cells (HUVECs) and showed that the first ones have enhanced junctions and sprouts in the capillary plexus compared with the second third ones.[42] Thereafter, others confirmed these observations showing an enhanced neoangiogenesis in the BM MM.[43-46] Moreover, it was demonstrated that the extent of angiogenesis is directly correlated with the PCs labeling index and the microvascular density (MVD) and that MM patients positive for the Angiopoietin-1 (Ang-1) expression have a major number of microvessels per field as compared to those negative for Ang-1.[47] Cibeira *et al.*[48] showed a statistically significant correlation between the grade of infiltration by PCs and MVD estimation; in patients with a major grade of BM PCs infiltration, the MVD was higher than in patients with a lower grade of BM involvement.

These findings were confirmed by Vacca *et al.*[41] and Rajkumar *et al*.[45], who also showed that patients with ≥ 50 microvessels per field had median survival of 2.6 years compared to the 5.1 years of those with < 50 microvessels.
In addition, several groups have demonstrated a significant relationship between increased BM angiogenesis and poor prognosis in MM patients.[43,49]

1.4.1. Molecules involved in angiogenesis

The development of new blood vessels is a complex process that involves both direct angiogenic cytokine production by PCs and their induction by the BM microenvironment. The increased BM angiogenesis in MM is substained by an imbalance between the production of pro-angiogenic and anti-angiogenic factors by both MM cells and microenvironment cells. MM cells interact with several BM microenvironment cells including stromal cells, fibroblasts, OBs, OCs, T lymphocytes, monocytes/macrophages and mast cells that produce growth and survival factors that sustain MM cell survival and trigger ECs proliferation and angiogenesis **(Figure C).** In the last years, several factors produced by MM cells and microenvironment have been identified:

- *Vascular Endothelial Growth Factor*

Various growth factors belonging to the VEGF family (VEGF, placenta growth factor [PlGF], VEGF-B, VEGF-C and VEGF-D) act as a modulators and inducers of angiogenesis *in vivo*.[50] Five molecular forms of VEGF are generated by alternative splicing of its RNA transcripts: $VEGF_{165,}$ $VEGF_{121}$, $VEGF_{145}$, $VEGF_{189}$ and $VEGF_{206}$.[2] A the same way exist different isoforms of VEGF receptors: VEGFR-1 or Flt-1, VEGFR-2 or VEGFR-3 or KDR/Flk-1 and Flt-4. VEGFR-1 and VEGFR-2 are both expressed by ECs and mediate the stimulatory effect of VEGF on survival, proliferation and migration of ECs.[51] The activity of VEGF is countered by the counterpart of soluble VEGFR-1 (sVEGFR-1 or sFlt-1), which is generated by a process of "splicing" alternative: sVEGFR-1 inhibits VEGF.[52] Importantly, increased BM angiogenesis in MM is supported mainly by the production of VEGF.
Podar et *al.*[2] in their study showed for the first time that VEGF induces proliferation and triggers migration of human MM cells, suggesting an autocrine VEGF loop in MM. MM cells produce VEGF directly which is able to stimulate the secretion of IL-6 and at the same time VEGF is produced by the stromal cells, which in turn induce the production of VEGF by the MM cells using a "loop" paracrine. There is also a "loop" autocrine where VEGF, stimulated by IL-6, acts

on its receptor VEGFR-1 on MM cells by inducing the secretion of VEGF.[2]
An increased angiogenic activity of mesenchymal stromal cells has also been demonstrated in MM with VEGF overexpression compared with healthy donors.[53] In 80-90% of MM patients, freshly purified PCs express VEGF mRNA, and high VEGF levels were detected in BM samples of MM patients.[51,54,55]
However, contrary to preclinical experiments, where long-term benefit of VEGF inhibition can be achieved, the clinical benefit in cancer patient survival with advance disease is limited, and a fraction of patients are intrinsically refractory or acquire resistance.[56-58]

- *Basic-Fibroblast Growth Factor-2 (bFGF-2)*

bFGF is another pro-angiogenic molecule regulating ECs proliferation, survival, migration and mobilization.[34,59] Bisping *et al.*[60] showed that, in BM MM microenvironment, malignant PCs are the predominant source of bFGF and its role in MM-induced angiogenesis has been demonstrated by the capacity of an anti-bFGF blocking antibody to inhibits *in vitro* vessels formation induced by BM PCs samples.[39]
It is thought to be also produced by ECs and stromal cells in the BM MM microenvironment. Colla *et al.*[61] demonstrated, in a cohort of newly diagnosed MM patients, that less than 50% of patients expressed bGF mRNA and a lower number of patients produced bFGF protein. These findings suggest that bFGF is not the major angiogenic factor produced by MM cells.

- *Angiopoietins*

Ang-1 is an important growth factor involving in the process of neo-angiogenesis, maturation and stabilization of new vascular walls. Ang-1, expressed and secreted by HMCLs, binds to its receptor Tie-2, expressed by ECs. This growth factor does not induce the proliferation of ECs directly, but acts as a survival factor for ECs[62], induces vessel stabilization, increases tubule formation[63] and plays a key role in mediating interactions between endothelial and matrix cells.[64] Nakayama *et al.*[65] underscored the critical role of the mast cell-derived Ang-1 in promoting PCs growth in tumor microenvironment in association with VEGF role. Angiopoietin-2 (Ang-2) is the natural antagonist of Ang-1and blocks the action of Tie-2 mediated by Ang-1 on ECs, leading the destabilization of the vessels.[66] Giuliani *et al*.[47] investigated the Ang-1 potential role in MM-induced angiogenesis and showed the expression and the secretion of Ang-1 by HMCLs, but not of its antagonist Ang-2. In analysis on newly diagnosed MM patients was demonstrated that Ang-1 is expressed in about 47% of patients, however, Ang-2 was not present in any patients tested.[47] In addition to the direct production of Ang-1, MM cells alter

the expression of angiopoietins and the Tie2 receptor in the BM microenvironment. In an *in vitro* co-culture system it has been demonstrated that several HMCLs up-regulated expression of Tie-2 by ECs at both mRNA and protein level.[47] This findings has been confirmed *in vivo* by studies of Vacca *et al*.[67] and Terpos *et al*.[68] However, the source of circulating Ang-2 is not clear, but since ECs and endothelial progenitor cells (EPCs) production of Ang-2 is well-established it is appropriate to consider ECs the primarily cells involving in regulating Ang-2 serum level.[69,70]

- *Metalloproteinases (MMPs)*

Matrix metalloproteinases (MMPs), a family of zinc-dependent endopeptidases involved in the "turnover" of the ECM and in physiological bone remodeling, play a fundamental role in the process of invasion, metastases, and tumor angiogenesis.[71] MMPs enhance angiogenesis by detaching pericytes from vessels undergoing angiogenesis, releasing and activating ECM-bound angiogenic factors, exposing cryptic pro-angiogenic integrin binding sites in the ECM, and by cleaving endothelial cell-cell adhesions.[72] MMPs also negatively regulate angiogenesis through the generation of endogenous angiogenesis inhibitors by proteolytic cleavage.[72] The secretion of the gelatinases MMP-9 and, MMP-2 and the collagenase MMP-1 by MM cells is enhanced by the interaction with ECs.[73,74] MMP-9 expression is similar between MGUS and MM patients, instead the expression of MMP-2 is enhanced in MM patients[39] MMP-1 and MMP-2, but not MMP-9, are expressed by tumor microenvironment BMSCs. While MMP-1 is positively regulated by TNF-α and oncostatin M (OSM), MMP-2 is not modulated by these cytokines. Finally, there are evidences that MMP-2 has a pivotal role in the spread of MM PCs and in their extramedullary localization. Since MMP-1, MMP-2 and MMP-9 have the ability to degrade collagens and fibronectin it is obvious that PCs of active MM patients are capable of invading both stroma and sub-endothelial basement membrane establishing intra- and extramedullary dissemination.[75]

- *Hepatocyte Growth Factor, Syndecan-1 and Heparanase*

HGF, secreted by mesenchymal cells and MM cells,[76] is a heparin-binding cytokine that, binding to the proto-oncogenic c-met receptor, mediates pleiotropic effects.[77] It stimulates ECs proliferation and survival, acts as a pro-angiogenic and pro-metastatic molecule and enhances MMP-9 production by MM cells.

In MM cells HGF, bFGF-2, epidermal growth factor (EGF) and VEGF activity and signaling are enhanced by syndecan-1. Syndecan-1 is a member of Syndecan family, transmembrane

proteoglycans involving in the organization of cytoskeleton and actin microfilaments, and in the cell-cell and cell-matrix interactions.[78,79] In particular, syndecan-1 acts as a tumor inhibitor by preventing tumor cells proliferation. In the epithelial-derived tumor cell-line S115, syndecan-1 ectodomain suppresses the growth of the malignant cells without affecting the growth of normal epithelial cells.[80] However, syndecan 1 expression also has a role in MM progression and angiogenesis, as well as in other cancers.[81] To explicate its functions syndecan-1 is shedded by Heparanase through the upregulation of MMP-9 and HGF activity and expression.[82,83]

- *Interleukin-6 and Interleukin-8 (IL-8)*

IL-6 is the major growth and survival factor for MM cells and is over-produced in a paracrine fashion by BMSCs.[84] This citockine stimulates the production of VEGF and OPN by MM cells.[84] Evidences suggest that IL-6 may exert a direct and indirect angiogenic effect in MM microenvironment.[85]

Interleukin-8 (IL-8), also known as CXCL8, is a chemokine that exerts a potent angiogenic activity binding CXCR1 and CXCR2 receptors on ECs.[86] The effects of IL-8 are independent of its chemotactic activity for neutrophils and other pro-inflammatory effects; indeed, promotes angiogenesis also in the absence of inflammatory cells. IL-8 is also able to inhibit apoptosis of ECs. Studies indicate that MM cells and BMSCs directly produce IL-8, and elevated BM levels of IL-8 have been demonstrated in MM patients.[87] Munshi *et al.*[88] compared the gene expression of MM PCs with healthy PCs and found increased expression of angiogenesis-related IL-8 in the first ones. Finally, with regard to angiogenesis mediated by IL-8, it was seen that it increases the MMP-2 and MMP-9 mRNA expression in ECs.[89]

- *Osteopontin*

OPN, directly produced by MM cells and OBs, is a pro-angiogenic factor promoting ECs migration and survival,[90] adhesion of both endothelial and smooth muscle cells.[91] Studies *in vitro*[92] and *in vivo*[93,94] associated OPN with tumor angiogenesis and, furthermore, showed a failure induction of pro-angiogenic effects of OPN-immuno-depleted CM (conditioned media) from MM cells and an arrest of MM-induced-angiogenesis by anti-OPN. In addition to its direct role in MM angiogenesis. Philip *et al.*[95] proposed an OPN possible indirect role through its modulation of MMP-2. These data suggest that OCs may have role in MM-induced angiogenesis, indeed, OPN is also secreted by OCs in the MM microenvironment. Data of Asou *et al*.[96] report a minimal bone resorption in OPN knockout mice compared with controls.

❖ *CCL2/MCP-1 (monocyte chemotactic protein-1)*

Monocyte chemotactic protein-1 (CCL2/MCP-1) is an important immune factor, secreted by both cancer cells and cells in the tumor microenvironment, including fibroblasts and ECs.[97] MCP-1 is a chemotactic protein, which attracts macrophages into the tumor microenvironment from the blood, that in turn release a series of factor, which promotes cancer cells generation and angiogenesis.[98] Indeed, Wu *et al.*[99] showed that MCP-1 is involved in regulating tumor cells migration, invasion and metastasis in Oral Squamous Cell Carcinoma (OSCC). Moreover, data on ECs in brain highlighted that MCP-1 induces the expression of several angiogenic factors.[100] More recently, these results were confirmed in *in vivo* studies where Bonapace *et al*.[101] showed that MCP-1 is involved in the enhancement of cancer cells mobilization, tumor formation and metastatic cell proliferation.
Other factors implicated in the angiogenic process are illustrated in the following table.

FACTOR	SITE	FUNCTIONS
Platelet Derived Growth Factor alpha (PDGFA)	MM cells	Stimulates cell proliferation, migration, survival and chemotaxis
Transforming Growth Factor beta-1 (TGFβ1)	Macrophages, Ecs, MM cells	Stimulates IL-6 production by BMSC
Platelet Endothelial Cell Adhesion Molecule 1 (PECAM1/CD31)	ECs	Stimulates angiogenesis
Melanoma Cell Adhesion Molecule (MCAM/CD146)	Ecs	Stimulates ECs proliferation and angiogenesis
Chemokine C-X-C motif Ligand 12 (CXCL12)	BMSCs	Stimulates proliferation and homing of MM cells
Chemokine (C-X-C motif) Ligand 10 (CXCL10)	Ecs, Monocytes, BMSCs, B cells, T cells, MM cells	Attenuates cell proliferation and tumor growth, promotes T cell adhesion to ECS, and inhibits bone marrow colony formation and angiogenesis

The process of angiogenesis is supported by both the over-expression of pro-angiogenic factors and the inhibition of anti-angiogenic factors. A number of these inhibitors are derived from the ECM, among these: thrombospondin, endostatin, angiostatin and tissue Inhibitor of Metalloproteinases (TIMP).[102]
Another important inhibitor of angiogenesis is semaphorin 3A (Sema3A). which is implicated in physiological function, such as immune responses, organogenesis, angiogenesis and in pathological function such as oncogenesis.[103] The expression of Sema3A supports both directly angiogenesis by inducing pericyte coverage of tumor vessels[104] and indirectly by

mediating recruitment of monocytes that express neuropilin 1 (NRP1), which in turn secrete several factors involved in vessel maturation.[105]

It has been showed that, in normal conditions, Sema3A inhibits, whereas VEGF stimulates the motility of vascular ECs expressing NRP1[106] and that the loss of endothelial Sema3A in favour of VEGF may be responsible for the angiogenic switch from MGUS to MM.[107]

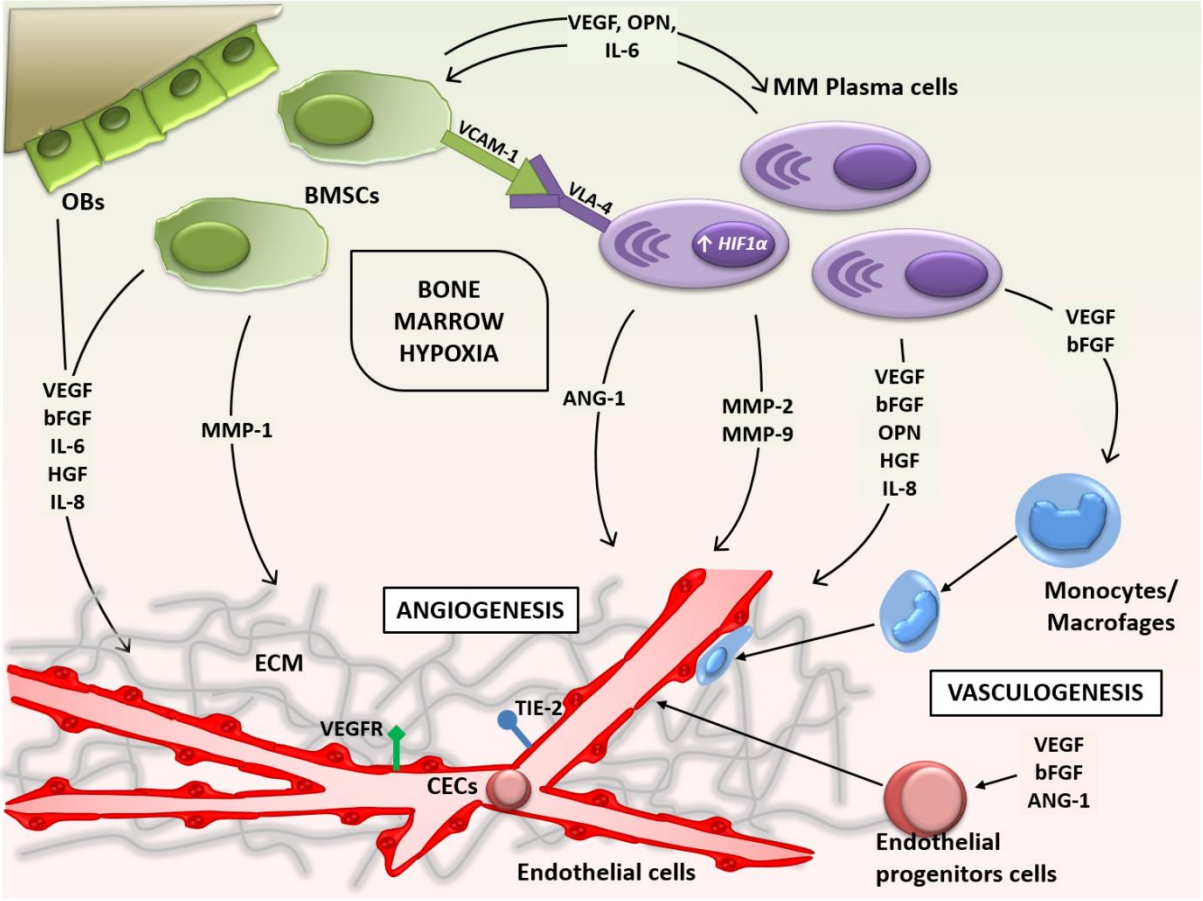

Figure C: Pathogenetic mechanisms of MM angiogenic switch. The interaction between MM plasma cells, BMSCs and OBs, mediated by cell-adhesion molecules, such VCAM1 and VLA-4, increases the production of growth factors, such as IL-6 and VEGF. These cytokines explain angiogenic activity supporting both angiogenesis and vasculogenesis.. (Modified from: Giuiani N et al. Ematologia Oncologica, Fondazione Matarelli. 2015.)

1.4.2. Role of Hypoxia and Hypoxia Inducible factor (HIF-1α) in tumor induced-angiogenesis

Hypoxia, resulting from poor perfusion and anemia, is a common feature of tumor microenvironment. Tumor hypoxia is associated with increased angiogenesis and malignant phenotype and has a critical role in the regulation of the angiogenic swith.[108,109] Hypoxia induces the expression of HIF-1α, a key transcription factor that regulates angiogenesis, cancer metabolism, invasion, maintenance of stem cell pools, cellular differentiation, genetic instability and metastases.[110-113]

HIF-1 consists of an oxygen-sensitive HIF-1α and constitutively expressed HIF-1β subunits. At oxygen levels > 5% HIF-1α is rapidly degradated by E3 ligase van Hippel-Lindau tumor suppressor protein, that modifies HIF-1α with polyubiquitin chains (ubiquitination) and thereby targets it for proteosomal degradation.[114] However, the reduced oxygen availability or treatment with hypoxia-mimetic agents (cobalt chloride) lead its translocation into nucleus where it forms heterodimer with its partner HIF-1β.[115,116] The HIF-1α/HIF-1β heterodimer binds to consensus sequence 5'-RCGTC-3', named hypoxia-responsive elements (HREs), on promoters of its target genes, such as VEGF and other pro-angiogenic molecules, required for the adaptation to hypoxia.[115-117]

Early xenograft studies in embryonic stem cells from HIF-1α$^{-/-}$ mice showed that VEGF levels and markers of vascularization were significantly reduced, indicating a key role of HIF-1α in angiogenesis.[118] Martin and collegues[114] reported that HIF-1α may contributes to increase angiogenesis also via upregulation of IL-8 and OPN.

However, even under normoxic conditions in different types of cancer cells, including MM cells, HIF-1α can be activated in an oxygen-independent manner by growth factors, oncogene products or by the accumulation of metabolic glucose intermediates.[114]

Studies of Ravi *et al.*[119] and Liao *et al*.[120] on genetic manipulation of HIF-1α in animal models demonstrated that its increased expression in human cells enhances tumor growth, angiogenesis and metastases. The same groups highlighted the importance of HIF-1α as a therapeutic target in solid tumors, in both preclinical models and early clinical trials, aimed to evaluate compounds interfering with HIF-1α regulation either indirectly (DNA intercalators, topoisomerase I, and mTOR inhibitors) or directly (HIF selective inhibitors).[119,120]

A growing number of evidences have provided insight into the importance role of HIF-1α in the pathophysiology of MM.[121] Indeed, numerous important genes for MM progression (VEGF, SC-derived factor 1, and myeloid cell leukemia sequence 1) are putative target of HIF-1α.[122] Asosingh *et al*.[123], underlining the important role of HIF-1α in MM BM microenvironment,

showed that it enhances VEGF production by malignant cells, promoting tumor progression and angiogenesis.

Colla and colleagues[124] reported that MM BM has a relatively low pO_2 and sO_2 as compared to healthy BM, even if there were no differences with BM pO_2 and sO_2 compared with MGUS BM. Some years before the same group showed that the oncogene, inhibitor of growth protein 4 (ING-4), directly regulates HIF-1α expression in MM cells inducing the angiogenic switch.[125] Furthermore, HIF-1α in MM cells induces the survival of malignant cells, the production of antiapoptotic proteins, bone resorption, immunosuppression and probably drug resistence.[114] **(Figure D)**

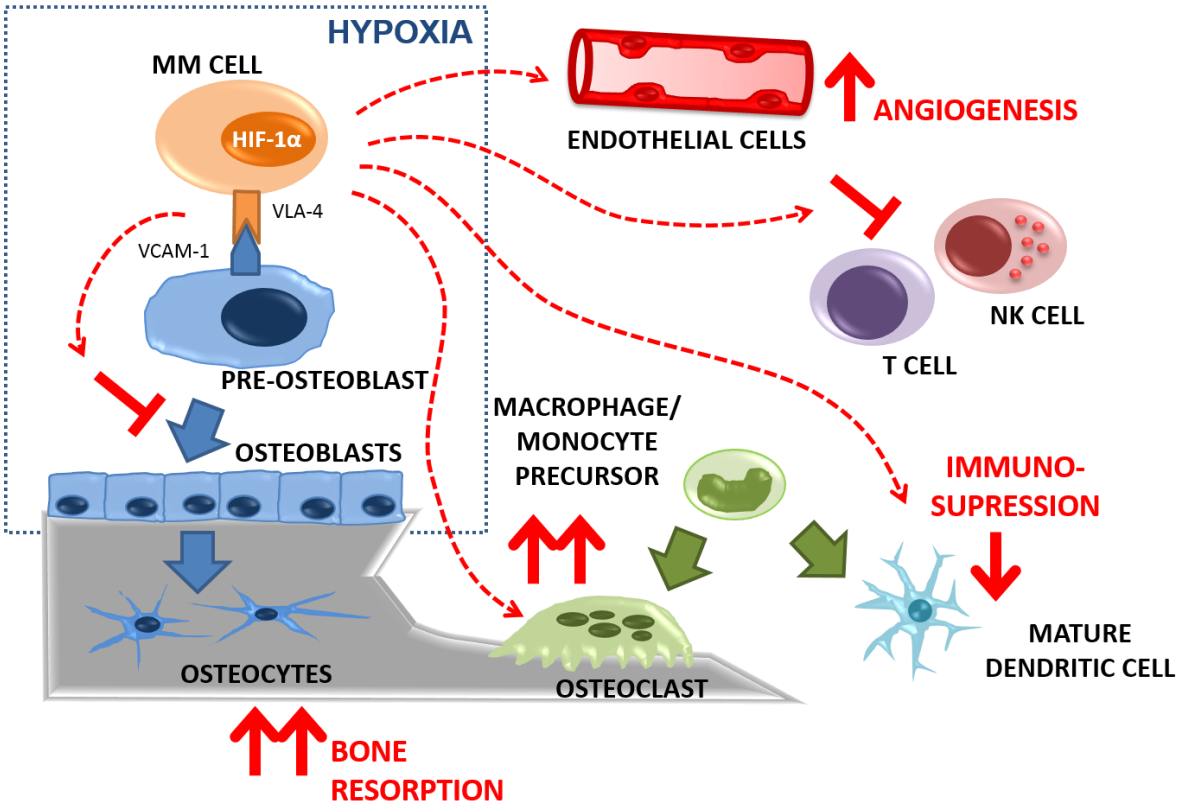

Figure D: Hypoxic MM BM microenvironment induces angiogenesis, immunosuppression and bone resorption, supporting the progression of the disease.

1.5. Galectins

In 1994 Barondes *et al*.[126] definited galectins as a phylogenetically conserved family of lectins with carbohydrate-binding specificity for N-acetyl-lactosamine-containing glycoproteins. The galectins share a carbohydrate recognition domain (CRD), consisting of about 130 amino acids, able to recognize the same structural determinant on lactose and related β-galactosides.[127]

Currently, 15 mammalian galectins have been identified and are classified into three types based on their distinct biochemical structures (**Figure E**):

1. Proto-type (galectin-1, -2, -5, -7, -10, -11, -13, -14, -15)
2. Tandem repeat-type (galectin-4, -6, -8, -9, -12)[128]
3. Chimera-type (galectin-3)

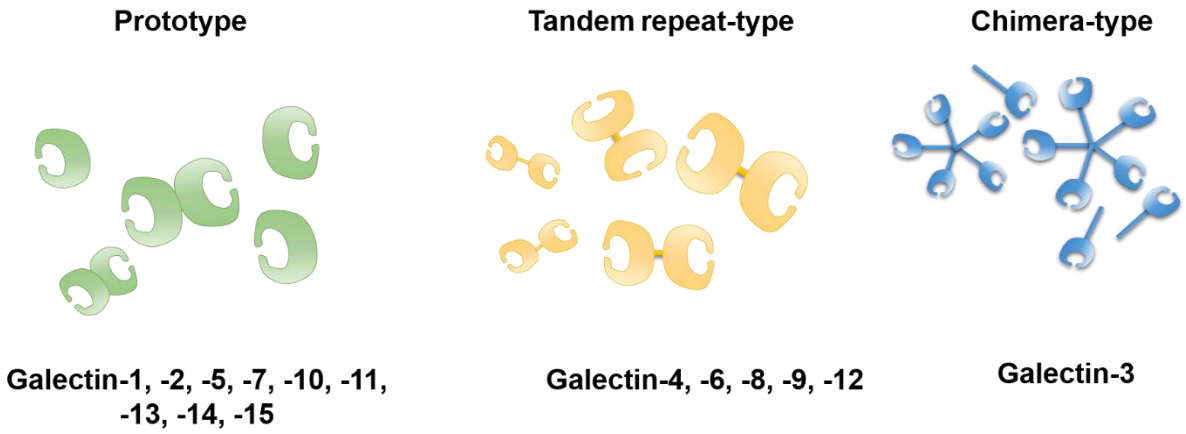

Figure E: Schematic representation of the structure of the different members of the galectin family.

Some lectins contain one CRD and are biologically active as monomers (galectin-5, -7, -10), as homodimers (galectin-1, -2, -11, -13, -14, -15) or as oligomers (galectin-3), whereas galectin-4, -6, -8, -9, -12 contain two CRDs. Studies have documented that galectins are confined to the cytosolic compartments where they have intracellular functions. However, evidences showed that galectins can be also externalized through non-classical pathways where they explain extracellularly functions.[126,127] Each member vary in their tissue distribution and are involved in difference biological activities, explained by their different glycan-binding properties.[128,129] Galectins display a wide range of biological functions in homeostasis,

apoptosis, vascular embryogenesis[130-132] and in pathological conditions (inflammation, diabetes, atherosclerosis and cancer)[133,134] by mediating communication between cells via cell–cell or cell–extracellular components. In particular, these functions are explicated by their binding to cell surface glyco-conjugated proteins or lipids, as well as to ECM components (laminin, fibronectin, thrombospondin, vitronectin).[135,136] Several lines of evidence showed that galectins play fundamental roles in tumor progression affecting on immune surveillance, angiogenesis, cell migration, tumor cell adhesion, and cellular response to chemotherapy.[137]
In this context, one member of this family, galectin-3 (Gal-3) is involved in several malignancies, including MM, by promoting cancer cell adhesion, angiogenesis and metastases.[127] Generally, is located in the cytoplasm, where it suppresses apoptosis, but it can be traslocated in the nucleus where it is involved in several biological process resulting in an increased cell survival.[138] Galectin-9 (Gal-9) is another galectin involved in a wide range of cellular functions, such as cell adhesion, proliferation and apoptosis.[139] In tumor microenvironment has been demonstrate that Gal-9 can activate caspase-8, -9 and -3 and thus inhibits the growth of MM cells.[140]
In this context, galectin-1 (Gal-1) is the most studied lectin with pro-tumor activity. Gal-1 is clearly involved in numerous processes related to cancer, including immunosuppression, angiogenesis, hypoxia, and metastases.[137]

1.5.1. Structure and function of Gal-1

Gal-1, the first protein discovered, is a lectin (14.5 KDa) that possesses one CRD. The structure of the CRD is highly conserved among many vertebrates throughout evolution. Gal-1 is encoded by the *LGALS1* (lectin galactoside binding soluble 1) gene located on chromosome 22q12.[141] Gal-1 includes 6 cysteines and can exist in either reduced or oxidized states. Oxidation of the cysteines in Gal-1 provides three intra-molecular disulfide bonds (Cys2-Cys130, Cys16-Cys88, Cys42-Cys60), causing conformational changes that hinder lectin activity (CDR capacity). The oxidized Gal-1 exists as a monomer and shows axonal regeneration-promoting activity, whereas reduced Gal-1 exists as a dimer with high CRD binding capacity.[142] Gal-1 is differentially expressed in normal tissues, such as in skeletal, smooth, cardiac muscle, kidney, thymus and placenta, and in pathological tissues where it explains a wide range of activity.[137] There is extensive literature reporting that in normal cells Gal-1 is in the cytoplasm and nucleus[142-144].However, Gal-1 appears to be secreted at higher level in the extracellular space of cancer cells and tumor-associated ECs compared to normal tissue.[145,146]

Important progresses were made in identifying Gal-1 binding partners. Nowadays is known that the lectin-carbohydrate interactions of Gal-1 occur in the extracellular compartment, whereas protein-protein interactions are intracellular.[141] NRP1, a type I transmembrane glycoprotein, is a Gal-1 extracellular binding partner[147] and is found on mesenchymal stem cells, tumor-associated stromal cells and ECs.[148] Hsieh *et al*.[149] showed for the first time that Gal-1 directly binds to NRP1 on ECs via CRD domain and promotes vascular endothelial growth factor receptor 2 (VEGFR2) phosphorylation and the activation of the extracellular signal-regulated kinases 1/2 (ERK 1/2) and c-Jun NH2-terminal kinases (JNK). The consequences of this binding are an increased proliferation, migration and adhesion of ECs.

1.5.2. Gal-1 in cancer

There is extensive literature reporting significant Gal-1 overexpression not only in a variety of cancer cell types, including melanoma, ovarian, lung, breast[150], gliomas[151], prostate, bladder, thyroid, head and neck[152], and colorectal cancers, but also in activated vascular ECs , stroma surrounding tumor cells and regulatory T (Treg) cells.[140] Gal-1 upregulation can dramatically influence tumor progression given its pleiotropic roles in cell transformation[153], cell proliferation, angiogenesis[154] ,cell adhesion and invasiveness,[155,156] and immunosuppression.[150,157]
Gal-1 has been showed to increase the adhesion of various normal and cancer cells to the ECM via cross-linking of integrins exposed on the cell surface with carbohydrate moieties of ECM components, such as laminin and fibronectin.[158,159] In addition, Gal-1 can also mediate homotypical cell interaction, favoring the aggregation of human melanoma cells[160], and interaction between cancer cells and ECs, favoring the tumor cells dissemination. Gal-1 causes the increased motility of glioma cells and the reorganization of the actin cytoskeleton associated with an increased expression of RhoA, a protein that modulates actin polymerization and depolymerization.[156] in this context, it was documented that the suppression of Gal-1 expression in glioma cells reduces motility and adhesion.[156] Harvey *et al.*[161] , using a proteomic approach, identified the Gal-1 membrane expression as a signature of cell invasiveness in mammary carcinoma cell lines. Moreover, Kim HJ *et al*.[162] highlighted, in their studies, a positive correlation between Gal-1 expression, tumor stage, tumor invasion and metastases. Other evidences showed significantly higher levels of Gal-1 in poorly differentiated and invasive colorectal, pancreatic and bladder tumors compared to different tumors or normal adjacent tissue.[163,164] Studies showed higher levels of extracellular Gal-1 in the plasma of poor prognosis patients with colorectal and head and neck squamous cell carcinomas.[165,166] Furthermore, *in vitro* studies showed that Gal-1 inhibition by antisense

mRNA or small interfering RNA (siRNA) suppresses cell proliferation in glioblastoma cells and cervical cancer, respectively.[138] Same results were observed in *in vivo* studies: Gal-1 down-regulation leaded a inhibition of ovarian[162], lung, and Kaposi's sarcoma growth.[146] Bacigalupo et *al.*[167] demonstrated that an augmented expression of Gal-1 in Hepatocellular Carcinoma cell line, HepG2, promotes the ephitelial-mesenchimal transition (EMT), important process for tumor dissemination, and induces the expression of mesenchymal marker vimentin and the loss of E-cadherin expression.

All these evidences show that Gal-1 expression or overexpression in tumor and/or in tissue surrounding them must be considered as a sign of malignant progression and dissemination into normal tissue and, consequently, of a poor prognosis for patients. (**Figure F**)

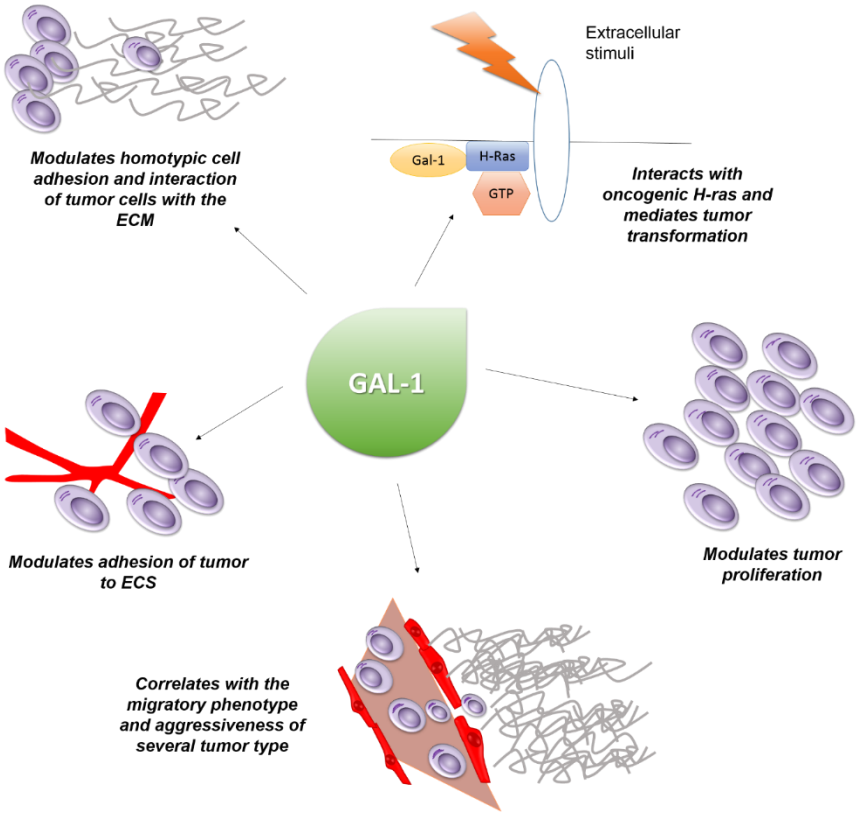

Figure F: Contribution of Gal-1 to tumor progression. Gal-1 interacts with oncogenic genes and promotes tumor transformation. In addition, this protein modulates cell growth, cell adhesion and cell migration, thereby supporting the tumor metastases.

1.5.3. Pro-angiogenic activity of Gal-1

Increasing evidences showed that endothelial galectins play a critical role in the endothelial adaptations associated with tumor angiogenesis.[140] Especially, among its numerous pro-cancer roles, Gal-1 seems to have a central role in the tumor vasculature stimulating vascular endothelial cells growth as well as provides physical support for newly formed capillaries. High Gal-1 expression has been reported in the vasculature of many tumors such as colon, head and neck, lung, and oral cancers. In 2006 Thijssen *et al*.[132] have showed that the knock-down of Gal-1 expression in ECs inhibits proliferation and migration, whereas Gal-1-null (gal-$1^{-/-}$) mice display hampered tumor growth due to decreased angiogeneic activity. In the same study, Thijssen have showed that tumors, in gal-$1^{-/-}$ mice, did not respond to Gal-1 targeted anti-angiogenesis therapy. Other studies suggested a role for exogenous Gal-1 in ECs functions; Gal-1 suppression in glioblastoma cells reduced the number of tumor vessels in mice[168]. In addition, exogenous Gal-1 was described to be involved in enhancing the viability and adhesion of cultured ECs.

More recently Thijssen *et al.*[154] provided evidences that tumor derived Gal-1 can act as a pro-angiogenic factor. Their data showed that, in gal-$1^{-/-}$ mice, tumor ECs take up Gal-1 from Gal-1-secreting tumor cells. In addition, it has been showed that Gal-1 inhibitors can prevent endothelial tube formation.[169]

In the tumor microenvironment Gal-1 is present in abundance and promotes the physical interactions between endothelial cell-cell or cell-ECM, helping to construct new blood capillaries via its homodimeric cross-linking property. Indeed, vascular endothelial cells are surrounded by considerable amounts of N-glycans on their surfaces and , in addition, the ECM in the tumor stroma contains high levels of laminin and fibronectin, which are known to be significant Gal-1 binding targets.[158]

1.5.4. Gal-1 expression in tumor hypoxia

It was observed that the expression of Gal-1 is up-regulated by the level of HIF-1α stabilization in the tumors. The hypoxia-responsive elements are located at 441 to 423 bp upstream of the transcriptional start site of the *LGALS1* gene and are essential for HIF-1α mediated Gal-1 expression.[170] The stabilized HIF-1α induces Gal-1 expression, which helps vascular endothelial cells to create new capillaries by activating ECs proliferation and migration, reinforcing cell-cell and cell-extracellular matrix and protecting them from the oxidative stress caused by the increased oxygen reactive species (ROS) levels existing within the tumor.

In 2005 Le *et al*.[171] have showed a significant relationship, in head and neck squamous cell carcinomas (HNC), between Gal-1 expression and the presence of hypoxia markers and an inverse correlation with T-cell infiltration, suggesting that hypoxia can affect malignant progression by regulating the tumor cells secretion of proteins, such as Gal-1, that modulate immune privilege.

These evidence was also observed in tongue (Scc4), pancreatic adenocarcinoma (Panc1) and immortalized B-cell line (V2P3). Increased circulating Gal-1 was observed in HNC tumor bearing mice after breathing 10% oxygen, which effectively increased tumor hypoxia.[171] Several studies have also showed that hypoxia-exposed cancer cells produce higher levels of Gal-1, which correlated with their levels of HIF-1α, as well as those of carbonic anhydrase IX (CA IX), whose expression is a late marker of hypoxia. Furthermore, Gal-1 upregulation by hypoxia has been documented also in prostate cancer cells and in acute myeloid leukemia cells. Finally, the knock-down of Gal-1 by its specific shRNA can significantly reduce hypoxia-induced invasion and migration of colon rectal cancer cells (SW620), and the ectopic expression of Gal-1 can remarkably restore invasion and migration abilities of HIF-1α-knocked SW620 cells.[172]

Recently Croci *et al.*[146] found that the Gal-1 interaction with *N*-glycans may link tumor hypoxia to vascularization in Kaposi's sarcoma. In this study they showed that these interactions promoted compensatory angiogenesis in tumor with limited sensitivity to anti-VEGF. **(Figure G)**

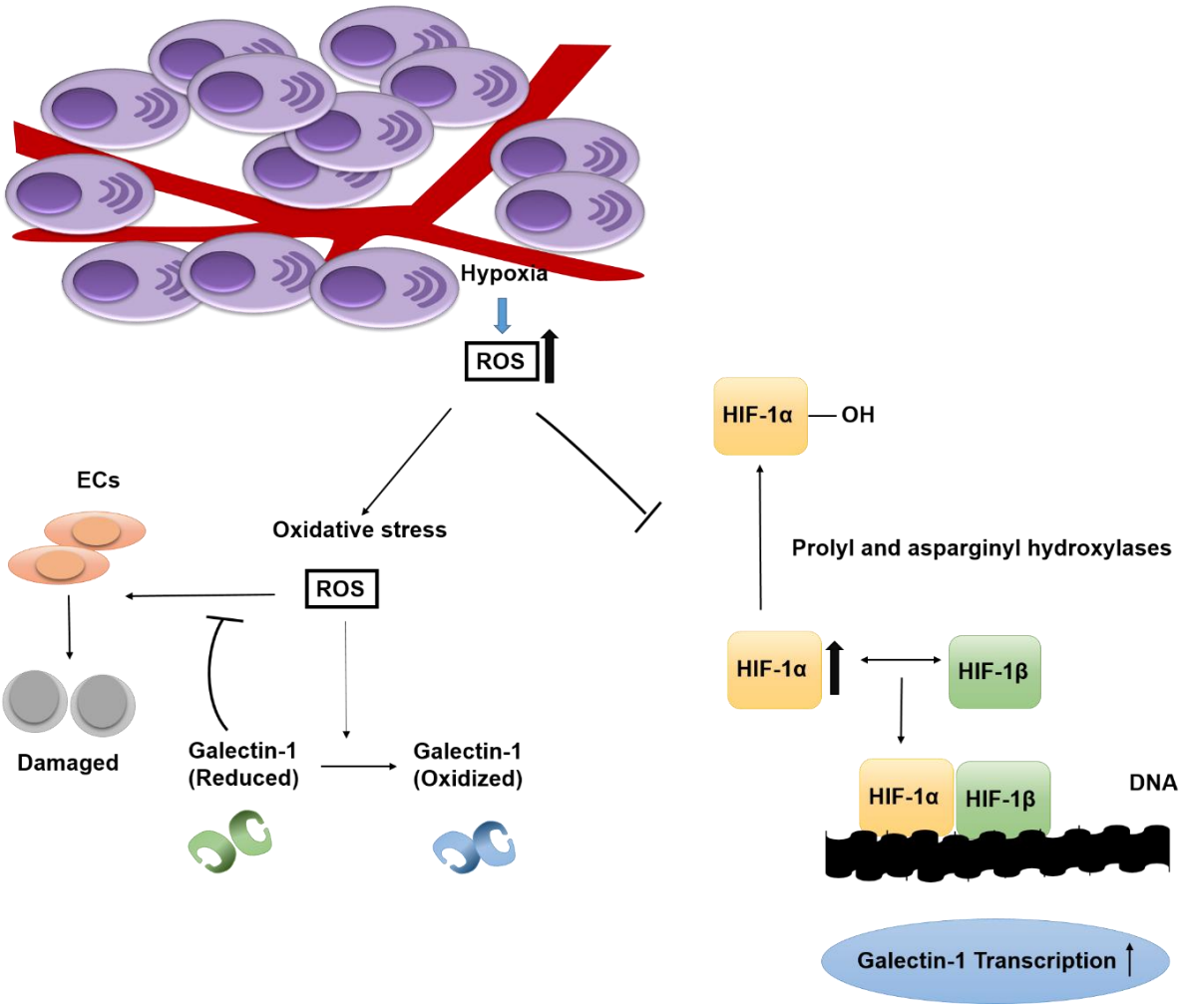

Figure G: Gal-1 pro-tumorigenic functions in the tumor microenvironment. Hypoxia, developing during tumor progression, increases ROS production in the hypoxia-exposed regions. Stabilized HIF-1α incorporates with HIF-1β and this complex binds DNA to promote transcription of Gal-1. Secreted Gal-1 may absorbs ROS to reduce the oxidized stress and will be converted into the oxidative state. Free Gal-1 binds to vascular endothelial cell surfaces and promotes tumor angiogenesis through promoting ECs proliferation and migration and reinforcing interactions of cell-cell or cell-extracellular matrix (laminin and fibronectin).

2. AIMS OF THE STUDY

Gal-1 is involved in several processes related to cancer, including immunosuppression, angiogenesis, hypoxia, and metastases. However, the role of Gal-1 in MM pathophysiology and in MM-induced angiogenesis is unknown.

In this study, we proposed to investigate the expression profile of Gal-1 in MM, its role in MM cell growth and in the MM-induced angiogenesis. Firstly, we have evaluated the expression of Gal-1 by malignant PCs in BM microenvironment and the association between *LGASL1* expression levels and patient clinical outcome in terms of overall survival. Secondly, we have investigated the role of Gal-1 on survival and proliferation of MM cells. Moreover, we explored the role of hypoxia and HIF-1α on Gal-1 expression checking the effect of hypoxic treatment (1% of O_2) and HIF-1α inhibition by shRNA lentivirus. Finally, we studied the effect of persistent Gal-1 inhibition in HMCLs on cell proliferation, survival, transcriptional and pro-angiogenic profiles, on tumor growth and on MM bone disease.

3. PATIENTS, MATERIALS AND METHODS

Patients

We studied a cohort of 24 patients with newly diagnosed active MM (ISS stage I-III), 9 patients with SMM and 9 patients with MGUS. BM aspirates (10 ml, treated with EDTA to prevent clotting) and bone biopsies were obtained from the iliac crest of all patients after informed consent, according to the Declaration of Helsinki. Ethical approval was obtained from the Institutional Review Board of our Hospital.

Expression analyses

LGALS1 expression analysis.

Gene expression profiles of highly purified PCs from 5 healthy subjects (N), 11 MGUS, 133 MM patients at diagnosis and 9 PCL (GSE16122),[173] and 23 HMCLs (GSE6205)[174], both generated on Affymetrix GeneChip HG-U133A arrays, were reannotated using GeneAnnot custom CDF annotation package (v2.2.0), leading to the definition of 12.364 unique, well-characterized genes. *LGALS1* expression level was evaluated across the different type of samples and of monoclonal gammopathies.

Association with prognosis.

Gene expression dataset from Millennium Pharmaceutical ("MP") and University of Arkansas for Medical Sciences ("UAMS"), NCBI GEO accession number GSE9782 and GSE2658, respectively, were used to test association between *LGASL1* expression and MM patient outcome. Cox proportional hazard model was also used in the *globaltest* function in R[175], under 100,000 permutation process, to test the positive or negative association between covariate (mRNA expression levels of *LGALS1*), assumed as continuous variable, and clinical outcome as response variable (in terms of overall survival, both UAMS and MP datasets or progression-free survival, only the MP dataset).

Immunohistochemistry

Gal-1 immunostaining on bone biopsies was performed in a cohort of 23 symptomatic MM patients, 9 SMM and 10 MGUS. Bone biopsy sections were incubated with rabbit monoclonal antibody against Gal-1 (1:500) (LifeSpan BioSciences Seattle, WA) for 60 min at room temperature. Gal-1 staining was revealed using the UltraVision LP Large Volume Detection System HRP polymer (Thermo Scientific, Erembodegem, Belgium).

Cells and cell culture conditions

Cell lines. HMCLs JJN3, OPM2, RPMI-8226 were purchased from DSMZ (Braunschweig, Germany), HMCL U266 was obtained from the American Type Culture Collection (Rockville, MD), HMCL XG1 was a generous gift of Prof. Antonino Neri (IRCCS, Milan) and HMCL INA-6 kindly provided by Prof. Francesco Piazza (Padova, Italy).

HMCLs were maintained in culture in RPMI 1640 medium supplemented with 10% of fetal bovine serum (FBS), Penicillin (100U/ml), Streptomycin (100µg/ml), L-Glutamine (2mM) and Fungizone. RPMI 1640 medium was also supplemented with IL-6 for XG1 and INA-6 (respectively 6ng/ml and 2,5ng/ml) (Pierce Biotechnology, Rockford, USA).

MM cells purification. Total MNCs were obtained from BM aspirates of 8 patients with newly diagnosed MM by density gradient centrifugation (Lympholite-H; Burlington, NC). BM $CD138^+$ PCs were purified from total MNCs by an immuno-magnetic method using anti-CD138 mAb coated microbeads (MACS, Miltenyi Biotec, Bergisch-Gladbach, Germany). Only samples with purity > of 90% checked by flow cytometry (BD FACS Canto II with Diva software; Becton, Dickinson and Company (BD); Franklin Lakes, NJ) were tested.

Hypoxic treatment. Normoxic condition was maintained at 20% of O_2 and 5% of CO_2 and hypoxic treatment was obtained by exposing cells at 1% O_2, 94% N_2 and 5% CO_2 for 48 hours. The effect of re-oxygenation was also tested by a subsequently incubation for 48 hours at 20% of O_2 and 5% of CO_2.

HIF-1α knock-down. HIF-1α knock-down in JJN3 was obtained by infection with a lentiviral shRNA vector anti-HIF-1α (Sigma-Aldrich, Milan, Italy) whereas the pLKO.1 lentiviral vector was used as empty control, as previously described.[176]

Gal-1 stable inhibition. Lentiviral shRNA vector anti-Gal-1 (OriGene, Rockville, MD) was used for Gal-1 stable knock-down in HMCLs, whereas the scramble lentiviral vector was used as control. Recombinant lentivirus was produced by transient transfection of 293T cells following a standard protocol. HMCLs were infected as previously described.[176] The efficiency of the infection was checked by flow cytometry for the green fluorescence protein (GFP) percentage. Cell pellets for Real-time PCR and Western Blot assays were also made to check *LGALS1* mRNA and Gal-1 protein expression, respectively.

Cell viability and proliferation assays. XG-1, JJN3 and RPMI-8226 were treated with recombinant human (rh)-Gal-1 (R&D System, Minneapolis, MN) at the concentration range 3-500 ng/ml for 48-72h in RPMI 1640 medium with 2% of FBS and viability was evaluated as previously reported.[176] Viability of JJN3 stably transfected with anti-Gal-1 and scramble vectors was evaluated after 48–72h of culture in RPMI 1640 medium with 2% of FBS or without FBS, as described above. JJN3 transfected with anti-Gal-1 and scramble vectors were cultured in 96-well microtiter plates for 48–72h in RPMI 1640 medium with 2% of FBS in the presence of 3H-thymidine (3H-TdR) (Biocompare

South San Francisco, CA, USA) and thymidine incorporation was detected by liquid scintillation spectroscopy (TopCount NXT; Packard; Meriden, Connecticut, US).

Qualitative and Real-time PCR

Total RNA was extracted from $CD138^+$ cells and HMCLs, after all different experimental conditions, using the RNeasy total RNA isolation kit (Qiagen, Hilden, Germany). 1 µg of RNA was reverse-transcribed with 400 U Moloney murine leukemia reverse transcriptase (Life Technologies, Carlsbad, California, US) in accordance with the manufacturer's protocol.

Qualitative PCR was performed using the following specific primer pairs:

LGALS1: F: 5′-CCTGACGCTAAGAGCTTCGT-3'; R: 5′- GGAAGGGAAAGACAGCCTCC-3'
MMP9: F: 5′-CGCAGACATCGTCATCCAGT-3′; R: 5′-GGATTGGCCTTGGAAGATGA-3′
CCL2: F: 5′-ACTGAAGCTCGTACTCTC-3′; R: 5′-CTTGGGTTGTGGAGTGAG-3′
*SEMA3A:*F 5'- GGCATATAATCAGACTCACTTGTACGC-3' R 5'-CTTGCATATCTGACCTATTCTAGCGTG-3'
GAPDH: F 5'-CAACGGATTTGGTCGTATTG-3'; R: 5'-GGAAGATGGTGATGGGATTT-3'

Annealing temperature: *LGALS1:* 60°C *VEGFA*: 60 °C; *CCL2*: 58 °C; *MMP9*: 60 °C; *SEMA3A:* 61°C and *GAPDH:* 58 °C. Product size: *LGALS1:* 166 bp; *CCL2*: 354 bp; *MMP9*: 369 bp; *SEMA3A:* 445 bp and *GAPDH*: 209 bp. Real-time PCR was performed by adding complementary DNA to a universal Light Cycler 480 Probes Master and RealTime ready Catalog Assay from Roche Diagnostics (Mannheim, Germany) for the following genes: *LGALS1*: Assay ID: 100568, *LGALS3*: Assay ID: 102651, *LGALS9:* Assay ID: 115117,*SEMA3A*: Assay ID: 137800, *MMP9*: Assay ID: 144030, and *GAPDH*: Assay ID 141139. The TaqMan Assay probes for *CCL2*: HS00234140_m1 and *HIF1A*: HS00936379_m1 genes were purchased from Life Technologies. The Custom RealTime Ready PCR Array (Roche Diagnostics) included 16 probes for the following genes: *ANGPT1*: Assay ID: 110625; *CCL2*: Assay ID: 141156; *CCL3:* Assay ID: 136214; *CXCL10:* Assay ID: 103807; *CXCL12:* Assay ID: 144645; *FGF2:* Assay ID: 147082; *HGF:* Assay ID: 108357; *HIF1A:* Assay ID: 141046; *IL8:* Assay ID: 103136; *MMP2:* Assay ID: 139230; *MMP9*: Assay ID: 144030; *PDGFA:* Assay ID: 147202; *PECAM1:* Assay ID: 137855; *TGFB1:* Assay ID: 101210; *VEGFA*: Assay ID:140191; *VEGFB:* Assay ID: 118328 and three reference genes *HPRT1:* Assay ID: 102079; *B2M:* Assay ID: 102065; *G6PD:* Assay ID: 102098. Real-time PCR experiments were performed on Light Cycler 480 (Roche Diagnostics), following a standard protocol. We applied the comparative Ct method using the endogenous reference gene *GAPDH*, to normalize the differences in RNA quality and reverse transcription efficiency. The relative mRNA quantification of each gene was performed by the ΔCt method (Δ=mean Ct–mean Ct *GAPDH*). ΔΔCt was evaluated as the difference between the ΔCt of a sample and the ΔCt of the control. The fold change in mRNA was calculated as $2^{-\Delta\Delta Ct}$. For PCR Array data analysis we applied the same ΔCt method described above, using as reference genes a mean of the three reference genes included in the plate layout.

Microarray analyses

Total RNA was extracted from JJN3 anti-Gal-1 and JJN3 scramble, after 48h of normoxic or hypoxic condition and 48h of re-oxygenation process, using the RNeasy total RNA isolation kit (Qiagen; Hilden, Germany). Gene expression profiles (GEPs) were generated on GeneChip® HG-U133 Plus 2.0 arrays (Affymetrix; Santa Clara, CA). The biotin-labeled cRNA of JJN3 scramble and JJN3 anti-Gal-1 was prepared according to the Affymetrix GeneChip Expression Analysis Technical Manual protocol. Normalized expression values were obtained by the RMA algorithm and reannotation of HG-U133 Plus 2.0 arrays was performed using the corresponding GeneAnnot custom chip definition files (GA v2.2.1), as previously described.[173] Hierarchical agglomerative clustering of the samples was carried out by DNA-Chip Analyzer (dChip) software,[177] using Pearson's correlation coefficient and average linkage as distance and linkage metrics, respectively, on those genes whose average change in expression levels varied at least 1.5-fold from the mean across the entire dataset, as previously reported.[178] In order to find the differentially expressed genes between anti-Gal-1 and scramble JJN3 samples in each experimental condition, for each gene, we calculated the ratio of the difference between the expression levels of the two experiments on the mean value of the same two variables. The most significant differentially expressed transcripts have been selected as those exceeding the mean plus 3 standard deviation of all the ratio values.

Protein expression analyses

Western Blot. Nuclear and cytosolic extracts were obtained using a commercial kit (Active Motif, Carlsbad, CA) following the manufacturer protocol. A total of 20 µg of cytosolic extracts were tested. For immunoblotting, the following antibodies were used: mouse monoclonal anti-Gal-1 antibody (1:500) (AbD Serotec, Kidlington, UK) and polyclonal goat anti-HIF-1α (1:1000) (R&D System, Minneapolis, MN) and mouse anti-β-actin monoclonal antibody (1:5000) (Sigma-Aldrich) as internal control. The secondary antibodies peroxidase conjugated were anti-mouse (1:10000) (BD Pharmingen, Franklin Lakes, NJ,) and anti-goat (1:30000) (Rockland Immunochemicals, Gilberrtsville, PA, USA). Chemiluminescence was detected using luminol solution (ECL Plus, GE Healthcare Amersham, Milan, Italy). The immunoreactive bands were visualized using an exposure time of min (Kodak XOMAT). Protein bands were quantified using ImageJ software.

ELISA assay. MMP-9 and MCP-1 levels in JJN3 scramble and anti-Gal-1 CM were detected by Human MMP-9 PicoKine™ ELISA Kit and Human MCP-1 PicoKine™ ELISA Kit (Boster, Pleasanton, CA, USA), following the manufacturer's protocol.

Immunoprecipitation. CM of JJN3 scramble and anti-Gal-1, in normoxic and hypoxic conditions were concentrated by centrifugation for 20 min at 2000 rpm with Amicon Ultra 15 (Millipore, Darmstadt, Germany). 500µg of protein of concentrated CM or rat brain extract (Santa Cruz Biotechnology), used as positive control, were immunoprecipitated with 2 µg rabbit anti-Sema3A antibody (Santa Cruz Biotechnology, Inc., Heidelberg, Germany) or 2 µg of IgG control (Santa Cruz

Biotechnology) for 2h at 4°C. Precipitates were recovered after an overnight incubation at 4°C with protein A/G Plus-Agarose (Santa Cruz Biotechnology), washed 3 times with PBS and resuspended in sample buffer. After separation of proteins by SDS–polyacrylamide gel electrophoresis, protein were stained with Silver Staining Plus Kit (Bio-Rad Laboratories, Hercules, California, US). Bands were quantified by ImageJ software.

Angiogenesis *in vitro* assay

In vitro angiogenesis was assessed by V2a angiogenesis assay Kit obtained from Cellworks (Buckingham, UK), as previously described.[125] In brief, cells were stimulated with VEGF (2 ng/mL, positive control) or suramin (20 μM, negative control) or with CM of JJN3 scramble or anti-Gal-1 cultured in normoxic (ratio CM/V2a Growth Medium 1:1) or hypoxic condition (ratio CM/V2a Growth Medium 1:1.5).

At day 14, cells were fixed and stained using an anti-CD31 Ab provided with the V2a angiogenesis assay Kit, following the manual instructions. Angioquant software was used for quantify number and length of formed tubules and number of junctions.

***In vivo* studies**

Two groups of 4 severe combined immunodeficiency/non obese diabetic (SCID-NOD) mice were housed under specific pathogen-free conditions and were injected subcutaneously with 5×10^6 JJN3 anti-GAL-1 vector or with JJN3 scramble. All procedures involving animals were performed in accordance with the National and International current regulations. Twenty-one days after tumor cell inoculation, mice were sacrificed and autopsies were performed. As previously described,[179] tumor volume (mm^3) was calculated according to the following formula: $0.523 \times length \times width^2$. Tumors were removed and sections of subcutaneous *ex vivo* plasmacytomas were stained with rabbit anti-mouse CD34 (1:100) (Santa Cruz Biotechnology). After the washing sections were incubated with a secondary antibody (1:250) (Rat anti-Immunoglobulin G horseradish peroxidase) (Millipore) and reaction revealed with a solution of 3-3′-diaminobenzidine tetrahydrochloride (liquid DAB substrate chromogen system) (DAKO, Glostrup, DK).

In a separate set of experiments, 3 groups of 11 SCID mice (Charles River, Wilmington, MA, USA) were irradiated 24 hours prior to injection with a single dose of 200cGy using a JL Shepherd MARK1 (San Fernando, CA, USA). Animals were injected intratibially with JJN3 wildtype, JJN3 scramble, or JJN3 anti-Gal-1 cells. Four weeks after injection, animals were euthanized, blood collected by cardiac puncture, radiographs taken, and bilateral tibias and femurs removed and fixed in 10% phosphate-buffered formalin for 48h and then transferred to 70% ethanol. Radiographs were taken using an XPERT 80 Digital Cabinet X-ray System (Kubtec Digital X-ray, Milford, CT, USA). Images of dissected tibiae were analyzed using a vivaCT 40 scanner (Scanco Medical, Brüttisellen, Switzerland) at resolution of 15 μm. Bone Volume/Total Volume (BV/TV) ratio was calculate for each

sample. Studies were approved by the Institutional Animal Care and Use Committee of the Indiana University School of Medicine. The sample size was calculated based on a previous study.[180] Plasmacytomas obtained from tumors removed from mice injected both subcutaneously and intratibially with JJN3 anti-Gal-1 and JJN3 scramble were fixed in 10% neutral buffered formalin, embedded in paraffin and stained with hematoxylin and eosin.

Statistical analysis

Non-parametric Mann-Whitney test and Kruskal-Wallis or parametric two tail Student's t test were used to compared quantitative variables. Results were considered significant at $p<0.05$. IBM SPSS™ (v.22) was used for all the statistical analyses.

4. RESULTS

Gal-1 is highly expressed in the BM microenvironment

We initially evaluated the expression of Gal-1 at mRNA and protein levels in BM PCs. Two datasets analyzed, including 5 healthy subjects, 11 MGUS, 133 MM patients at diagnosis and 9 PCL (GSE16122), and 23 HMCLs (GSE6205) showed an high expression of *LGALS1* in all samples without significant differences across the different types of samples (**Figure S1a**). Consistent to these data, Real-time PCR and Western Blot analysis on 8 samples of freshly purified BM $CD138^+$ cells from newly diagnosed MM patients (**Figure 1a**) and on 6 HMCLs (**Figure 1b**) revealed high expression levels of *LGALS1* mRNA and Gal-1 protein in all samples, even if with variability of expression between the samples. Immunohistochemistry analysis performed on bone biopsies from 23 MM symptomatic patients, 9 SMM and 10 MGUS confirmed the high levels of Gal-1 expression in MM cells and revealed a markedly positivity to Gal-1 of BM OBs and vessels without a significant difference across the different types of monoclonal gammopathies. A representative example of Gal-1 immunostaining was reported in **Figure 1c** and the immunohistochemical data were summarized in **Table S1**.

Gal-1 expression levels are correlated with MM patient outcome in terms of overall survival

Subsequently, to verify a possible correlation between *LGALS1* expression levels and MM patient clinical outcome in terms of overall survival, we used two gene expression datasets from Millennium Pharmaceutical ("MP") and University of Arkansas for Medical Sciences ("UAMS") NCBI GEO accession number GSE9782 and GSE2658, respectively. Notably, a significant association has been demonstrated between *LGASL1* expression levels and overall survival in both MP (P=0.00105) and UAMS (P=0.00428) datasets by a *globaltest* analysis. Indeed, high *LGALS1* expression levels were associated with a poor prognosis in term of overall survival, whereas low *LGALS1* expression levels correlated with an increased clinical outcome as shown the Kaplan Meier estimated curves reported in **Figure S1b** (MP P=2.709e-06; UAMS P=2.341e-04).

Gal-1 is a hypoxia and HIF-1α-induced protein in MM

We then asked whether hypoxic MM microenvironment could influence Gal-1 expression. To address this question we conducted a series of *in vitro* experiments on two HMCLs, JJN3 and OPM2. Both HMCLs were incubated in normoxic (20% of O_2 and 5% of CO_2), and then in hypoxic treatment

(1% O_2, 94% N_2 and 5% CO_2 for 48 hours) and finally in reoxygenation condition (20% of O_2 and 5% of CO_2 for 48 hours). We compared mRNA levels of Gal-1 between normoxic, hypoxic and reoxygenation cells by Real-time PCR analysis. The data showed a significant induction of Gal-1 mRNA levels following hypoxic exposure as compared to normoxic exposure, and a consistent restoration of mRNA levels of Gal-1 after reoxygenation treatment (**Figure 2a**). Consistent to Real-time PCR results, Western Blot analysis revealed a marked upregulation of Gal-1 protein levels in HMCLs following hypoxic exposure respect to normoxic exposure, and a restoration of *LGALS1* mRNA levels after re-oxygenation treatment, as reported in **Figure 2b** and **Figure 2c**. Given the relevance of transcription factor HIF-1α in driven MM hypoxia[176], we then examined whether HIF-1α may control Gal-1 expression in MM. JJN3 cell line was stably transfected with shRNA lentiviral vector anti-HIF-1α, whereas the pLKO.1 lentiviral vector was used as empty control, as recently reported.[176] We evaluated Gal-1 mRNA levels and Gal-1 protein expression of JJN3 anti-HIF-1α, compared with JJN3 pLKO.1, in both normoxic and hypoxic conditions.

Real-time PCR and Western blot analyses showed that hypoxia increased *LGALS1* mRNA (**Figure 2d**) and Gal-1 protein (**Figure 2e**) levels in both JJN3 pLKO.1 and JJN3 anti-HIF-1α, and that stable knock-down of HIF-1α significantly down-regulated Gal-1 expression both in normoxic and in hypoxic conditions.

Effect of Gal-1 on MM cell viability and proliferation and stable inhibition of Gal-1 in HMCLs

Cell viability (XG1, RPMI-82226 (data not shown) and JJN3) was assessed by MTT assay after exposure to several concentrations of rh-Gal-1 at different time points. As reported in **Figure S2a**, the viability of the cells was not modified by rh-Gal-1 treatment.

Moreover, to evaluate the putative role of Gal-1 in the MM cells, we stably knocked-down Gal-1 in JJN3 and OPM2 with shRNA lentiviral vector anti-Gal-1 (JJN3 anti-Gal-1 and OPM2 anti-Gal-1). The scramble vector was used as control (JJN3 scramble and OPM2 scramble). Gal-1 inhibition was confirmed by Real-time PCR and Western Blot, as shown in **Figures 3a-b.**

Subsequently, we tested the specificity of the lentiviral vector anti-Gal-1 evaluating the mRNA expression levels of other galectins known to be active in the MM microenvironment: Gal-3[181,182] and Gal-9.[183] Real-time PCR did not show a significant reduction of *LGALS3* mRNA, coding for Gal-3 protein, and *LGALS9* mRNA, coding for Gal-9 protein, expression in JJN3 anti-Gal-1 compared with JJN3 scramble (**Figure 3c**).

The stable inhibition of Gal-1 did not affect the proliferation rate and viability of JJN3 compared to JJN3 scramble at all the time point considered (**Figure S2b-c**), as reported in another tumor model.[184]

Gal-1 specific silencing affects the transcriptional profile of HMCLs

In addition, we performed a transcriptional profile analysis, using U133 Plus2.0 Arrays, on JJN3 cell line transfected with shRNA anti-Gal-1 and those transfected with the control vector, following normoxic, hypoxic and re-oxygenation exposures. The data showed that Gal-1 knock-down significantly modulated 269 genes in normoxia (of these 140 genes were specific for this condition), 279 genes in hypoxia (148 genes specific for this condition) and 279 genes after re-oxygenation process (152 genes specific for this condition). There were 71 common genes in all three conditions. (**Figure 3d**) The modulated genes are listed in the **Tables S2-8**. As expected, hypoxia up-regulated the expression of several proangiogenic genes, in particular *MMP9, CCL2, IL8* and *VEGFA*. The pro-angiogenic gene *CCL2* was significantly down-regulated by Gal-1 inhibition in normoxic, hypoxic conditions and re-oxygenation conditions, and the other pro-angiogenic gene *MMP9* was significantly down-regulated after hypoxia treatment. Interestingly, Gal-1 inhibition did not modify the expression levels of *VEGFA* in JJN3 in all three conditions considered and induced a slight upregulation of *IL8* in hypoxia. Moreover, Gal-1 inhibition in hypoxic condition up-regulated the anti-angiogenic genes *SEMA3A* and *CXCL10*. Furthermore, some adhesion molecules were modulated by Gal-1 suppression, including *MCAM*, down-regulated in normoxic condition, and *STEAP*, down-regulated in all the three experimental conditions. Finally, anti-tumor genes were up-regulated in JJN3 anti-Gal-1 compared to JJN3 scramble: *EGR1*, in hypoxic condition, *SPARC* in all three experimental conditions and *TGFBI* in hypoxia and, slightly, after the re-oxygenation process.

Gal-1 specific silencing reduces the pro-angiogenic properties of HMCLs

Based on the GEP analyses, we focalized our attention on the potential relationship between Gal-1 and the production of pro-angiogenic molecules by MM cells. Real-time PCR and qualitative PCR confirmed a down-regulation of *MMP9* and *CCL2* expression and an up-regulation of *SEMA3A* expression in JJN3 anti-Gal-1 compared to JJN3 scramble, both in normoxic and hypoxic conditions (**Figures 4a** and **4b**). These observations were confirmed by ELISA assay on JJN3 anti-Gal-1 CM and JJN3 scramble CM. Indeed, Gal-1 suppression significantly decreased the soluble MMP9 (P=0.025) and MCP1 proteins (P=0.022), in both normoxic and hypoxic conditions. (**Figure 4c**). Immunoprecipitation analysis on concentrated CM of JJN3 scramble and JJN3 anti-Gal-1 revealed that hypoxia reduced the protein levels of Sema3A and that the suppression of Gal-1 up-regulated Sema3A protein expression, both in normoxic and hypoxic conditions (**Figure 4d** and **4e**). Finally, the expression levels of 16 genes involved in the angiogenic process were analyzed by PCR array in JJN3 scramble compared with JJN3 anti-Gal-1, in both normoxic and hypoxic conditions. The analysis did not show significant variations of expression levels of the majority of the molecules

analyzed, but in hypoxic condition, JJN3 anti-Gal-1 displayed a significant increase of the *CXCL10* expression level, an anti-angiogenic and anti-tumor gene, consistent with the GEP analyses. Moreover, the PCR array confirmed the down-regulation of *MMP9* and *CCL2* mRNA expression. Consistent with the GEP data, we also confirmed that *VEGFA* is up-regulated in JJN3 by hypoxia treatment, but Gal-1 inhibition did not modify its expression both in normoxia and in hypoxia (**Figure 4f**).

Gal-1 depletion impairs the pro-angiogenic properties of HMCLs in *in vitro* angiogenesis assay

To elucidate the functional significance of these findings, we subsequently examined the effect of Gal-1 suppression on the ability of MM cells to mediate angiogenesis process by an *in vitro* angiogenesis assay. Consistent with the angiogenic role of Gal-1 reported in literature[132,146,168,185], we found that CM of JJN3 anti-Gal-1 significantly reduced the capacity by HUVECs to form vessels, evaluated as number of junctions, number of tubules, and total tubule length (*P*=0.000, *P*=0.003 and *P*=0.000, respectively in normoxic condition) compared with CM of JJN3 scramble (**Figure 5a** and **5b**).

Gal-1 depletion in HMCLs blocks the tumor growth in *in vivo* models and inhibits angiogenesis and bone destruction

Subsequently, we conducted a series of *in vivo* experiments in both subcutaneously and intratibial mouse models to investigate whether Gal-1 inhibition may influence tumor growth *in vivo*. NOD-SCID mice were injected subcutaneously with JJN3-anti-Gal-1 or OPM2-anti-Gal-1 and JJN3-scramble or OPM2 scramble and 3 weeks after cell inoculation, mice were sacrificed, tumors removed and measured. At this time point, all animals developed tumors that grew at the site of injection in the absence of metastases to distant sites. We observed a significant reduction in the tumor volume of mice injected with JJN3-anti-Gal-1 or OPM2-anti-Gal-1 respect to mice injected with JJN3-scramble (*P*=0.05) or OPM2 scramble (*P*=0.0055) (**Figure 6a**). **Figure 6b** shows two representative tumors removed from each mice group.

Interestingly, in the plasmacytomas removed from JJN3 anti-Gal-1 and OPM2 anti-Gal-1 mice the MVD (number of vessels positive for CD34/mm^3) was significantly reduced as compared with that obtained from the scramble control cells (JJN3 anti-Gal-1 vs. JJN3 scramble: *P*=0.002; OPM2 anti-Gal-1 vs. OPM2 scramble: *P*=0.019) (**Figure 6c**). Photos in **Figure 6d** show exemplifying CD34 immunostaining on the plasmacytomas. Moreover, to further investigate the effect of Gal-1

suppression in MM cells, NIH-III SCID mice, an intratibial mouse model, were injected with JJN3-anti-Gal-1 and JJN3 scramble and lytic lesions were allowed to develop for 4 weeks before the mice were analyzed. A significant reduction in the tumor length (*P*=0.019), thickness (*P*=0.047), width and volume size (*P*=0.028) were observed in the anti-Gal-1 group as compared to the scramble group (**Figure 7a**). Histological analysis confirmed the reduction of the tumor burden in JJN3-anti-Gal-1 as compared to JJN3-scramble (**Figure 7b**). Moreover, JJN3 anti-Gal-1 mice developed fewer and smaller lytic lesions on x-ray compared to the controls (**Figure 7c**). Finally, µQCT analysis on bone samples showed fewer osteolytic lesions in JJN3-anti-Gal-1 mice compared to JJN3 scramble mice (**Figure 7d**). Histomorphometric analyses revealed a significant higher bone volume on total volume (BV/TV as mm^3/mm^3) in mice injected with JJN3-anti-Gal-1 (median BV/TV 0.004636 ± 0.0108486 and median BV/TV 0.000500) compared to mice injected with JJN3 scramble (mean BV/TV 0.000209 ± 0.0006610 and median BV/TV 0.000000) (*P*=0.008 calculated by Mann-Whitney test).

5. DISCUSSION AND CONCLUSIONS

MM is a neoplastic disorder characterized by the clonal expansion of terminally differentiated PCs that accumulate in the BM. The clinical features of MM are osteolytic lesions, renal impairment, anemia and immunodeficiency.[4] Several studies have showed that an abnormal angiogenesis contribute to tumor progression and poor prognosis in MM patients.[39,40,42,44] Indeed, the aberrant angiogenesis represents the rationale for the development of novel therapeutic treatments with antiangiogenic property in the treatment of MM.[186] Moreover, it has been reported that hypoxia is a hallmark of the MM microenvironment and that consequently HIF-1α activation trigger the angiogenic switch and induce alterations in the malignant PCs metabolism supporting MM progression.[176]

Recent evidence shows a central role for galectins, a family of β-galactoside-binding lectins, in several processes related to cancer, including angiogenesis.[126,127,140] In particular, Gal-3 and Gal-9 can control tumor angiogenesis involving in different events in the angiogenic process.[187] Based on these data, galectins targeted therapies may offer new strategy in the treatment of MM. Indeed, experimental evidence *in vitro* and *in vivo* indicate that the protease-resistant Gal-9 inhibits MM cell growth[183] and that the N-terminally truncated form of Gal-3, Gal-3C, inhibits MM cell proliferation and result is additive to the anti-myeloma effects in association with Bortezomib.[181,182] In this regard, another member of this family, Gal-1, is expressed in a large set of solid tumor types[159,160,167,188] and promotes tumor progression by influencing cell adhesion, immunosuppression, hypoxia, angiogenesis and metastases.[128,167,185] In hematological malignancies, Gal-1 is highly present in the plasma of patients with cutaneous T-cell lymphoma and is correlated with aggressiveness in murine T-cell lymphoma model.[189] Exposure to hypoxic condition up-regulated Gal-1 expression through HIF-1α within the tumor microenvironment.[172,190] Furthermore, Croci et *al.*[146,184] showed that direct interactions of Gal-1 with complex *N*-glycans may link tumor hypoxia and angiogenesis process in models of melanoma and Kaposi's sarcoma. Currently, the role of Gal-1 in the MM pathophysiology, in the MM BM angiogenic switch and in the tumor burden is unknown.

Based on this evidence, in the present study we evaluated the role of Gal-1 in the MM BM microenvironment and its regulation by hypoxia, its role in MM cell proliferation and pro-angiogenic properties, and in tumor growth *in vivo.*

Our study first documented that Gal-1 is highly expressed by BM PCs, without significant difference between MGUS, SMM and active MM cells, assessed by Real-time PCR and Western Blot. Shaughnessy *et al*.[191] identified *LGALS1* in a signature of 70 genes that can define the high-risk MM. Accordingly, our further analysis on two independent datasets, Millennium Pharmaceutical and University of Arkansas for Medical Sciences, comprehending matching MM PCs RNA expression and patient clinical data, revealed that high expression of *LGALS1* correlated with lower overall survival. Consistent with the study on solid tumors,[171,190] we found that, in HMCLs, tumor hypoxia increases Gal-1 expression compared with normoxic condition, and that the process of re-

oxygenation restored the levels of Gal-1, at RNA and protein levels. Furthermore, the stable knock-down of HIF-1α, the master regulator of tumor cells hypoxia adaptation, by shRNA lentivirus significantly down-regulated Gal-1 expression, both in normoxic and hypoxic conditions, indicating that Gal-1 is a hypoxia and HIF-1α- induced protein in MM.

Then we evaluated the possible effect of rh-Gal-1 on three HMCLs viability. In contrast with the paper of Abroun *et al*.,[192] we did not find any significant modulation on cell viability by Gal-1 treatment in all time points either in RPMI-8226 (CD45-), XG1 (CD45RA-) and in JJN3 (CD45RO+): this could be due to the different methods of viability analysis (flow cytometry *versus* MTT assay) and different culture media. Consistent with previously reported data on Lewis lung carcinoma, melanoma and T cell lymphoma cell lines,[184] we found that also Gal-1 inhibition by stable lentiviral vector did not modify JJN3 viability and proliferation. Although we did not find a significant effect on cell proliferation and survival by Gal-1 suppression, our data revealed that Gal-1 depletion in HMCLs affects their transcriptional profile. Since several studies have showed that Gal-1 is implicated in tumor angiogenesis we focused on molecules involved in this process. GEP analyses demonstrated that Gal-1 depletion reduces the expression levels of pro-angiogenic genes, such as *CCL2*, a chemotactic protein that attracts macrophages into the tumor microenvironment[98] and *MMP9*, an enzyme highly expressed by MM cells that proteolytically degrades components of ECM and promotes tumor invasion, metastases and angiogenesis.[71] Moreover, Gal-1 depletion reduces the expression levels of several adhesion genes, including *MCAM* and *STEAP1*, and increases the expression levels of genes with anti-tumor properties, such as *EGR1*, *SPARC*, *TGFBI*, and with anti-angiogenic properties, such as *SEMA3A* and *CXCL10*, an angiostatic chemokine[193] with antiangiogenic and anti-tumor properties in MM.[194] Our results on Sema3A are in agreement with the literature reporting that the loss of endothelial Sema3A in favour of VEGF may be responsible for the angiogenic switch from MGUS to MM.[107] Interestingly, the GEP analysis did not reveal a down regulation of the strong pro-angiogenic molecule VEGFA. Supporting these findings, a functional *in vitro* angiogenesis assay showed a reduction of vessels formation capacity by HUVECs seeded with CM of HMCLs transfected with anti-Gal-1 shRNA lentivirus, in both hypoxic and normoxic conditions. Because, our study aimed at testing the potential angiogenic role of Gal-1 that could suggest its clinical employment, we inoculated HMCLs, carrying a stable infection with lentiviral vector shRNA anti-Gal-1 or carrying a stable infection with the control vector, in two *in vivo* models. In agreement with the *in vitro* data, we demonstrated a significant inhibition of the tumor growth by Gal-1 depletion, leading to a significant reduction of tumor mass. Since we did not observe a significant effect of Gal-1 suppression on cell viability and proliferation of JJN3 *in vitro*, we propose that the *in vivo* anti-MM effect was mainly due to the inhibitory effects on angiogenesis process, in keeping with our *in vitro* data showing that Gal-1 suppression reduces the pro-angiogenic properties of MM cells. The reduction of the MVD in the plasmacytomas removed from mice injected subcutaneously with JJN3-anti-Gal-1 compared to those injected with JJN3 scramble supports further that the antitumor effect

of Gal-1 suppression was mainly due to the inhibition of angiogenesis. In line with our data, it has been reported that Gal-1 expression correlates with the number of blood vessels in biopsies of several tumor types, including prostate carcinoma[195] and Kaposi's sarcoma.[146] Finally, in the intratibial mouse model we showed that Gal-1 suppression also impairs MM-induced formation of osteolytic bone lesions, suggesting its possible role in MM bone disease. On the hand this could be due to an indirect effect by reducing vascularization process and tumor growth, on the other hand to a direct effect leading the over-production of Sema3A, as shown by *in vitro* experiments. Indeed, the literature reports that the antiangiogenic molecule Sema3A exerts a strong osteoprotection effect by inhibiting osteoclast differentiation and simulating osteoblast differentiation.[196] Supporting our *in vivo* findings, Gal-1 inhibition has been shown to suppress *in vivo* angiogenesis in mice in other tumor models, such as glioblastoma.[132,197] Altogether, our data indicate that selective Gal-1 inhibition results in an anti-MM effect by suppressing angiogenesis and the development of osteolytic bone lesions, suggesting that Gal-1 is a new potential therapeutic target in MM. Our evidence is in agreement with the literature reporting that targeting Gal-1 expression leads a suppression of vascular process and growth of breast[150], Kaposi's sarcoma[146] and prostate carcinoma.[195] Thus, targeting Gal-1 could be a support to anti-VEGF therapy in MM cell that actually is ineffective, as recently reported.[198] Croci et *al.*[184] showed that Gal-1 is implicated in the resistance to the anti-VEGF therapy of different tumor by stabilizing cell-surface retention of VEGFR2 and stimulates VEGF-independent tumor angiogenesis. Supporting these findings, in the recent years, several Gal-1 inhibitors have been developed. The galactomannan of plant origin Davanat® (GM-CT-01) inhibits Gal-1 binding to a different site from the conventional galectin binding domain.[199] In colorectal carcinoma patients, GM-CT-01 completed a phase I clinical trial and, now, three phase II open label clinical trials are ongoing. The molecule OTX008, which targets Gal-1, is currently undergoing a phase I clinical trial. Effects of OTX008 in cancer cells are related to down-regulation of Gal-1 protein and modulation of the Gal-1/SEMA3A/NRP-1 system,[200] moreover has been showed that it can inhibit tumor angiogenesis and tumor growth in both melanoma and ovarian tumor models[201] that tumor treated with OTX008 showed a reduction of microvessels diameter and VEGFR2 expression.[200] Given its contribution in MM angiogenesis, the introduction of compounds that targets Gal-1 in the treatment of MM could potentiate the therapeutic effects of the current treatments.

6. REFERENCES

1. Chapman, M.A.*, et al.* Initial genome sequencing and analysis of multiple myeloma. *Nature* **471**, 467-472 (2011).
2. Podar, K.*, et al.* Vascular endothelial growth factor triggers signaling cascades mediating multiple myeloma cell growth and migration. *Blood* **98**, 428-435 (2001).
3. Mahindra, A., Hideshima, T. & Anderson, K.C. Multiple myeloma: biology of the disease. *Blood reviews* **24 Suppl 1**, S5-11 (2010).
4. Kyle, R.A. & Rajkumar, S.V. Multiple myeloma. *The New England journal of medicine* **351**, 1860-1873 (2004).
5. Barlogie, B.*, et al.* Standard chemotherapy compared with high-dose chemoradiotherapy for multiple myeloma: final results of phase III US Intergroup Trial S9321. *Journal of clinical oncology : official journal of the American Society of Clinical Oncology* **24**, 929-936 (2006).
6. Hallek, M., Bergsagel, P.L. & Anderson, K.C. Multiple myeloma: increasing evidence for a multistep transformation process. *Blood* **91**, 3-21 (1998).
7. Kyle, R.A.*, et al.* Clinical course and prognosis of smoldering (asymptomatic) multiple myeloma. *The New England journal of medicine* **356**, 2582-2590 (2007).
8. Palumbo, A. & Anderson, K. Multiple myeloma. *The New England journal of medicine* **364**, 1046-1060 (2011).
9. Bourguet, C.C., Grufferman, S., Delzell, E., DeLong, E.R. & Cohen, H.J. Multiple myeloma and family history of cancer. A case-control study. *Cancer* **56**, 2133-2139 (1985).
10. Fritschi, L. & Siemiatycki, J. Lymphoma, myeloma and occupation: results of a case-control study. *International journal of cancer. Journal international du cancer* **67**, 498-503 (1996).
11. Avet-Loiseau, H.*, et al.* Genetic abnormalities and survival in multiple myeloma: the experience of the Intergroupe Francophone du Myelome. *Blood* **109**, 3489-3495 (2007).
12. Kuehl, W.M. & Bergsagel, P.L. Multiple myeloma: evolving genetic events and host interactions. *Nature reviews. Cancer* **2**, 175-187 (2002).
13. Liu, P.*, et al.* Activating mutations of N- and K-ras in multiple myeloma show different clinical associations: analysis of the Eastern Cooperative Oncology Group Phase III Trial. *Blood* **88**, 2699-2706 (1996).
14. Bergsagel, P.L. & Kuehl, W.M. Chromosome translocations in multiple myeloma. *Oncogene* **20**, 5611-5622 (2001).
15. Dewald, G.W., Kyle, R.A., Hicks, G.A. & Greipp, P.R. The clinical significance of cytogenetic studies in 100 patients with multiple myeloma, plasma cell leukemia, or amyloidosis. *Blood* **66**, 380-390 (1985).
16. Sawyer, J.R., Waldron, J.A., Jagannath, S. & Barlogie, B. Cytogenetic findings in 200 patients with multiple myeloma. *Cancer genetics and cytogenetics* **82**, 41-49 (1995).
17. Ribatti, D., Moschetta, M. & Vacca, A. Microenvironment and multiple myeloma spread. *Thrombosis research* **133 Suppl 2**, S102-106 (2014).
18. Dankbar, B.*, et al.* Vascular endothelial growth factor and interleukin-6 in paracrine tumor-stromal cell interactions in multiple myeloma. *Blood* **95**, 2630-2636 (2000).
19. Cavo, M.*, et al.* International Myeloma Working Group consensus approach to the treatment of multiple myeloma patients who are candidates for autologous stem cell transplantation. *Blood* **117**, 6063-6073 (2011).
20. Dimopoulos, M.*, et al.* Lenalidomide plus dexamethasone for relapsed or refractory multiple myeloma. *The New England journal of medicine* **357**, 2123-2132 (2007).
21. Roodman, G.D. Pathogenesis of myeloma bone disease. *Blood cells, molecules & diseases* **32**, 290-292 (2004).
22. Melton, L.J., 3rd, Kyle, R.A., Achenbach, S.J., Oberg, A.L. & Rajkumar, S.V. Fracture risk with multiple myeloma: a population-based study. *Journal of bone and mineral research : the official journal of the American Society for Bone and Mineral Research* **20**, 487-493 (2005).
23. Kyle, R.A.*, et al.* Review of 1027 patients with newly diagnosed multiple myeloma. *Mayo Clinic proceedings* **78**, 21-33 (2003).
24. Giuliani, N., Rizzoli, V. & Roodman, G.D. Multiple myeloma bone disease: Pathophysiology of osteoblast inhibition. *Blood* **108**, 3992-3996 (2006).

25. Roodman, G.D. Pathogenesis of myeloma bone disease. *Leukemia* **23**, 435-441 (2009).
26. Boyle, W.J., Simonet, W.S. & Lacey, D.L. Osteoclast differentiation and activation. *Nature* **423**, 337-342 (2003).
27. Yaccoby, S. Advances in the understanding of myeloma bone disease and tumour growth. *British journal of haematology* **149**, 311-321 (2010).
28. Yaccoby, S.*, et al.* Myeloma interacts with the bone marrow microenvironment to induce osteoclastogenesis and is dependent on osteoclast activity. *British journal of haematology* **116**, 278-290 (2002).
29. Trouvin, A.P. & Goeb, V. Receptor activator of nuclear factor-kappaB ligand and osteoprotegerin: maintaining the balance to prevent bone loss. *Clinical interventions in aging* **5**, 345-354 (2010).
30. Roodman, G.D. Targeting the bone microenvironment in multiple myeloma. *Journal of bone and mineral metabolism* **28**, 244-250 (2010).
31. Pearse, R.N.*, et al.* Multiple myeloma disrupts the TRANCE/ osteoprotegerin cytokine axis to trigger bone destruction and promote tumor progression. *Proceedings of the National Academy of Sciences of the United States of America* **98**, 11581-11586 (2001).
32. Giuliani, N.*, et al.* Myeloma cells block RUNX2/CBFA1 activity in human bone marrow osteoblast progenitors and inhibit osteoblast formation and differentiation. *Blood* **106**, 2472-2483 (2005).
33. Bolzoni, M.*, et al.* Myeloma cells inhibit non-canonical wnt co-receptor ror2 expression in human bone marrow osteoprogenitor cells: effect of wnt5a/ror2 pathway activation on the osteogenic differentiation impairment induced by myeloma cells. *Leukemia* **27**, 451-463 (2013).
34. Carmeliet, P. Angiogenesis in health and disease. *Nature medicine* **9**, 653-660 (2003).
35. Potente, M., Gerhardt, H. & Carmeliet, P. Basic and therapeutic aspects of angiogenesis. *Cell* **146**, 873-887 (2011).
36. Folkman, J. Angiogenesis: an organizing principle for drug discovery? *Nature reviews. Drug discovery* **6**, 273-286 (2007).
37. Folkman, J. Tumor angiogenesis: therapeutic implications. *The New England journal of medicine* **285**, 1182-1186 (1971).
38. Munshi, N.C. & Wilson, C. Increased bone marrow microvessel density in newly diagnosed multiple myeloma carries a poor prognosis. *Seminars in oncology* **28**, 565-569 (2001).
39. Sezer, O.*, et al.* Bone marrow microvessel density is a prognostic factor for survival in patients with multiple myeloma. *Annals of hematology* **79**, 574-577 (2000).
40. Vacca, A.*, et al.* Bone marrow neovascularization, plasma cell angiogenic potential, and matrix metalloproteinase-2 secretion parallel progression of human multiple myeloma. *Blood* **93**, 3064-3073 (1999).
41. Vacca, A.*, et al.* Bone marrow of patients with active multiple myeloma: angiogenesis and plasma cell adhesion molecules LFA-1, VLA-4, LAM-1, and CD44. *American journal of hematology* **50**, 9-14 (1995).
42. Vacca, A. & Ribatti, D. Bone marrow angiogenesis in multiple myeloma. *Leukemia* **20**, 193-199 (2006).
43. Rajkumar, S.V. & Greipp, P.R. Angiogenesis in multiple myeloma. *British journal of haematology* **113**, 565 (2001).
44. Rajkumar, S.V.*, et al.* Prognostic value of bone marrow angiogenesis in multiple myeloma. *Clinical cancer research : an official journal of the American Association for Cancer Research* **6**, 3111-3116 (2000).
45. Rajkumar, S.V.*, et al.* Bone marrow angiogenesis in 400 patients with monoclonal gammopathy of undetermined significance, multiple myeloma, and primary amyloidosis. *Clinical cancer research : an official journal of the American Association for Cancer Research* **8**, 2210-2216 (2002).
46. Dominici, M.*, et al.* Angiogenesis in multiple myeloma: correlation between in vitro endothelial colonies growth (CFU-En) and clinical-biological features. *Leukemia* **15**, 171-176 (2001).
47. Giuliani, N.*, et al.* Proangiogenic properties of human myeloma cells: production of angiopoietin-1 and its potential relationship to myeloma-induced angiogenesis. *Blood* **102**, 638-645 (2003).

48. Cibeira, M.T.*, et al.* Bone marrow angiogenesis and angiogenic factors in multiple myeloma treated with novel agents. *Cytokine* **41**, 244-253 (2008).
49. Sezer, O.*, et al.* Relationship between bone marrow angiogenesis and plasma cell infiltration and serum beta2-microglobulin levels in patients with multiple myeloma. *Annals of hematology* **80**, 598-601 (2001).
50. Neufeld, G., Cohen, T., Gengrinovitch, S. & Poltorak, Z. Vascular endothelial growth factor (VEGF) and its receptors. *FASEB journal : official publication of the Federation of American Societies for Experimental Biology* **13**, 9-22 (1999).
51. Giuliani, N., Colla, S. & Rizzoli, V. Angiogenic switch in multiple myeloma. *Hematology* **9**, 377-381 (2004).
52. Giuliani, N., Storti, P., Bolzoni, M., Palma, B.D. & Bonomini, S. Angiogenesis and multiple myeloma. *Cancer microenvironment : official journal of the International Cancer Microenvironment Society* **4**, 325-337 (2011).
53. Wang, X., Zhang, Z. & Yao, C. Angiogenic activity of mesenchymal stem cells in multiple myeloma. *Cancer investigation* **29**, 37-41 (2011).
54. Kumar, S.*, et al.* Expression of VEGF and its receptors by myeloma cells. *Leukemia* **17**, 2025-2031 (2003).
55. Bellamy, W.T. Expression of vascular endothelial growth factor and its receptors in multiple myeloma and other hematopoietic malignancies. *Seminars in oncology* **28**, 551-559 (2001).
56. Bergers, G. & Hanahan, D. Modes of resistance to anti-angiogenic therapy. *Nature reviews. Cancer* **8**, 592-603 (2008).
57. Ebos, J.M. & Kerbel, R.S. Antiangiogenic therapy: impact on invasion, disease progression, and metastasis. *Nature reviews. Clinical oncology* **8**, 210-221 (2011).
58. Ferrara, N. Pathways mediating VEGF-independent tumor angiogenesis. *Cytokine & growth factor reviews* **21**, 21-26 (2010).
59. Carmeliet, P. & Jain, R.K. Angiogenesis in cancer and other diseases. *Nature* **407**, 249-257 (2000).
60. Bisping, G.*, et al.* Paracrine interactions of basic fibroblast growth factor and interleukin-6 in multiple myeloma. *Blood* **101**, 2775-2783 (2003).
61. Colla, S.*, et al.* Do human myeloma cells directly produce basic FGF? *Blood* **102**, 3071-3072; author reply 3072-3073 (2003).
62. Kwak, H.J., So, J.N., Lee, S.J., Kim, I. & Koh, G.Y. Angiopoietin-1 is an apoptosis survival factor for endothelial cells. *FEBS letters* **448**, 249-253 (1999).
63. Hayes, A.J.*, et al.* Angiopoietin-1 and its receptor Tie-2 participate in the regulation of capillary-like tubule formation and survival of endothelial cells. *Microvascular research* **58**, 224-237 (1999).
64. Tsigkos, S., Koutsilieris, M. & Papapetropoulos, A. Angiopoietins in angiogenesis and beyond. *Expert opinion on investigational drugs* **12**, 933-941 (2003).
65. Nakayama, T., Yao, L. & Tosato, G. Mast cell-derived angiopoietin-1 plays a critical role in the growth of plasma cell tumors. *The Journal of clinical investigation* **114**, 1317-1325 (2004).
66. Albini, A. & Noonan, D.M. Angiopoietin2 and tie2: tied to lymphangiogenesis and lung metastasis. New perspectives in antimetastatic antiangiogenic therapy. *Journal of the National Cancer Institute* **104**, 429-431 (2012).
67. Vacca, A.*, et al.* Endothelial cells in the bone marrow of patients with multiple myeloma. *Blood* **102**, 3340-3348 (2003).
68. Terpos, E.*, et al.* Circulating angiopoietin-1 to angiopoietin-2 ratio is an independent prognostic factor for survival in newly diagnosed patients with multiple myeloma who received therapy with novel antimyeloma agents. *International journal of cancer. Journal international du cancer* **130**, 735-742 (2012).
69. Holash, J., Wiegand, S.J. & Yancopoulos, G.D. New model of tumor angiogenesis: dynamic balance between vessel regression and growth mediated by angiopoietins and VEGF. *Oncogene* **18**, 5356-5362 (1999).
70. Plank, M.J., Sleeman, B.D. & Jones, P.F. The role of the angiopoietins in tumour angiogenesis. *Growth factors* **22**, 1-11 (2004).

71. Barille, S.*, et al.* Metalloproteinases in multiple myeloma: production of matrix metalloproteinase-9 (MMP-9), activation of proMMP-2, and induction of MMP-1 by myeloma cells. *Blood* **90**, 1649-1655 (1997).
72. Rundhaug, J.E. Matrix metalloproteinases and angiogenesis. *Journal of cellular and molecular medicine* **9**, 267-285 (2005).
73. Van Valckenborgh, E.*, et al.* Upregulation of matrix metalloproteinase-9 in murine 5T33 multiple myeloma cells by interaction with bone marrow endothelial cells. *International journal of cancer. Journal international du cancer* **101**, 512-518 (2002).
74. Van Valckenborgh, E.*, et al.* Multifunctional role of matrix metalloproteinases in multiple myeloma: a study in the 5T2MM mouse model. *The American journal of pathology* **165**, 869-878 (2004).
75. Vacca, A., Ribatti, D., Roccaro, A.M., Frigeri, A. & Dammacco, F. Bone marrow angiogenesis in patients with active multiple myeloma. *Seminars in oncology* **28**, 543-550 (2001).
76. Borset, M., Hjorth-Hansen, H., Seidel, C., Sundan, A. & Waage, A. Hepatocyte growth factor and its receptor c-met in multiple myeloma. *Blood* **88**, 3998-4004 (1996).
77. Galimi, F., Brizzi, M.F. & Comoglio, P.M. The hepatocyte growth factor and its receptor. *Stem cells* **11 Suppl 2**, 22-30 (1993).
78. Seidel, C.*, et al.* High levels of soluble syndecan-1 in myeloma-derived bone marrow: modulation of hepatocyte growth factor activity. *Blood* **96**, 3139-3146 (2000).
79. Derksen, P.W.*, et al.* Cell surface proteoglycan syndecan-1 mediates hepatocyte growth factor binding and promotes Met signaling in multiple myeloma. *Blood* **99**, 1405-1410 (2002).
80. Zhang, Y.*, et al.* Targeting of heparanase-modified syndecan-1 by prosecretory mitogen lacritin requires conserved core GAGAL plus heparan and chondroitin sulfate as a novel hybrid binding site that enhances selectivity. *The Journal of biological chemistry* **288**, 12090-12101 (2013).
81. Choi, S.*, et al.* Transmembrane domain-induced oligomerization is crucial for the functions of syndecan-2 and syndecan-4. *The Journal of biological chemistry* **280**, 42573-42579 (2005).
82. Yang, Y.*, et al.* Heparanase enhances syndecan-1 shedding: a novel mechanism for stimulation of tumor growth and metastasis. *The Journal of biological chemistry* **282**, 13326-13333 (2007).
83. Ramani, V.C., Yang, Y., Ren, Y., Nan, L. & Sanderson, R.D. Heparanase plays a dual role in driving hepatocyte growth factor (HGF) signaling by enhancing HGF expression and activity. *The Journal of biological chemistry* **286**, 6490-6499 (2011).
84. Anderson, K.C. & Carrasco, R.D. Pathogenesis of myeloma. *Annual review of pathology* **6**, 249-274 (2011).
85. Motro, B., Itin, A., Sachs, L. & Keshet, E. Pattern of interleukin 6 gene expression in vivo suggests a role for this cytokine in angiogenesis. *Proceedings of the National Academy of Sciences of the United States of America* **87**, 3092-3096 (1990).
86. Belperio, J.A.*, et al.* CXC chemokines in angiogenesis. *Journal of leukocyte biology* **68**, 1-8 (2000).
87. Kline, M.*, et al.* Cytokine and chemokine profiles in multiple myeloma; significance of stromal interaction and correlation of IL-8 production with disease progression. *Leukemia research* **31**, 591-598 (2007).
88. Munshi, N.C.*, et al.* Identification of genes modulated in multiple myeloma using genetically identical twin samples. *Blood* **103**, 1799-1806 (2004).
89. Brat, D.J., Bellail, A.C. & Van Meir, E.G. The role of interleukin-8 and its receptors in gliomagenesis and tumoral angiogenesis. *Neuro-oncology* **7**, 122-133 (2005).
90. Senger, D.R.*, et al.* Stimulation of endothelial cell migration by vascular permeability factor/vascular endothelial growth factor through cooperative mechanisms involving the alphavbeta3 integrin, osteopontin, and thrombin. *The American journal of pathology* **149**, 293-305 (1996).
91. Liaw, L., Almeida, M., Hart, C.E., Schwartz, S.M. & Giachelli, C.M. Osteopontin promotes vascular cell adhesion and spreading and is chemotactic for smooth muscle cells in vitro. *Circulation research* **74**, 214-224 (1994).

92. Colla, S.*, et al.* Human myeloma cells express the bone regulating gene Runx2/Cbfa1 and produce osteopontin that is involved in angiogenesis in multiple myeloma patients. *Leukemia* **19**, 2166-2176 (2005).
93. Takahashi, F.*, et al.* Osteopontin induces angiogenesis of murine neuroblastoma cells in mice. *International journal of cancer. Journal international du cancer* **98**, 707-712 (2002).
94. Hirama, M.*, et al.* Osteopontin overproduced by tumor cells acts as a potent angiogenic factor contributing to tumor growth. *Cancer letters* **198**, 107-117 (2003).
95. Philip, S., Bulbule, A. & Kundu, G.C. Osteopontin stimulates tumor growth and activation of promatrix metalloproteinase-2 through nuclear factor-kappa B-mediated induction of membrane type 1 matrix metalloproteinase in murine melanoma cells. *The Journal of biological chemistry* **276**, 44926-44935 (2001).
96. Asou, Y.*, et al.* Osteopontin facilitates angiogenesis, accumulation of osteoclasts, and resorption in ectopic bone. *Endocrinology* **142**, 1325-1332 (2001).
97. Lazennec, G. & Richmond, A. Chemokines and chemokine receptors: new insights into cancer-related inflammation. *Trends in molecular medicine* **16**, 133-144 (2010).
98. Chen, Q.*, et al.* Monocyte chemotactic protein-1 promotes the proliferation and invasion of osteosarcoma cells and upregulates the expression of AKT. *Molecular medicine reports* **12**, 219-225 (2015).
99. Wu, M.H.*, et al.* Targeting galectin-1 in carcinoma-associated fibroblasts inhibits oral squamous cell carcinoma metastasis by downregulating MCP-1/CCL2 expression. *Clinical cancer research : an official journal of the American Association for Cancer Research* **17**, 1306-1316 (2011).
100. Stamatovic, S.M., Keep, R.F., Mostarica-Stojkovic, M. & Andjelkovic, A.V. CCL2 regulates angiogenesis via activation of Ets-1 transcription factor. *Journal of immunology* **177**, 2651-2661 (2006).
101. Bonapace, L.*, et al.* Cessation of CCL2 inhibition accelerates breast cancer metastasis by promoting angiogenesis. *Nature* **515**, 130-133 (2014).
102. Visse, R. & Nagase, H. Matrix metalloproteinases and tissue inhibitors of metalloproteinases: structure, function, and biochemistry. *Circulation research* **92**, 827-839 (2003).
103. Yu, W.*, et al.* Inhibition of pathological retinal neovascularization by semaphorin 3A. *Molecular vision* **19**, 1397-1405 (2013).
104. Casazza, A.*, et al.* Systemic and targeted delivery of semaphorin 3A inhibits tumor angiogenesis and progression in mouse tumor models. *Arteriosclerosis, thrombosis, and vascular biology* **31**, 741-749 (2011).
105. Plein, A., Fantin, A. & Ruhrberg, C. Neuropilin regulation of angiogenesis, arteriogenesis, and vascular permeability. *Microcirculation* **21**, 315-323 (2014).
106. Miao, H.Q.*, et al.* Neuropilin-1 mediates collapsin-1/semaphorin III inhibition of endothelial cell motility: functional competition of collapsin-1 and vascular endothelial growth factor-165. *The Journal of cell biology* **146**, 233-242 (1999).
107. Vacca, A.*, et al.* Loss of inhibitory semaphorin 3A (SEMA3A) autocrine loops in bone marrow endothelial cells of patients with multiple myeloma. *Blood* **108**, 1661-1667 (2006).
108. Brahimi-Horn, M.C., Chiche, J. & Pouyssegur, J. Hypoxia and cancer. *Journal of molecular medicine* **85**, 1301-1307 (2007).
109. Liao, D. & Johnson, R.S. Hypoxia: a key regulator of angiogenesis in cancer. *Cancer metastasis reviews* **26**, 281-290 (2007).
110. Hickey, M.M. & Simon, M.C. Regulation of angiogenesis by hypoxia and hypoxia-inducible factors. *Current topics in developmental biology* **76**, 217-257 (2006).
111. Zhong, H.*, et al.* Overexpression of hypoxia-inducible factor 1alpha in common human cancers and their metastases. *Cancer research* **59**, 5830-5835 (1999).
112. Semenza, G.L. Oxygen homeostasis. *Wiley interdisciplinary reviews. Systems biology and medicine* **2**, 336-361 (2010).
113. Semenza, G.L. Targeting HIF-1 for cancer therapy. *Nature reviews. Cancer* **3**, 721-732 (2003).
114. Martin, S.K., Diamond, P., Gronthos, S., Peet, D.J. & Zannettino, A.C. The emerging role of hypoxia, HIF-1 and HIF-2 in multiple myeloma. *Leukemia* **25**, 1533-1542 (2011).

115. Semenza, G.L. Hypoxia-inducible factor 1 (HIF-1) pathway. *Science's STKE : signal transduction knowledge environment* **2007**, cm8 (2007).
116. Song, L.P.*, et al.* Hypoxia-inducible factor-1alpha-induced differentiation of myeloid leukemic cells is its transcriptional activity independent. *Oncogene* **27**, 519-527 (2008).
117. Wenger, R.H., Stiehl, D.P. & Camenisch, G. Integration of oxygen signaling at the consensus HRE. *Science's STKE : signal transduction knowledge environment* **2005**, re12 (2005).
118. Ryan, H.E., Lo, J. & Johnson, R.S. HIF-1 alpha is required for solid tumor formation and embryonic vascularization. *The EMBO journal* **17**, 3005-3015 (1998).
119. Ravi, R.*, et al.* Regulation of tumor angiogenesis by p53-induced degradation of hypoxia-inducible factor 1alpha. *Genes & development* **14**, 34-44 (2000).
120. Liao, D., Corle, C., Seagroves, T.N. & Johnson, R.S. Hypoxia-inducible factor-1alpha is a key regulator of metastasis in a transgenic model of cancer initiation and progression. *Cancer research* **67**, 563-572 (2007).
121. Borsi, E.*, et al.* HIF-1alpha inhibition blocks the cross talk between multiple myeloma plasma cells and tumor microenvironment. *Experimental cell research* **328**, 444-455 (2014).
122. Rankin, E.B. & Giaccia, A.J. The role of hypoxia-inducible factors in tumorigenesis. *Cell death and differentiation* **15**, 678-685 (2008).
123. Asosingh, K.*, et al.* Role of the hypoxic bone marrow microenvironment in 5T2MM murine myeloma tumor progression. *Haematologica* **90**, 810-817 (2005).
124. Colla, S.*, et al.* Low bone marrow oxygen tension and hypoxia-inducible factor-1alpha overexpression characterize patients with multiple myeloma: role on the transcriptional and proangiogenic profiles of CD138(+) cells. *Leukemia* **24**, 1967-1970 (2010).
125. Colla, S.*, et al.* The new tumor-suppressor gene inhibitor of growth family member 4 (ING4) regulates the production of proangiogenic molecules by myeloma cells and suppresses hypoxia-inducible factor-1 alpha (HIF-1alpha) activity: involvement in myeloma-induced angiogenesis. *Blood* **110**, 4464-4475 (2007).
126. Barondes, S.H.*, et al.* Galectins: a family of animal beta-galactoside-binding lectins. *Cell* **76**, 597-598 (1994).
127. Barondes, S.H., Cooper, D.N., Gitt, M.A. & Leffler, H. Galectins. Structure and function of a large family of animal lectins. *The Journal of biological chemistry* **269**, 20807-20810 (1994).
128. Ito, K.*, et al.* Galectin-1 as a potent target for cancer therapy: role in the tumor microenvironment. *Cancer metastasis reviews* **31**, 763-778 (2012).
129. Hirabayashi, J.*, et al.* Oligosaccharide specificity of galectins: a search by frontal affinity chromatography. *Biochimica et biophysica acta* **1572**, 232-254 (2002).
130. Wells, V. & Mallucci, L. Identification of an autocrine negative growth factor: mouse beta-galactoside-binding protein is a cytostatic factor and cell growth regulator. *Cell* **64**, 91-97 (1991).
131. Matarrese, P.*, et al.* Galectin-1 sensitizes resting human T lymphocytes to Fas (CD95)-mediated cell death via mitochondrial hyperpolarization, budding, and fission. *The Journal of biological chemistry* **280**, 6969-6985 (2005).
132. Thijssen, V.L.*, et al.* Galectin-1 is essential in tumor angiogenesis and is a target for antiangiogenesis therapy. *Proceedings of the National Academy of Sciences of the United States of America* **103**, 15975-15980 (2006).
133. de la Fuente, H., Cibrian, D. & Sanchez-Madrid, F. Immunoregulatory molecules are master regulators of inflammation during the immune response. *FEBS letters* **586**, 2897-2905 (2012).
134. Moiseeva, E.P., Javed, Q., Spring, E.L. & de Bono, D.P. Galectin 1 is involved in vascular smooth muscle cell proliferation. *Cardiovascular research* **45**, 493-502 (2000).
135. Moiseeva, E.P., Spring, E.L., Baron, J.H. & de Bono, D.P. Galectin 1 modulates attachment, spreading and migration of cultured vascular smooth muscle cells via interactions with cellular receptors and components of extracellular matrix. *Journal of vascular research* **36**, 47-58 (1999).
136. Rabinovich, G.A. & Toscano, M.A. Turning 'sweet' on immunity: galectin-glycan interactions in immune tolerance and inflammation. *Nature reviews. Immunology* **9**, 338-352 (2009).
137. Camby, I., Le Mercier, M., Lefranc, F. & Kiss, R. Galectin-1: a small protein with major functions. *Glycobiology* **16**, 137R-157R (2006).

138. Astorgues-Xerri, L.*, et al.* Unraveling galectin-1 as a novel therapeutic target for cancer. *Cancer treatment reviews* **40**, 307-319 (2014).
139. Thijssen, V.L., Heusschen, R., Caers, J. & Griffioen, A.W. Galectin expression in cancer diagnosis and prognosis: A systematic review. *Biochimica et biophysica acta* **1855**, 235-247 (2015).
140. Thijssen, V.L., Poirier, F., Baum, L.G. & Griffioen, A.W. Galectins in the tumor endothelium: opportunities for combined cancer therapy. *Blood* **110**, 2819-2827 (2007).
141. Cho, M. & Cummings, R.D. Galectin-1, a beta-galactoside-binding lectin in Chinese hamster ovary cells. II. Localization and biosynthesis. *The Journal of biological chemistry* **270**, 5207-5212 (1995).
142. Hirabayashi, J. & Kasai, K. Effect of amino acid substitution by sited-directed mutagenesis on the carbohydrate recognition and stability of human 14-kDa beta-galactoside-binding lectin. *The Journal of biological chemistry* **266**, 23648-23653 (1991).
143. Moutsatsos, I.K., Wade, M., Schindler, M. & Wang, J.L. Endogenous lectins from cultured cells: nuclear localization of carbohydrate-binding protein 35 in proliferating 3T3 fibroblasts. *Proceedings of the National Academy of Sciences of the United States of America* **84**, 6452-6456 (1987).
144. Thijssen, V.L., Hulsmans, S. & Griffioen, A.W. The galectin profile of the endothelium: altered expression and localization in activated and tumor endothelial cells. *The American journal of pathology* **172**, 545-553 (2008).
145. Sanjuan, X.*, et al.* Differential expression of galectin 3 and galectin 1 in colorectal cancer progression. *Gastroenterology* **113**, 1906-1915 (1997).
146. Croci, D.O.*, et al.* Disrupting galectin-1 interactions with N-glycans suppresses hypoxia-driven angiogenesis and tumorigenesis in Kaposi's sarcoma. *The Journal of experimental medicine* **209**, 1985-2000 (2012).
147. Ellis, L.M. The role of neuropilins in cancer. *Molecular cancer therapeutics* **5**, 1099-1107 (2006).
148. Guttmann-Raviv, N.*, et al.* The neuropilins and their role in tumorigenesis and tumor progression. *Cancer letters* **231**, 1-11 (2006).
149. Hsieh, S.H.*, et al.* Galectin-1, a novel ligand of neuropilin-1, activates VEGFR-2 signaling and modulates the migration of vascular endothelial cells. *Oncogene* **27**, 3746-3753 (2008).
150. Dalotto-Moreno, T.*, et al.* Targeting galectin-1 overcomes breast cancer-associated immunosuppression and prevents metastatic disease. *Cancer research* **73**, 1107-1117 (2013).
151. Rorive, S.*, et al.* Galectin-1 is highly expressed in human gliomas with relevance for modulation of invasion of tumor astrocytes into the brain parenchyma. *Glia* **33**, 241-255 (2001).
152. Saussez, S., Camby, I., Toubeau, G. & Kiss, R. Galectins as modulators of tumor progression in head and neck squamous cell carcinomas. *Head & neck* **29**, 874-884 (2007).
153. Paz, A., Haklai, R., Elad-Sfadia, G., Ballan, E. & Kloog, Y. Galectin-1 binds oncogenic H-Ras to mediate Ras membrane anchorage and cell transformation. *Oncogene* **20**, 7486-7493 (2001).
154. Thijssen, V.L.*, et al.* Tumor cells secrete galectin-1 to enhance endothelial cell activity. *Cancer research* **70**, 6216-6224 (2010).
155. Jung, T.Y.*, et al.* Role of galectin-1 in migration and invasion of human glioblastoma multiforme cell lines. *Journal of neurosurgery* **109**, 273-284 (2008).
156. Camby, I.*, et al.* Galectin-1 modulates human glioblastoma cell migration into the brain through modifications to the actin cytoskeleton and levels of expression of small GTPases. *Journal of neuropathology and experimental neurology* **61**, 585-596 (2002).
157. Salatino, M.*, et al.* Galectin-1 as a potential therapeutic target in autoimmune disorders and cancer. *Expert opinion on biological therapy* **8**, 45-57 (2008).
158. van den Brule, F.*, et al.* Galectin-1 accumulation in the ovary carcinoma peritumoral stroma is induced by ovary carcinoma cells and affects both cancer cell proliferation and adhesion to laminin-1 and fibronectin. *Laboratory investigation; a journal of technical methods and pathology* **83**, 377-386 (2003).

159. Ellerhorst, J., Troncoso, P., Xu, X.C., Lee, J. & Lotan, R. Galectin-1 and galectin-3 expression in human prostate tissue and prostate cancer. *Urological research* **27**, 362-367 (1999).
160. Tinari, N.*, et al.* Glycoprotein 90K/MAC-2BP interacts with galectin-1 and mediates galectin-1-induced cell aggregation. *International journal of cancer. Journal international du cancer* **91**, 167-172 (2001).
161. Harvey, S., Zhang, Y., Landry, F., Miller, C. & Smith, J.W. Insights into a plasma membrane signature. *Physiological genomics* **5**, 129-136 (2001).
162. Kim, H.J.*, et al.* Galectin 1 expression is associated with tumor invasion and metastasis in stage IB to IIA cervical cancer. *Human pathology* **44**, 62-68 (2013).
163. Nagy, N.*, et al.* Refined prognostic evaluation in colon carcinoma using immunohistochemical galectin fingerprinting. *Cancer* **97**, 1849-1858 (2003).
164. Langbein, S.*, et al.* Gene-expression signature of adhesion/growth-regulatory tissue lectins (galectins) in transitional cell cancer and its prognostic relevance. *Histopathology* **51**, 681-690 (2007).
165. Watanabe, M.*, et al.* Clinical significance of circulating galectins as colorectal cancer markers. *Oncology reports* **25**, 1217-1226 (2011).
166. Saussez, S.*, et al.* The determination of the levels of circulating galectin-1 and -3 in HNSCC patients could be used to monitor tumor progression and/or responses to therapy. *Oral oncology* **44**, 86-93 (2008).
167. Bacigalupo, M.L.*, et al.* Galectin-1 triggers epithelial-mesenchymal transition in human hepatocellular carcinoma cells. *Journal of cellular physiology* **230**, 1298-1309 (2015).
168. Le Mercier, M.*, et al.* Knocking down galectin 1 in human hs683 glioblastoma cells impairs both angiogenesis and endoplasmic reticulum stress responses. *Journal of neuropathology and experimental neurology* **67**, 456-469 (2008).
169. Rabinovich, G.A.*, et al.* Synthetic lactulose amines: novel class of anticancer agents that induce tumor-cell apoptosis and inhibit galectin-mediated homotypic cell aggregation and endothelial cell morphogenesis. *Glycobiology* **16**, 210-220 (2006).
170. Hughes, A.E.*, et al.* Mutations in TNFRSF11A, affecting the signal peptide of RANK, cause familial expansile osteolysis. *Nature genetics* **24**, 45-48 (2000).
171. Le, Q.T.*, et al.* Galectin-1: a link between tumor hypoxia and tumor immune privilege. *Journal of clinical oncology : official journal of the American Society of Clinical Oncology* **23**, 8932-8941 (2005).
172. Zhao, X.Y.*, et al.* Hypoxia inducible factor-1 mediates expression of galectin-1: the potential role in migration/invasion of colorectal cancer cells. *Carcinogenesis* **31**, 1367-1375 (2010).
173. Agnelli, L.*, et al.* A SNP microarray and FISH-based procedure to detect allelic imbalances in multiple myeloma: an integrated genomics approach reveals a wide gene dosage effect. *Genes, chromosomes & cancer* **48**, 603-614 (2009).
174. Lombardi, L.*, et al.* Molecular characterization of human multiple myeloma cell lines by integrative genomics: insights into the biology of the disease. *Genes, chromosomes & cancer* **46**, 226-238 (2007).
175. Goeman, J.J. & le Cessie, S. A goodness-of-fit test for multinomial logistic regression. *Biometrics* **62**, 980-985 (2006).
176. Storti, P.*, et al.* Hypoxia-inducible factor (HIF)-1alpha suppression in myeloma cells blocks tumoral growth in vivo inhibiting angiogenesis and bone destruction. *Leukemia* **27**, 1697-1706 (2013).
177. Schadt, E.E., Li, C., Ellis, B. & Wong, W.H. Feature extraction and normalization algorithms for high-density oligonucleotide gene expression array data. *Journal of cellular biochemistry. Supplement* **Suppl 37**, 120-125 (2001).
178. Mattioli, M.*, et al.* Gene expression profiling of plasma cell dyscrasias reveals molecular patterns associated with distinct IGH translocations in multiple myeloma. *Oncogene* **24**, 2461-2473 (2005).
179. Storti, P.*, et al.* HOXB7 expression by myeloma cells regulates their pro-angiogenic properties in multiple myeloma patients. *Leukemia* **25**, 527-537 (2011).
180. D'Souza, S.*, et al.* Gfi1 expressed in bone marrow stromal cells is a novel osteoblast suppressor in patients with multiple myeloma bone disease. *Blood* **118**, 6871-6880 (2011).

181. Streetly, M.J.*, et al.* GCS-100, a novel galectin-3 antagonist, modulates MCL-1, NOXA, and cell cycle to induce myeloma cell death. *Blood* **115**, 3939-3948 (2010).
182. Mirandola, L.*, et al.* Galectin-3C inhibits tumor growth and increases the anticancer activity of bortezomib in a murine model of human multiple myeloma. *PloS one* **6**, e21811 (2011).
183. Kobayashi, T.*, et al.* Galectin-9 exhibits anti-myeloma activity through JNK and p38 MAP kinase pathways. *Leukemia* **24**, 843-850 (2010).
184. Croci, D.O.*, et al.* Glycosylation-dependent lectin-receptor interactions preserve angiogenesis in anti-VEGF refractory tumors. *Cell* **156**, 744-758 (2014).
185. Clausse, N., van den Brule, F., Waltregny, D., Garnier, F. & Castronovo, V. Galectin-1 expression in prostate tumor-associated capillary endothelial cells is increased by prostate carcinoma cells and modulates heterotypic cell-cell adhesion. *Angiogenesis* **3**, 317-325 (1999).
186. Ribatti, D., Nico, B. & Vacca, A. Importance of the bone marrow microenvironment in inducing the angiogenic response in multiple myeloma. *Oncogene* **25**, 4257-4266 (2006).
187. Andre, S.*, et al.* Galectins-1 and -3 and their ligands in tumor biology. Non-uniform properties in cell-surface presentation and modulation of adhesion to matrix glycoproteins for various tumor cell lines, in biodistribution of free and liposome-bound galectins and in their expression by breast and colorectal carcinomas with/without metastatic propensity. *Journal of cancer research and clinical oncology* **125**, 461-474 (1999).
188. Demydenko, D. & Berest, I. Expression of galectin-1 in malignant tumors. *Experimental oncology* **31**, 74-79 (2009).
189. Cedeno-Laurent, F.*, et al.* Galectin-1 inhibits the viability, proliferation, and Th1 cytokine production of nonmalignant T cells in patients with leukemic cutaneous T-cell lymphoma. *Blood* **119**, 3534-3538 (2012).
190. White, N.M.*, et al.* Galectin-1 has potential prognostic significance and is implicated in clear cell renal cell carcinoma progression through the HIF/mTOR signaling axis. *British journal of cancer* **110**, 1250-1259 (2014).
191. Shaughnessy, J.D., Jr.*, et al.* A validated gene expression model of high-risk multiple myeloma is defined by deregulated expression of genes mapping to chromosome 1. *Blood* **109**, 2276-2284 (2007).
192. Abroun, S.*, et al.* Galectin-1 supports the survival of CD45RA(-) primary myeloma cells in vitro. *British journal of haematology* **142**, 754-765 (2008).
193. Keeley, E.C., Mehrad, B. & Strieter, R.M. Chemokines as mediators of neovascularization. *Arteriosclerosis, thrombosis, and vascular biology* **28**, 1928-1936 (2008).
194. Barash, U.*, et al.* Heparanase enhances myeloma progression via CXCL10 downregulation. *Leukemia* **28**, 2178-2187 (2014).
195. Laderach, D.J.*, et al.* A unique galectin signature in human prostate cancer progression suggests galectin-1 as a key target for treatment of advanced disease. *Cancer research* **73**, 86-96 (2013).
196. Hayashi, M.*, et al.* Osteoprotection by semaphorin 3A. *Nature* **485**, 69-74 (2012).
197. Le Mercier, M., Fortin, S., Mathieu, V., Kiss, R. & Lefranc, F. Galectins and gliomas. *Brain pathology* **20**, 17-27 (2010).
198. White, D.*, et al.* Results from AMBER, a randomized phase 2 study of bevacizumab and bortezomib versus bortezomib in relapsed or refractory multiple myeloma. *Cancer* **119**, 339-347 (2013).
199. Miller, M.C., Klyosov, A. & Mayo, K.H. The alpha-galactomannan Davanat binds galectin-1 at a site different from the conventional galectin carbohydrate binding domain. *Glycobiology* **19**, 1034-1045 (2009).
200. Astorgues-Xerri, L.*, et al.* OTX008, a selective small-molecule inhibitor of galectin-1, downregulates cancer cell proliferation, invasion and tumour angiogenesis. *European journal of cancer* **50**, 2463-2477 (2014).
201. Zucchetti, M.*, et al.* Pharmacokinetics and antineoplastic activity of galectin-1-targeting OTX008 in combination with sunitinib. *Cancer chemotherapy and pharmacology* **72**, 879-887 (2013).

7. LEGENDS OF FIGURES

Figure 1: Expression of Gal-1 in MM patients and HMCLs.

(a) The expression of *LGALS1* mRNA and Gal-1 protein was evaluated respectively by Real-time PCR and Western Blot both in 8 freshly purified BM CD138+ from newly diagnosed MM patients (positive control: PC3 cell line) and **(b)** in 6 HMCLs. **(c)** Gal-1 protein was evaluated by immunohistochemistry in fixed bone biopsies obtained from 23 MM, 9 SMM and 10 MGUS patients. The photos show Gal-1 protein immunostaining on osteomedullary biopsies of three representative MM patients, one SMM patient and one MGUS patient is reported. (positive control: colorectal cancer).

Figure 2: Effect of hypoxia and HIF-1α inhibition on Gal-1 expression

(a) JJN3 and OPM2 cells were incubated at 1%O_2 for 48h, followed by 48 h at 20% O_2, and *LGALS1* mRNA and **(b)** Gal-1 protein expressions were evaluated by Real-time PCR and Western Blot, respectively**.** Graph represents mean fold change (± Standard Deviation, S.D.) calculated assuming JJN3 normoxia and OPM2 normoxia as control condition of 3 independent experiments in duplicate. (*P* calculated by two tail Student's t test) **(c)** Protein bands were calculated and normalized by β-actin using ImageJ software**. (d)** Anti-HIF-1α lentivirus shRNA pool was used for HIF-1α stable knock-down in JJN3, whereas the pLKO.1 lentiviral vector was used as the empty control vector as previously described.[176] *LGALS1* mRNA expression was evaluated by Real-time PCR in normoxic and hypoxic conditions. Graph represents mean fold change (± S.D.) of two independent experiments in duplicate, calculated assuming JJN3 pLKO.1 normoxia as control condition. (*P* calculated by two tail Student's t test) **(e)** Gal-1 protein expression at cytoplasmic level was evaluated by Western Blot in JJN3 pLKO.1 and JJN3 anti-HIF-1α in normoxic and hypoxic condition. β-actin was used as internal control**.**

Figure 3: Gal-1 stable inhibition in HMCLs and its effect on JJN3 transcriptional profile

(a) Gal-1 stable knock-down in JJN3 and OPM2 was obtained using an anti-Gal-1 lentivirus shRNA, whereas the scramble lentiviral vector was used as control. *LGALS1* mRNA expression was checked by Real-time PCR. Graph represents mean fold change (± S.D.) of three independent experiments**.** (*P* calculated by two tail Student's t test) **(b)** Gal-1 protein expression at cytoplasmic level was evaluated by Western blot in JJN3 scramble/OPM2 scramble and JJN3 anti-Gal-1/OPM2 anti-Gal-1 and β-actin was used as internal control**. (c)** To verify the specificity for *LGALS1* of the anti-Gal-1 lentiviral vector, mRNA levels of *LGALS3* and *LGALS9* were evaluated in JJN3 scramble ad JJN3 anti-Gal-1 by Real-time PCR. Graphs represent the median fold change of three independent experiments performed in duplicate**. (d)** Heatmap of the differentially expressed genes resulted after

hierarchical agglomerative clustering of JJN3 scramble and JJN3 anti-Gal-1 in normoxia, hypoxia and re-oxygenation conditions performed by dChip software**.**

Figure 4: Effect of Gal-1 inhibition on MM cells pro-angiogenic profiles.

(a) The levels of mRNA transcripts for the pro-angiogenic genes *MMP9, CCL2* and for the anti-angiogenic gene *SEMA3A* were evaluated in JJN3 scramble and JJN3 anti-Gal-1 under both normoxic and hypoxic conditions by Real-time PCR and **(b)** qualitative PCR. *GAPDH* was used as reference gene. Graphs represents mean fold change (± S.D.) of three independent experiments performed in duplicate, calculated assuming JJN3 scramble in normoxia and hypoxia as control. (*P* calculated by two tail Student's t test) **(c)** CM of JJN3 scramble and JJN3 anti-Gal-1 incubated in normoxic and hypoxic conditions were tested by ELISA for MMP-9 and CCL2/MCP-1. Graphs represent the median value, reported as pg/µg, of three independent experiments. The statistical analysis was performed by Kruskal–Wallis test**. (d)** Immunoprecipitation was performed on JJN3 scramble and JJN3 anti-Gal-1 concentrated CM in normoxic and hypoxic conditions, using an anti-Sema3A antibody and IgG as negative control. The samples were separated by SDS-Page and the bands were revealed by silver staining. (Positive control: rat brain extract) (CTRL=control). **(e)** Immunoprecipitated bands by anti-Sema3A antibody were quantify by ImageJ software. **(f)** JJN3 scramble and JJN3 anti-Gal-1 mRNA expression levels of 16 genes involved in the angiogenic process in the MM BM were evaluated by Real-time PCR array in condition of normoxia and hypoxia. Graph represents mean fold change (± S.D.) of two independent experiments. JJN3 scramble in normoxia was assumed as control condition (* $P<0.05$).

Figure 5: Stable inhibition of Gal-1 reduces the JJN3 CM angiogenic proprieties.

(a) The Angiokit co-culture of HUVECs and fibroblasts cells was stimulated for 14 days with the CM of JJN3 scramble and JJN3 anti-Gal-1 and incubated under normoxic (dilution 1:1) or hypoxic (dilution 1:1.5) conditions. (Positive control: V2a Growth Medium added with VEGFA 2 ng/mL; negative control: V2a Growth Medium added with suramin 2µM) **(b)** Graphs represent the mean ± S.D. values of the number of junction, number of tubules and total tubule length (reported as number of pixels), respectively of two independent experiments. (*P* calculated by two tail Student's t test) (px=pixels) (CTRL=control).

Figure 6: *In vivo* effect of Gal-1 inhibition on HMCLs growth and on MM-induced angiogenesis

Two groups of four NOD/SCID animals each were injected subcutaneously with 5×10^6 of JJN3 scramble or JJN3 anti-Gal-1 or with 30×10^6 of OPM2 scramble or OPM2 anti-Gal-1. Three weeks after cell inoculation, mice were sacrificed, tumors removed, weighed and measured as described in the methods. Tissue samples from the *ex vivo* plasmacytomas were obtained for immunohistochemical staining. **(a)** Box plots represent the median volume of the masses removed

from all the mice injected with JJN3 scramble or JJN3 anti-Gal-1 and OPM2 scramble or OPM2 anti-Gal-1. (*P* calculated by Mann-Whitney test) **(b)** Photographs represent one representative tumor mass from each mice group, removed from JJN3 scramble or JJN3 anti-Gal-1 or from OPM2 scramble or OPM2 anti-Gal-1 mice. **(c)** Box plots represent the median values of plasmacytomas MVD (number of vessels positive for CD34/mm^3) of all the mice injected with JJN3 scramble or JJN3 anti-Gal-1 and OPM2 scramble or OPM2 anti-Gal-1. (*P* calculated by two tail Student's t test) **(d)** Images represent the immunostaining of CD34 antigen performed on formalin fixed paraffin-embedded samples, respectively, obtained from the plasmacytomas masses of two representative mice injected with JJN3 scramble and JJN3 anti-Gal-1, and the plasmacytomas masses of two representative mice injected with OPM2 scramble and OPM2 anti-Gal-1. Original magnification 400X.

Figure 7: Gal-1 inhibition in JJN3 blunts tumor burden and MM-induced bone destruction after intratibial inoculation in mice.

SCID and NIH-III nude mice each were injected intratibially with 5×10^4 cells of JJN3-anti-Gal-1 or JJN3 scramble. At 4 weeks after injection, the animals were sacrificed and the tibias were dissected out. Tissue samples were obtained for the histological evaluation and immunoistochemistry. **(a)** Box plots represent the median length, width, thickness and volume of the masses removed from all the mice injected with JJN3 scramble or JJN3 anti-Gal-1. (Statistical analyses performed by Mann-Whitney test) **(b)** Hematoxylin and eosin staining of tissues samples obtained from one representative mice of each mice injected with JJN3 scramble or JJN3-anti-Gal-1. **(c)** X rays images form all the mice injected with JJN3 scramble or JJN3-anti-Gal-1. **(d)** Images show the dissected tibias of all the mice (JJN3 scramble and JJN3-anti-Gal-1) acquired on vivaCT 40 scanner at resolution of 15 µm, reconstructed and segmented for 3-dimensional display using the instrument's analysis algorithm software.

8. FIGURES

Figure 1

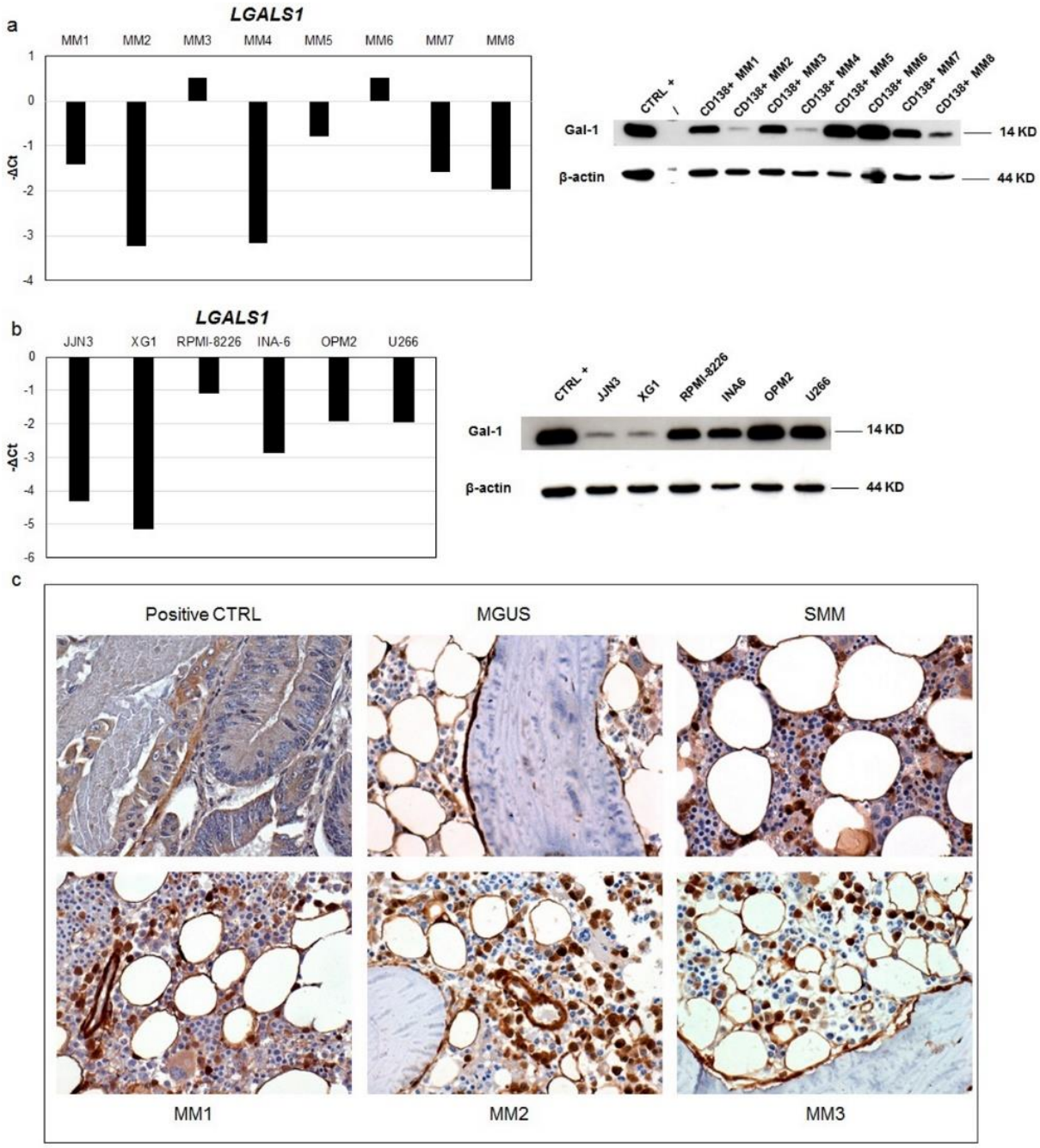

Figure 2

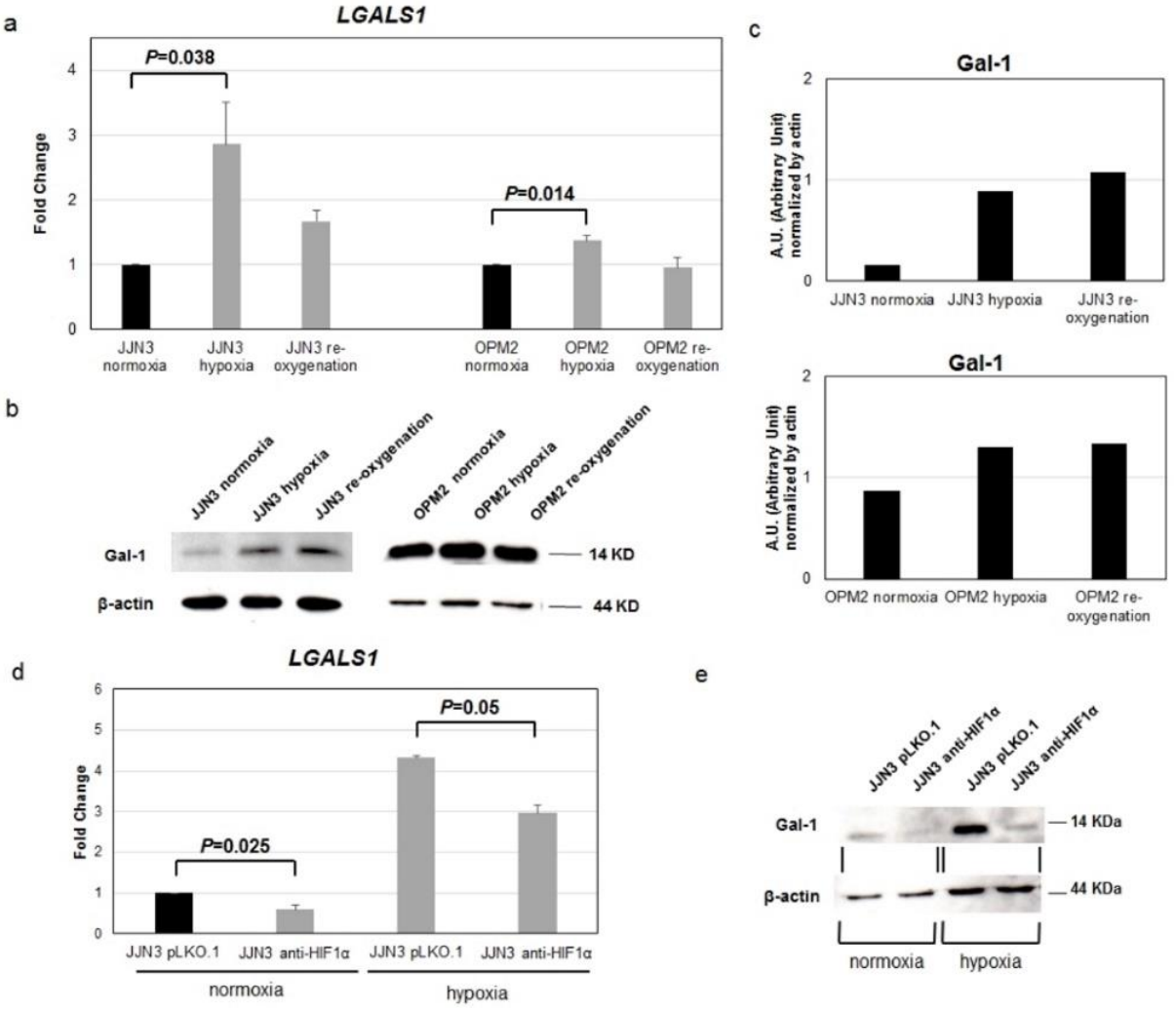
a
LGALS1
P=0.038
P=0.014
Fold Change
JJN3 normoxia
JJN3 hypoxia
JJN3 re-oxygenation
OPM2 normoxia
OPM2 hypoxia
OPM2 re-oxygenation
b
JJN3 normoxia
JJN3 hypoxia
JJN3 re-oxygenation
OPM2 normoxia
OPM2 hypoxia
OPM2 re-oxygenation
Gal-1
β-actin
14 KD
44 KD
c
Gal-1
A.U. (Arbitrary Unit) normalized by actin
JJN3 normoxia
JJN3 hypoxia
JJN3 re-oxygenation
Gal-1
A.U. (Arbitrary Unit) normalized by actin
OPM2 normoxia
OPM2 hypoxia
OPM2 re-oxygenation
d
LGALS1
P=0.05
P=0.025
Fold Change
JJN3 pLKO.1
JJN3 anti-HIF1α
JJN3 pLKO.1
JJN3 anti-HIF1α
normoxia
hypoxia
e
JJN3 pLKO.1
JJN3 anti-HIF1α
JJN3 pLKO.1
JJN3 anti-HIF1α
Gal-1
β-actin
14 KDa
44 KDa
normoxia
hypoxia

Figure 3

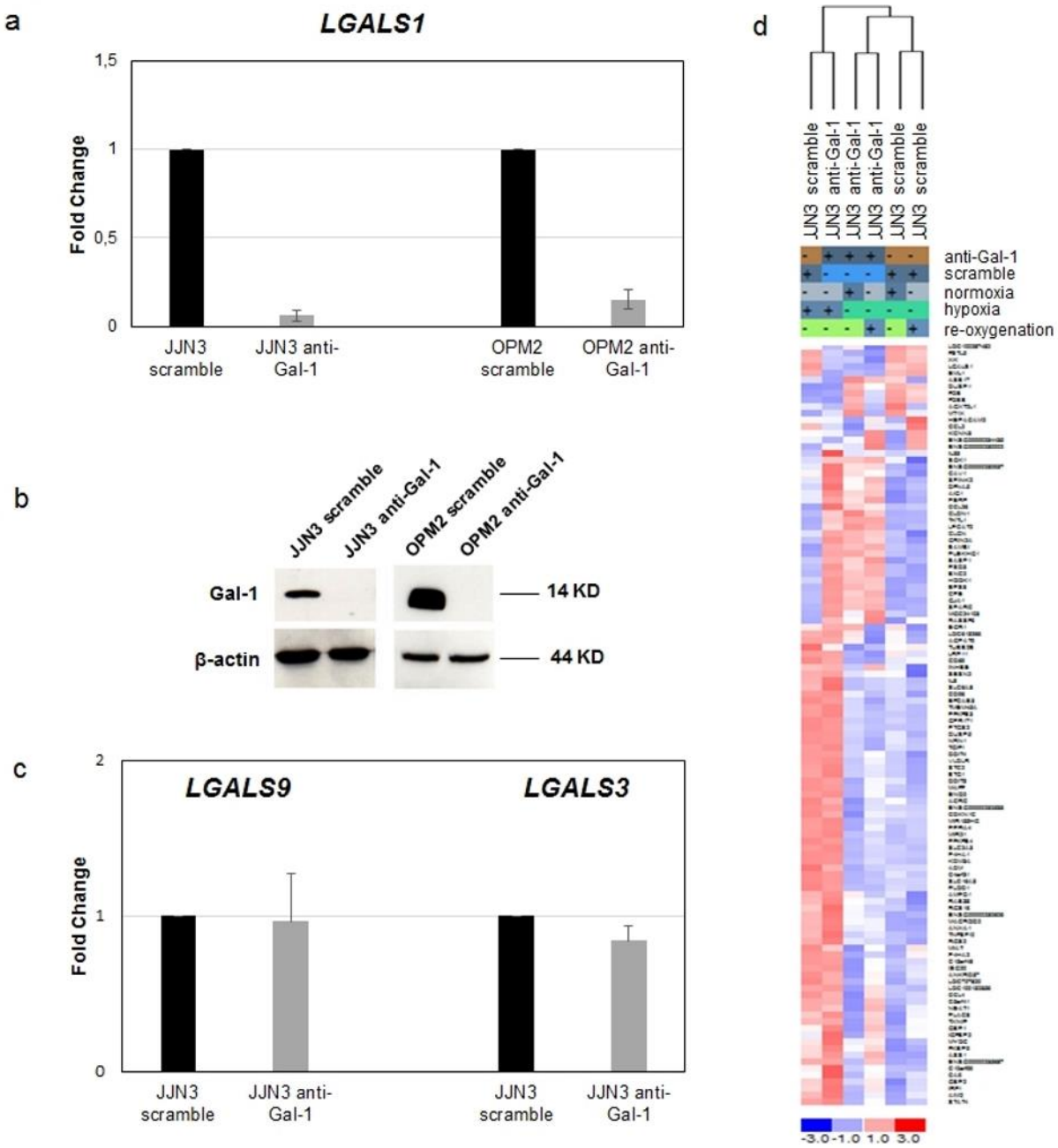
a
LGALS1
Fold Change
1,5
1
0,5
0
JJN3 scramble
JJN3 anti-Gal-1
OPM2 scramble
OPM2 anti-Gal-1
b
JJN3 scramble
JJN3 anti-Gal-1
OPM2 scramble
OPM2 anti-Gal-1
Gal-1
β-actin
14 KD
44 KD
c
LGALS9
LGALS3
Fold Change
2
1
0
JJN3 scramble
JJN3 anti-Gal-1
JJN3 scramble
JJN3 anti-Gal-1
d
JJN3 scramble
JJN3 anti-Gal-1
JJN3 anti-Gal-1
JJN3 anti-Gal-1
JJN3 scramble
JJN3 scramble
anti-Gal-1
scramble
normoxia
hypoxia
re-oxygenation
-3.0 -1.0 1.0 3.0

Figure 4

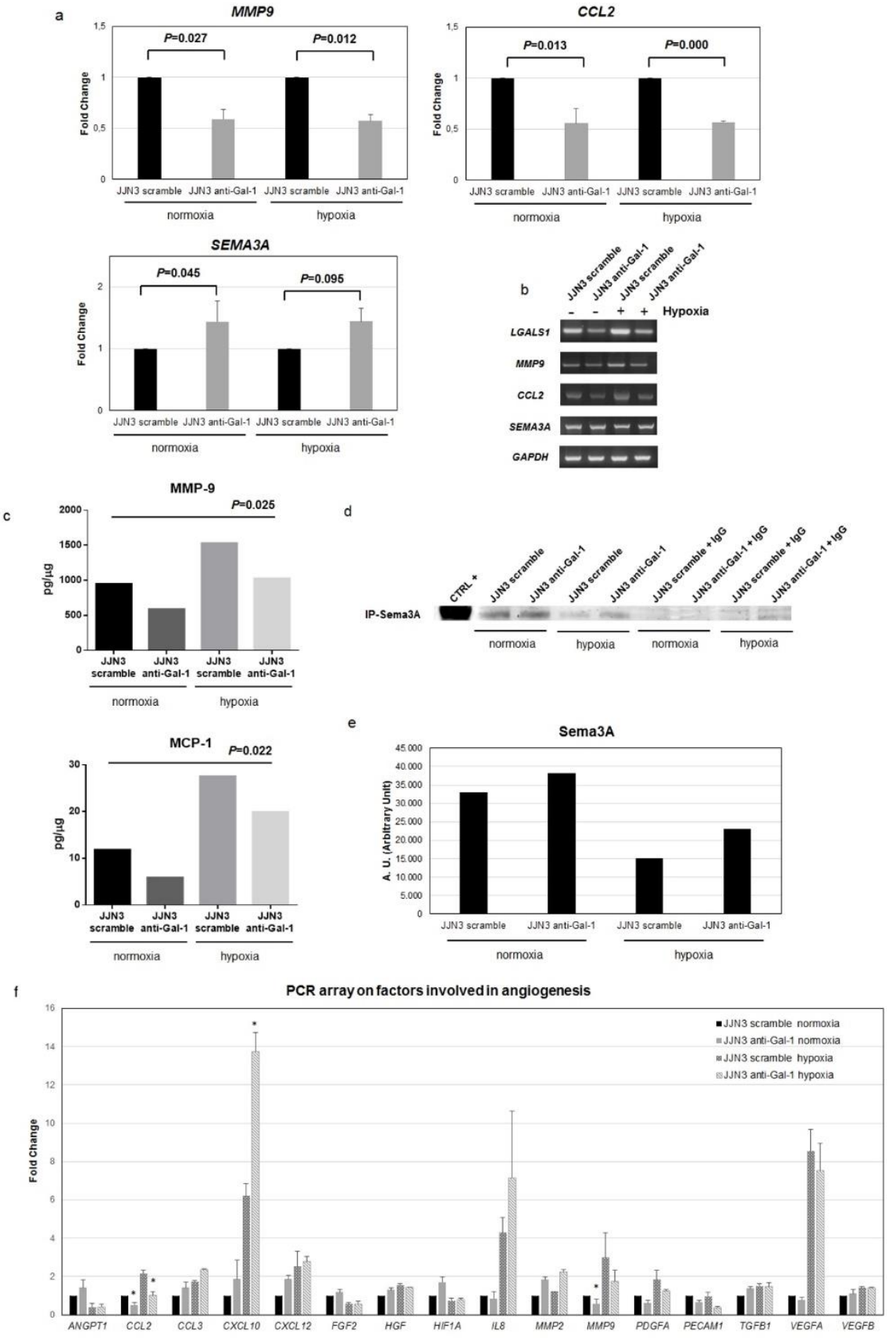
a
MMP9
P=0.027
P=0.012
Fold Change
JJN3 scramble
JJN3 anti-Gal-1
normoxia
hypoxia
CCL2
P=0.013
P=0.000
SEMA3A
P=0.045
P=0.095
b
Hypoxia
LGALS1
MMP9
CCL2
SEMA3A
GAPDH
c
MMP-9
P=0.025
pg/µg
MCP-1
P=0.022
d
CTRL +
IP-Sema3A
JJN3 scramble + IgG
JJN3 anti-Gal-1 + IgG
e
Sema3A
A. U. (Arbitrary Unit)
f
PCR array on factors involved in angiogenesis
JJN3 scramble normoxia
JJN3 anti-Gal-1 normoxia
JJN3 scramble hypoxia
JJN3 anti-Gal-1 hypoxia
ANGPT1
CCL2
CCL3
CXCL10
CXCL12
FGF2
HGF
HIF1A
IL8
MMP2
MMP9
PDGFA
PECAM1
TGFB1
VEGFA
VEGFB

Figure 5

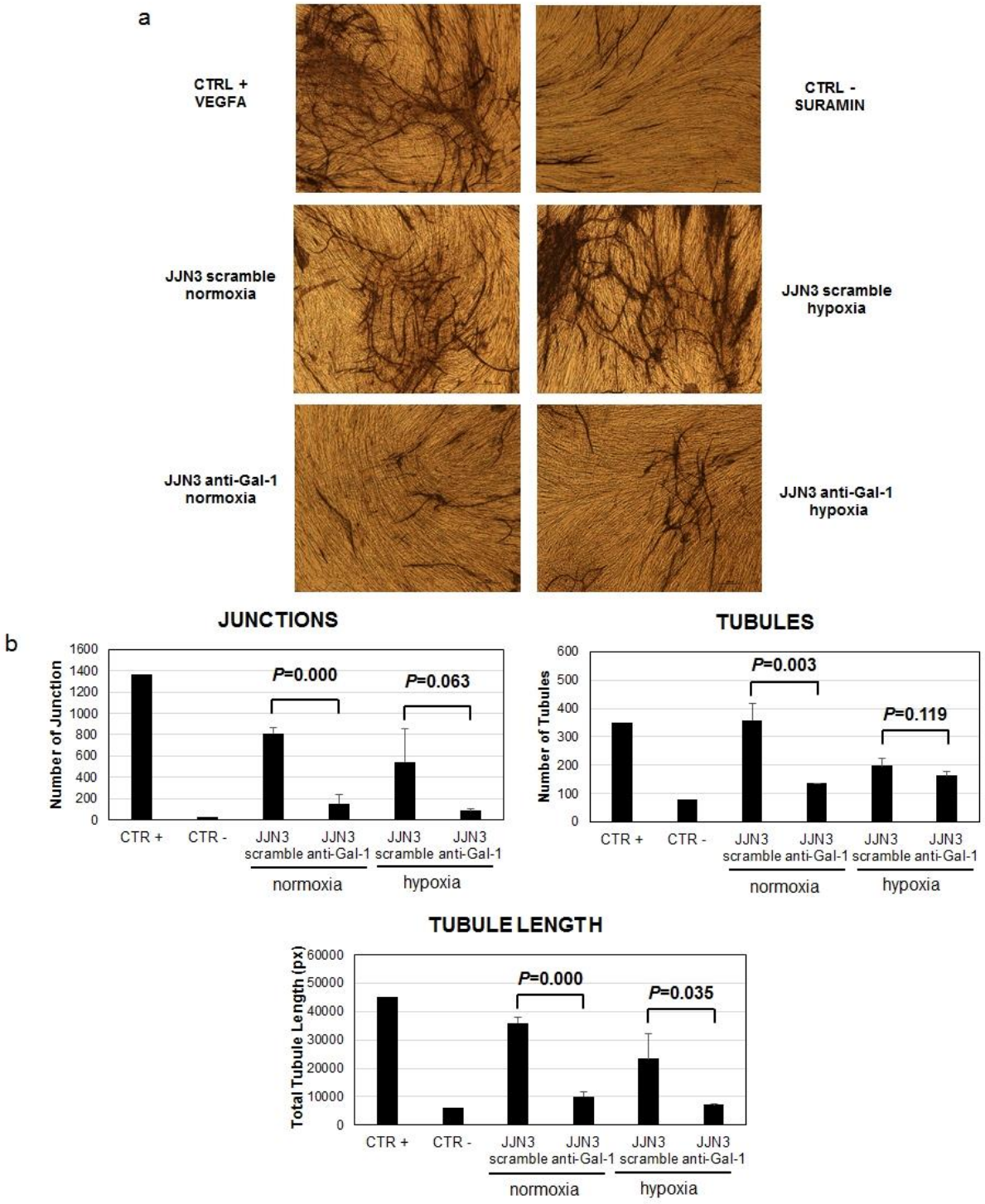
a
CTRL + VEGFA
CTRL - SURAMIN
JJN3 scramble normoxia
JJN3 scramble hypoxia
JJN3 anti-Gal-1 normoxia
JJN3 anti-Gal-1 hypoxia
b
JUNCTIONS
Number of Junction
P=0.000
P=0.063
CTR +
CTR -
JJN3 scramble
JJN3 anti-Gal-1
normoxia
hypoxia
TUBULES
Number of Tubules
P=0.003
P=0.119
TUBULE LENGTH
Total Tubule Length (px)
P=0.000
P=0.035

Figure 6

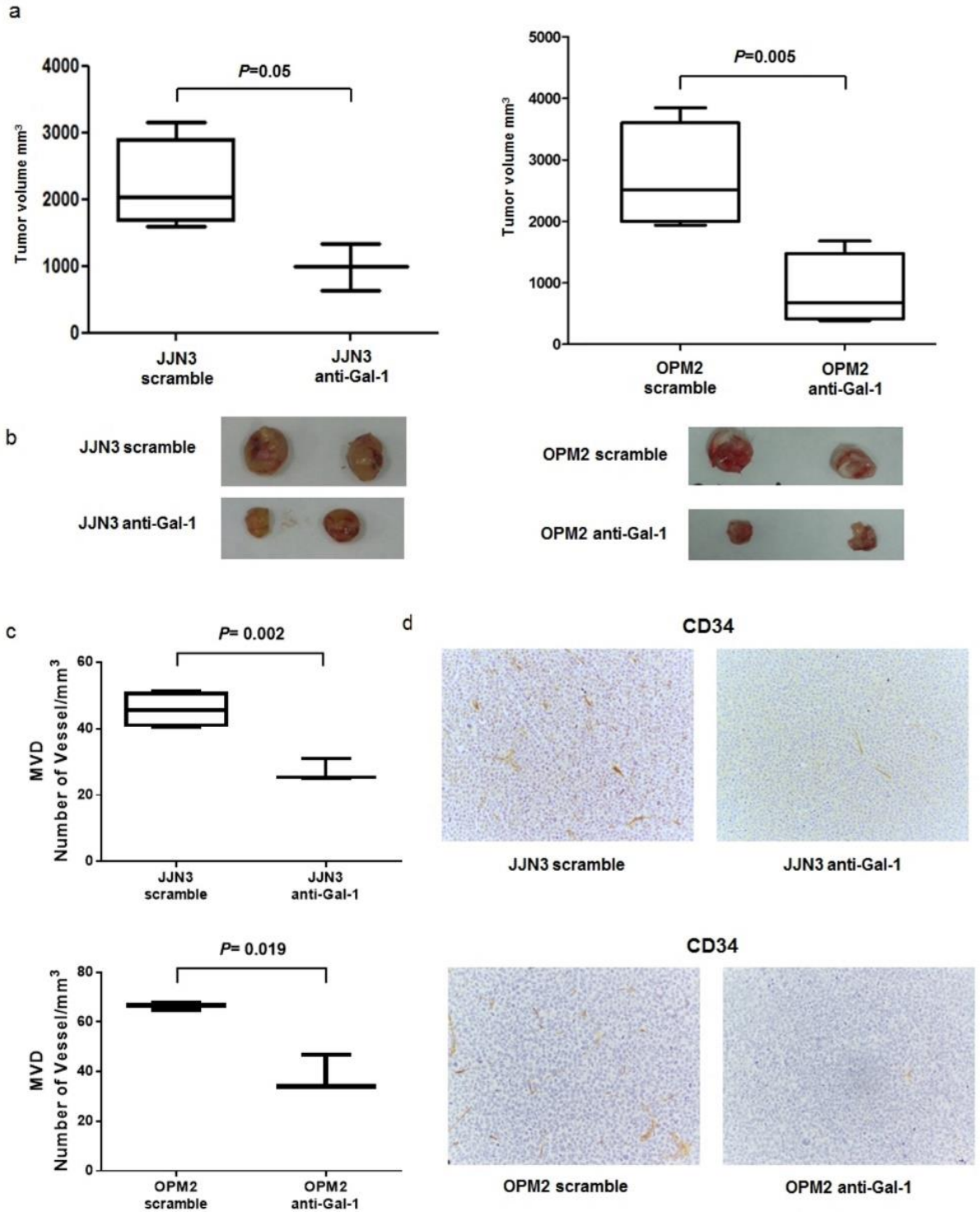
a
Tumor volume mm3
4000
3000
2000
1000
0
P=0.05
JJN3 scramble
JJN3 anti-Gal-1
5000
4000
3000
2000
1000
0
P=0.005
OPM2 scramble
OPM2 anti-Gal-1
b
JJN3 scramble
JJN3 anti-Gal-1
OPM2 scramble
OPM2 anti-Gal-1
c
MVD Number of Vessel/mm3
60
40
20
0
P= 0.002
JJN3 scramble
JJN3 anti-Gal-1
80
60
40
20
0
P= 0.019
OPM2 scramble
OPM2 anti-Gal-1
d
CD34
JJN3 scramble
JJN3 anti-Gal-1
CD34
OPM2 scramble
OPM2 anti-Gal-1

Figure 7

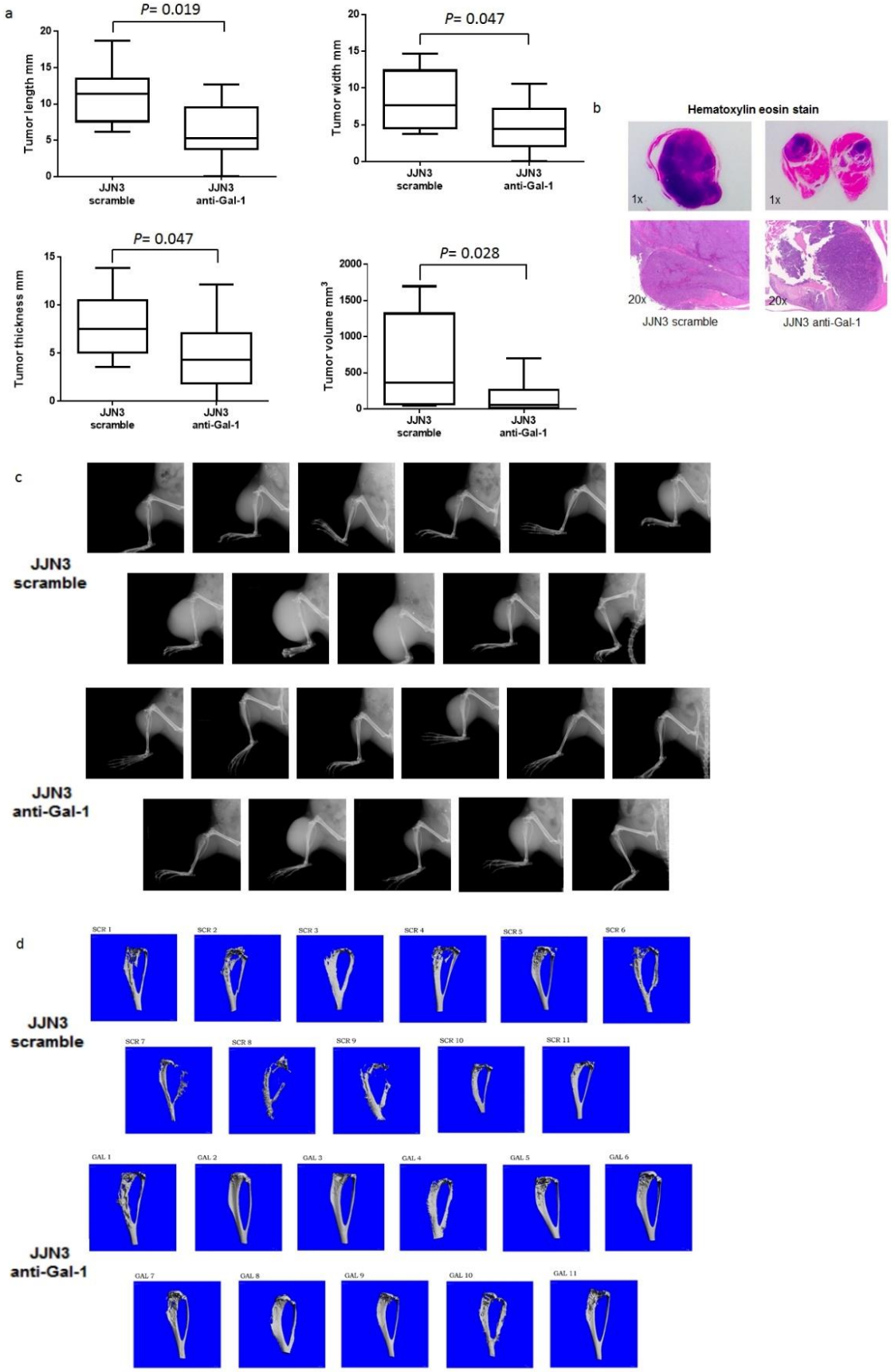
a
P= 0.019
Tumor length mm
JJN3 scramble
JJN3 anti-Gal-1
P= 0.047
Tumor width mm
P= 0.047
Tumor thickness mm
P= 0.028
Tumor volume mm3
b
Hematoxylin eosin stain
1x
20x
JJN3 scramble
JJN3 anti-Gal-1
c
JJN3 scramble
JJN3 anti-Gal-1
d
JJN3 scramble
JJN3 anti-Gal-1

9. LEGENDS OF SUPPLEMENTARY FIGURES

Figure S1: LGALS1 expression levels in MM cells and its association with overall survival.
(a) Box plot represents the median level of *LGALS1* expression of 5 healthy subjects (N), 11 MGUS, 133 MM patients at diagnosis and 9 PCL (GSE16122), and 23 HMCLs (GSE6205). **(b)** Kaplan Meier estimated curves represent the percentage of overall survival of MM patients included in two datasets MP and UAMS, divided in two group as patients with low (in red) and high (in blue) *LGALS1* expression levels.

Figure S2: Role of Gal-1 on JJN3 viability and proliferation.
(a) JJN3 cells were treated with rh-Gal-1 at 3, 20 and 500 ng/ml for 48-72h in RPMI 1640 medium with 2% of FBS and viability was evaluated by MTT assay. (CTRL= control: JJN3 not treated) Graphs represent mean percentage variation (± S.D.) of two independent experiments in quintuplicate. **(b)** Viability of JJN3 stably transfected with anti-Gal-1 and scramble vectors was evaluated by MTT assay after 48–72 h of culture in RPMI 1640 medium with 2% of FBS or without FBS. (CTRL= control: JJN3 scramble) **(c)** JJN3 scramble and JJN3 anti-Gal-1 vectors were incubated for 48–72h in RPMI 1640 medium with 2% of FBS, 3H-TdR was added for the lasts 8h of culture and thymidine incorporation was detected by liquid scintillation spectroscopy. (CTRL= control: JJN3 scramble) All the graphs represent mean percentage variation (± S.D.) of three independent experiments in quintuplicate, calculated assuming JJN3 scramble as control condition.

10. SUPPLEMENTARY FIGURES

Figure S1

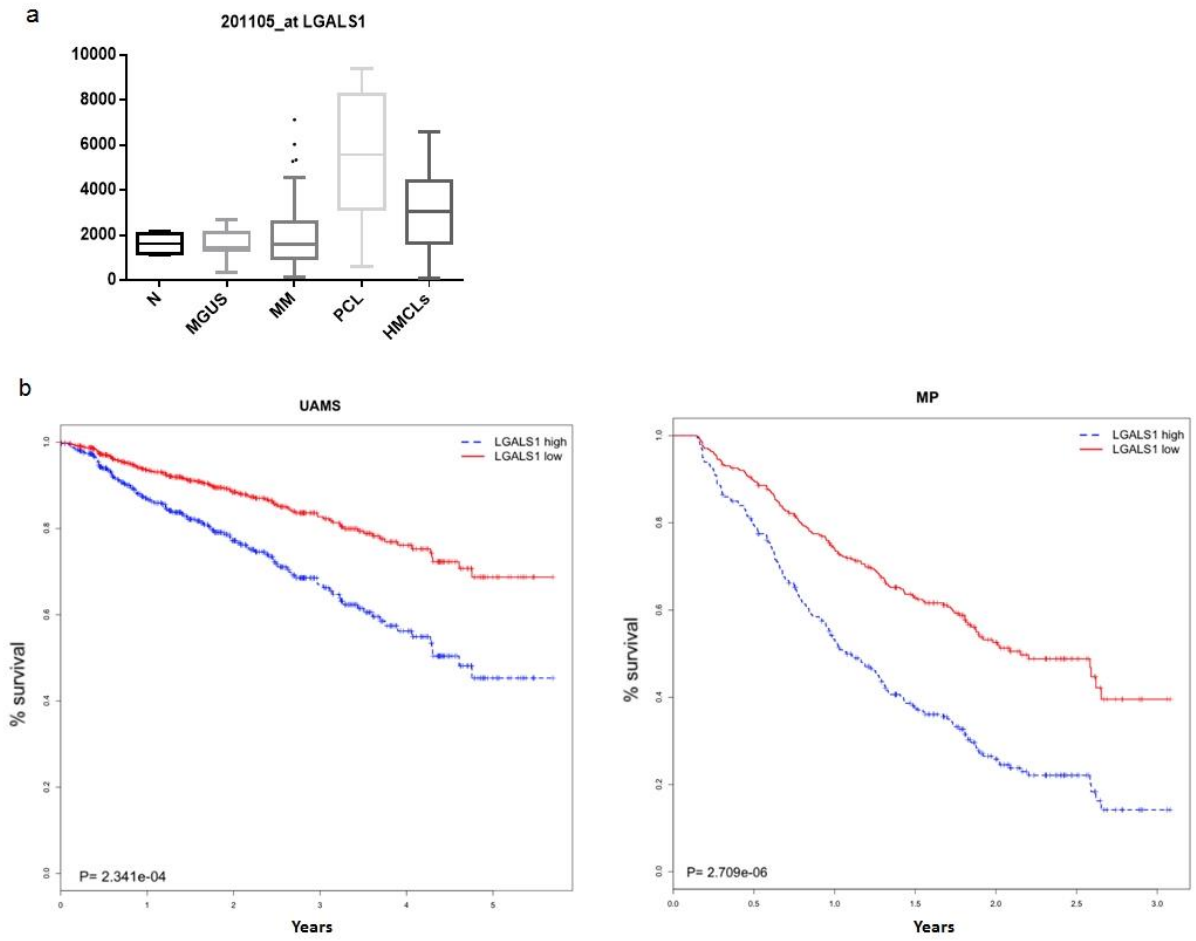

Figure S2

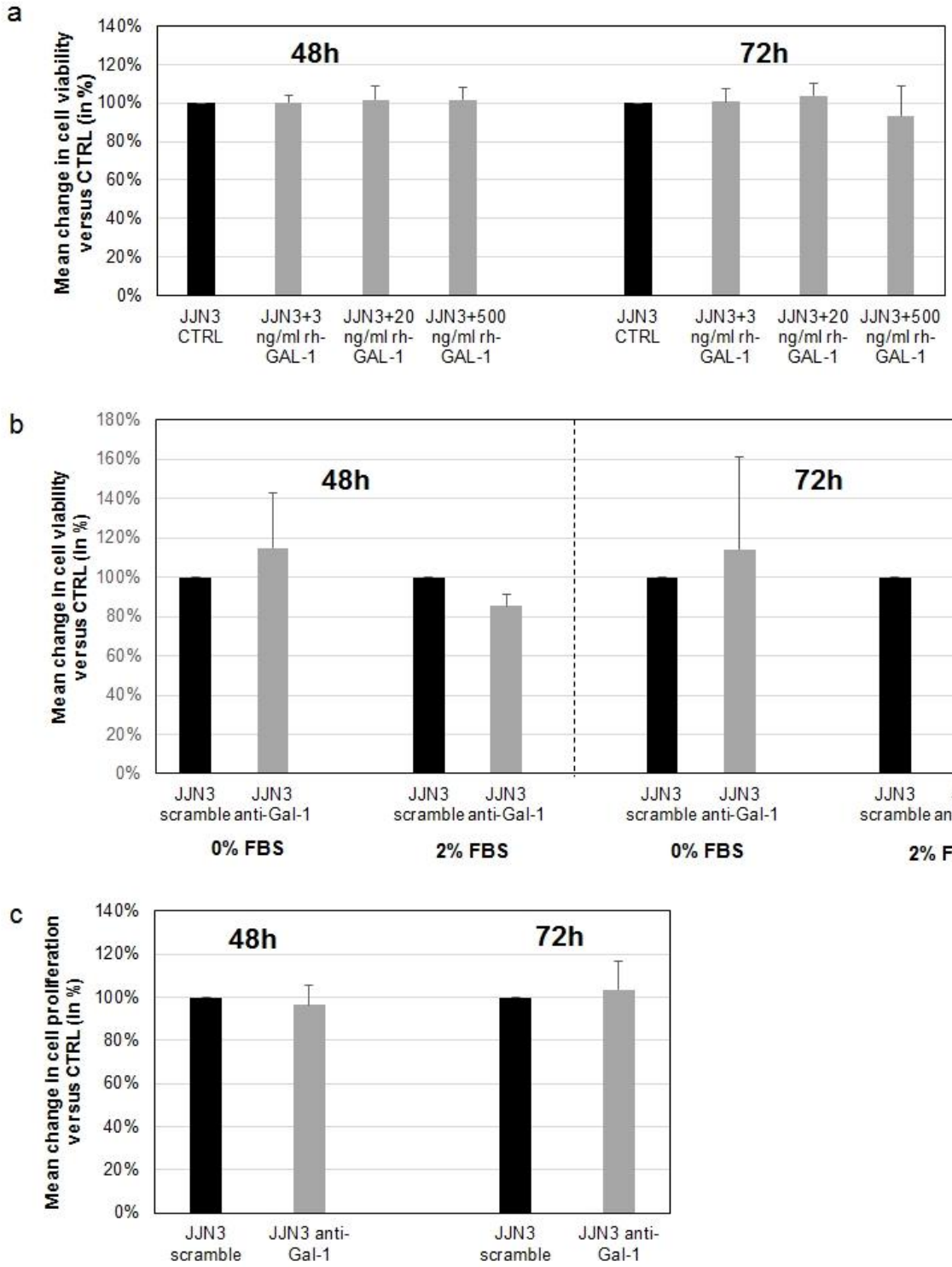
a
Mean change in cell viability versus CTRL (in %)
140%
120%
100%
80%
60%
40%
20%
0%
48h
72h
JJN3 CTRL
JJN3+3 ng/ml rh-GAL-1
JJN3+20 ng/ml rh-GAL-1
JJN3+500 ng/ml rh-GAL-1
JJN3 CTRL
JJN3+3 ng/ml rh-GAL-1
JJN3+20 ng/ml rh-GAL-1
JJN3+500 ng/ml rh-GAL-1
b
Mean change in cell viability versus CTRL (in %)
180%
160%
140%
120%
100%
80%
60%
40%
20%
0%
48h
72h
JJN3 scramble
JJN3 anti-Gal-1
0% FBS
2% FBS
c
Mean change in cell proliferation versus CTRL (in %)
140%
120%
100%
80%
60%
40%
20%
0%
48h
72h
JJN3 scramble
JJN3 anti-Gal-1

11. SUPPLEMENTARY TABLES

Table S1: The table reassumes the results of Gal-1 immunohistochemical staining on osteomedullary biopsies of 24 MM, 9 SMM and 9 MGUS patients. (NA= not analyzable)

DIAGNOSIS	VESSELS	OSTEOBLASTS	PLASMA CELLS
MGUS1	+	+	-
MGUS2	+	+	+
MGUS3	+	+	+
MGUS4	+	+	-
MGUS5	+	+	+
MGUS6	+	+	-
MGUS7	+	+	+
MGUS8	-	-	-
MGUS9	+	+	+
SMM1	+	+	+
SMM2	+	+	+
SMM3	+	+	+
SMM4	+	+	+
SMM5	+	+	+
SMM6	+	+	+
SMM7	+	+	+
SMM8	+	+	+
SMM9	-	+	-
MM1	+	+	+
MM2	+	+	+
MM3	+	+	+
MM4	+	+	NA
MM5	+	+	+
MM6	+	+	+
MM7	+	+	+
MM8	+	+	+
MM9	+	+	+
MM10	+	+	+/-
MM11	+	+	+
MM12	+	+	-
MM13	+	+	+
MM14	-	-	-
MM15	+	+	+
MM16	+	+	+
MM17	+	+	+
MM18	+	+	+
MM19	+	+	+
MM20	+	+	+
MM21	+	+	+
MM22	+	+	+
MM23	+	+	+
MM24	+	+	+

Table S2: Differentially expressed genes in the analysis of JJN3 anti-Gal-1 vs JJN3 scramble in normoxia. (Variation = ratio of the difference between the expression level of the two experiments on the mean value of the same two variables. The most significant differentially expressed transcripts have been selected as those exceeding the mean plus 3 standard deviation of all the ratio values.)

Gene symbol	Variation	Gene name
LGALS1	-1.857917838	lectin. galactoside-binding. soluble. 1
FSTL5	-0.96383885	follistatin-like 5
C15orf48	-0.786760771	chromosome 15 open reading frame 48
PXDN	-0.766106873	peroxidasin homolog (Drosophila)
TUBB2B	-0.757299963	tubulin. beta 2B
ENSG00000237940	-0.742918596	
FBXW10	-0.731076108	F-box and WD repeat domain containing 10; similar to FBXW10 protein
ENSG00000240207	-0.724072714	
XK	-0.701087712	X-linked Kx blood group (McLeod syndrome)
ZSCAN1	-0.681691789	zinc finger and SCAN domain containing 1
C3orf79	-0.678776406	hypothetical protein LOC152118
EML1	-0.667884045	echinoderm microtubule associated protein like 1
LOC100134937	-0.666634183	hypothetical LOC100134937
LOC284898	-0.639633783	hypothetical protein LOC284898
CDKN1C	-0.638870953	cyclin-dependent kinase inhibitor 1C (p57. Kip2)
LOC100127972	-0.619592303	hypothetical LOC100127972
NCRNA00182	-0.619232115	
ENSG00000240405	-0.602508922	
ARRB1	-0.599410162	arrestin. beta 1
ENSG00000145965	-0.592024723	
ACRC	-0.589474207	acidic repeat containing
MCAM	-0.585821502	melanoma cell adhesion molecule
TMEM51	-0.575392698	transmembrane protein 51
RAPGEF4	-0.566548071	Rap guanine nucleotide exchange factor (GEF) 4
CUX2	-0.563868641	cut-like homeobox 2
ZNF57	-0.562895377	zinc finger protein 57
ANG	-0.562180627	angiogenin. ribonuclease. RNase A family. 5
LRP11	-0.561862368	low density lipoprotein receptor-related protein 11
ZNF257	-0.55938877	zinc finger protein 257
ENSG00000238217	-0.555715651	
ENSG00000222017	-0.553635776	
HIST1H2BC	-0.547363692	histone cluster 1. H2bi; histone cluster 1. H2bg; histone cluster 1. H2be; histone cluster 1. H2bf; histone cluster 1. H2bc
ENSG00000237512	-0.547052253	
GPR20	-0.544671111	G protein-coupled receptor 20
MEX3B	-0.542694005	mex-3 homolog B (C. elegans)
PCP4L1	-0.540770892	Purkinje cell protein 4 like 1

ENSG00000222044	-0.537298033	
APOBEC3A	-0.536634271	apolipoprotein B mRNA editing enzyme. catalytic polypeptide-like 3A
C1orf104	-0.530258026	chromosome 1 open reading frame 104
WNT5A	-0.529356513	wingless-type MMTV integration site family. member 5A
PTP4A3	-0.52885229	protein tyrosine phosphatase type IVA. member 3
LOC285692	-0.528751825	hypothetical LOC285692
LOC375295	-0.525181452	hypothetical protein LOC375295
ENSG00000223750	-0.525017154	
C1orf38	-0.518513274	chromosome 1 open reading frame 38
KRTAP9-2	-0.518079867	keratin associated protein 9-9; keratin associated protein 9-2
CCL2	-0.5144572	chemokine (C-C motif) ligand 2
MAML2	-0.510626931	mastermind-like 2 (Drosophila)
ELOVL2	-0.508411036	elongation of very long chain fatty acids (FEN1/Elo2. SUR4/Elo3. yeast)-like 2
LOC100129917	-0.507857608	hypothetical protein LOC100129917
LOC400965	-0.50696023	hypothetical LOC400965
ADAM19	-0.501676621	ADAM metallopeptidase domain 19 (meltrin beta)
HIST2H2BE	-0.49210203	histone cluster 2. H2be
ENSG00000237101	-0.487594433	
EFNA1	-0.484713716	ephrin-A1
FLJ37786	-0.482272974	hypothetical LOC100133086; hypothetical LOC642691
RIN2	-0.479999321	Ras and Rab interactor 2
MAGEB6	-0.475886303	melanoma antigen family B. 6
STEAP1	-0.475103542	six transmembrane epithelial antigen of the prostate 1
LOC144481	-0.47450745	hypothetical protein LOC144481
LOC285033	-0.469010875	hypothetical protein LOC285033
GPX7	-0.467049667	glutathione peroxidase 7
ENSG00000234264	-0.466840168	
ENSG00000228372	-0.465756469	
RAB39B	-0.465293153	RAB39B. member RAS oncogene family
OR2K2	-0.465054236	olfactory receptor. family 2. subfamily K. member 2
LOC100129845	-0.462329945	hypothetical LOC100129845
GABARAPL3	-0.461384738	GABA(A) receptors associated protein like 3 (pseudogene); GABA(A) receptor-associated protein like 1
DDIT3	-0.460708999	DNA-damage-inducible transcript 3
IRX4	-0.459209872	iroquois homeobox 4
SPIB	-0.457788016	Spi-B transcription factor (Spi-1/PU.1 related)
CENPW	-0.454033514	
LOC285281	-0.452989668	hypothetical protein LOC285281
ORM1	-0.447307982	orosomucoid 1
IRF8	-0.445972726	interferon regulatory factor 8

POU3F4	-0.445338379	POU class 3 homeobox 4
OR1A1	-0.444838725	olfactory receptor. family 1. subfamily A. member 1
ENSG00000238184	-0.444243589	
RIC3	-0.443180725	resistance to inhibitors of cholinesterase 3 homolog (C. elegans)
CCL4	-0.440815571	chemokine (C-C motif) ligand 4
PTMS	-0.439533677	parathymosin
MYO5C	-0.439189957	myosin VC
MEFV	-0.437120833	Mediterranean fever
GPR160	-0.436597073	G protein-coupled receptor 160
SLIT1	-0.435783441	slit homolog 1 (Drosophila)
RAMP1	-0.433245825	receptor (G protein-coupled) activity modifying protein 1
NRTN	-0.431173751	neurturin
LOC100132815	-0.430097696	hypothetical protein LOC100132815
LOC100287482	-0.429793253	similar to hCG2038584
DRD4	-0.428309956	dopamine receptor D4
PRKACG	-0.428205281	protein kinase. cAMP-dependent. catalytic. gamma
KCNJ2	-0.427815987	potassium inwardly-rectifying channel. subfamily J. member 2
MEP1B	-0.427040264	meprin A. beta
TNIP3	-0.426325685	TNFAIP3 interacting protein 3
SLC41A2	-0.425061039	solute carrier family 41. member 2
UST	-0.423658416	uronyl-2-sulfotransferase
KCNT2	-0.423501771	potassium channel. subfamily T. member 2
C5orf20	-0.42349135	TRAF-interacting protein with forkhead-associated domain. family member B; chromosome 5 open reading frame 20
LOC642776	-0.422608134	hypothetical protein LOC642776
ENSG00000234350	-0.420386309	
TIMD4	-0.420272208	T-cell immunoglobulin and mucin domain containing 4
DOC2B	-0.420023931	double C2-like domains. beta
MGC2889	-0.419750448	hypothetical protein MGC2889
PRKAG3	-0.419534273	protein kinase. AMP-activated. gamma 3 non-catalytic subunit
C1orf192	-0.417702973	chromosome 1 open reading frame 192
ENSG00000232533	-0.416863725	
HS3ST5	-0.416635492	heparan sulfate (glucosamine) 3-O-sulfotransferase 5
LRRC55	-0.415811079	leucine rich repeat containing 55
HBBP1	-0.414821336	hemoglobin. beta pseudogene 1
ENSG00000236714	-0.413973681	
CBLN2	0.405043279	cerebellin 2 precursor
JAKMIP2	0.405058761	Janus kinase and microtubule interacting protein 2
IRS4	0.406333396	insulin receptor substrate 4

ENSG00000226363	0.409154289	
TSSK4	0.410245338	testis-specific serine kinase 4
ENSG00000234352	0.410343998	
NKX6-3	0.412314733	NK6 homeobox 3
TNFSF4	0.412792412	tumor necrosis factor (ligand) superfamily. member 4
ENSG00000227290	0.413248111	
ENC1	0.413615985	ectodermal-neural cortex (with BTB-like domain)
LOC285423	0.414614334	hypothetical LOC285423
ENSG00000203691	0.415418644	
PENK	0.416115361	proenkephalin
LOC285547	0.416429206	hypothetical protein LOC285547
ENPP4	0.41702068	ectonucleotide pyrophosphatase/phosphodiesterase 4 (putative function)
SPINT2	0.41707633	serine peptidase inhibitor. Kunitz type. 2
MAPK10	0.417145335	mitogen-activated protein kinase 10
HTR2C	0.418981126	5-hydroxytryptamine (serotonin) receptor 2C
ENSG00000224189	0.419448943	
LOC503519	0.420109684	hypothetical LOC503519
PON3	0.420205465	paraoxonase 3
TMEM200A	0.421984586	transmembrane protein 200A
IL29	0.422023578	interleukin 29 (interferon. lambda 1)
PNPO	0.423915218	pyridoxamine 5'-phosphate oxidase
SGK3	0.424756509	serum/glucocorticoid regulated kinase family. member 3
LOC653160	0.428251141	Hypothetical protein LOC653160
C6orf147	0.428604833	chromosome 6 open reading frame 147
ENSG00000230606	0.428816735	
ENSG00000232058	0.429132071	
LOC285000	0.429541559	hypothetical protein LOC285000
ANKRD22	0.429563463	ankyrin repeat domain 22
FOXB1	0.430413582	forkhead box B1
NPTXR	0.430470752	neuronal pentraxin receptor
SI	0.430867892	sucrase-isomaltase (alpha-glucosidase)
GPR180	0.431351636	G protein-coupled receptor 180
TSPAN10	0.431432276	tetraspanin 10
ENSG00000227877	0.432988357	
KIF24	0.433898455	kinesin family member 24
CHRM5	0.434656416	cholinergic receptor. muscarinic 5
C21orf117	0.436652469	chromosome 21 open reading frame 117
ELOVL7	0.436838672	ELOVL family member 7. elongation of long chain fatty acids (yeast)
RORB	0.436883961	RAR-related orphan receptor B
LRP4	0.436982343	low density lipoprotein receptor-related protein 4
BASE	0.439507267	breast cancer and salivary gland expression gene
TRIB2	0.440259573	tribbles homolog 2 (Drosophila)

TRDV2	0.440900937	T cell receptor alpha constant; T cell receptor alpha locus; T cell receptor alpha variable 20; T cell receptor delta locus; T cell receptor delta variable 2
PLXDC2	0.443047662	plexin domain containing 2
ENSG00000232655	0.443822416	
OR51B5	0.444268553	olfactory receptor. family 51. subfamily B. member 5
CNTNAP4	0.445283251	contactin associated protein-like 4
TANC1	0.446364717	tetratricopeptide repeat. ankyrin repeat and coiled-coil containing 1
ENSG00000206552	0.447753282	
LOC100170939	0.448229792	glucuronidase. beta pseudogene
LPAR1	0.449695167	lysophosphatidic acid receptor 1
ENSG00000233061	0.449863329	
TP73	0.449942688	tumor protein p73
LOC441086	0.452747573	hypothetical protein LOC441086
C20orf197	0.455369695	chromosome 20 open reading frame 197
MAP3K9	0.455801573	mitogen-activated protein kinase kinase kinase 9
ENSG00000244210	0.461007755	
ABLIM1	0.46386719	actin binding LIM protein 1
IFNG	0.464469129	interferon. gamma
ENSG00000236094	0.465187277	
C9orf66	0.467292618	chromosome 9 open reading frame 66
BAI3	0.472251666	brain-specific angiogenesis inhibitor 3
LOC727944	0.472325604	similar to hCG2042412
KDR	0.472763161	kinase insert domain receptor (a type III receptor tyrosine kinase)
REEP3	0.476689001	receptor accessory protein 3
UCHL3	0.481680281	ubiquitin carboxyl-terminal esterase L3 (ubiquitin thiolesterase)
FBXL2	0.482172332	F-box and leucine-rich repeat protein 2
GRIA4	0.482743507	glutamate receptor. ionotrophic. AMPA 4
TWIST1	0.483635886	twist homolog 1 (Drosophila)
ANXA13	0.483858162	annexin A13
FSCN1	0.49065447	fascin homolog 1. actin-bundling protein (Strongylocentrotus purpuratus)
LOC283270	0.490920034	hypothetical protein LOC283270
PCDHB4	0.495888919	protocadherin beta 4
IGSF5	0.498732806	immunoglobulin superfamily. member 5
PPARGC1A	0.499260711	peroxisome proliferator-activated receptor gamma. coactivator 1 alpha
ENSG00000224397	0.503965129	
EFNA5	0.508829895	ephrin-A5
ULBP2	0.509587279	UL16 binding protein 2
ENSG00000237807	0.509696432	
IL21R	0.509949353	interleukin 21 receptor
C3orf52	0.513539094	chromosome 3 open reading frame 52
MUC8	0.516289563	mucin 8

MGST2	0.519106699	microsomal glutathione S-transferase 2
GPR37	0.520039677	G protein-coupled receptor 37 (endothelin receptor type B-like)
SH3BGRL2	0.521382058	SH3 domain binding glutamic acid-rich protein like 2
PTPLA	0.522660791	protein tyrosine phosphatase-like (proline instead of catalytic arginine). member A
CD109	0.523125273	CD109 molecule
ENSG00000226383	0.528011306	
SOX21	0.533023985	SRY (sex determining region Y)-box 21
FEZ1	0.533294452	fasciculation and elongation protein zeta 1 (zygin I)
C11orf84	0.536901261	chromosome 11 open reading frame 84
MME	0.537971371	membrane metallo-endopeptidase
ENSG00000229051	0.540419522	
TSPY1	0.545501753	testis specific protein. Y-linked 3; testis specific protein. Y-linked 2; testis specific protein. Y-linked 1; testis specific protein. Y-linked pseudogene 7
ENSG00000229689	0.546299559	
ASB17	0.549903955	ankyrin repeat and SOCS box-containing 17
LHX2	0.549938269	LIM homeobox 2
CA2	0.549986879	carbonic anhydrase II
LOC100128554	0.550344944	hypothetical protein LOC100128554
CAV1	0.555900419	caveolin 1. caveolae protein. 22kDa
LOC286184	0.564682345	hypothetical protein LOC286184
ENSG00000223786	0.56593985	
GABRB2	0.567217633	gamma-aminobutyric acid (GABA) A receptor. beta 2
LRIG3	0.571966241	leucine-rich repeats and immunoglobulin-like domains 3
EDNRB	0.572831914	endothelin receptor type B
GRIP1	0.576616191	glutamate receptor interacting protein 1
BLNK	0.577390378	B-cell linker
ENSG00000236700	0.585609923	
ENSG00000230937	0.59046546	
NPAS4	0.591502459	neuronal PAS domain protein 4
GCNT2	0.602899875	glucosaminyl (N-acetyl) transferase 2. I-branching enzyme (I blood group)
PALLD	0.603643178	palladin. cytoskeletal associated protein
GSTA1	0.605678444	glutathione S-transferase alpha 1
ABCA12	0.609389114	ATP-binding cassette. sub-family A (ABC1). member 12
NAP1L3	0.613187619	nucleosome assembly protein 1-like 3
GBP2	0.617241606	guanylate binding protein 2. interferon-inducible
LOC283914	0.617863604	hypothetical protein LOC283914
LOC646241	0.621453798	hypothetical protein LOC646241
FKBP9	0.645384479	FK506 binding protein 9. 63 kDa
SLC22A24	0.650800121	solute carrier family 22. member 24

KBTBD11	0.660976204	kelch repeat and BTB (POZ) domain containing 11
FAM19A2	0.667001837	family with sequence similarity 19 (chemokine (C-C motif)-like). member A2
ENSG00000234435	0.669658621	
PRKCH	0.677402674	protein kinase C. eta
CCL26	0.683414497	chemokine (C-C motif) ligand 26
DFNA5	0.684272939	deafness. autosomal dominant 5
CCL20	0.684375273	chemokine (C-C motif) ligand 20
NXN	0.689526843	nucleoredoxin
MACROD2	0.704190389	MACRO domain containing 2
ENSG00000230627	0.708327529	
BNC2	0.71678925	basonuclin 2
PPAP2B	0.727105134	phosphatidic acid phosphatase type 2B
FAM49A	0.734321664	family with sequence similarity 49. member A
PLK2	0.736693116	polo-like kinase 2 (Drosophila)
BASP1	0.750217513	brain abundant. membrane attached signal protein 1
MYOC	0.756187636	myocilin. trabecular meshwork inducible glucocorticoid response
LOC441268	0.759164839	hypothetical LOC441268
PERP	0.763144003	PERP. TP53 apoptosis effector
RASSF6	0.815902846	Ras association (RalGDS/AF-6) domain family member 6
CTGF	0.819730653	connective tissue growth factor
PSD3	0.831606933	pleckstrin and Sec7 domain containing 3
BAMBI	0.842391188	hypothetical LOC729590; BMP and activin membrane-bound inhibitor homolog (Xenopus laevis)
AIG1	0.850346377	androgen-induced 1
ZNF521	0.862741547	zinc finger protein 521
HOOK1	0.895694667	hook homolog 1 (Drosophila)
GRIN2A	0.956550634	glutamate receptor. ionotropic. N-methyl D-aspartate 2A
CLDN1	0.979162003	claudin 1
PLEKHG1	1.006657943	pleckstrin homology domain containing. family G (with RhoGef domain) member 1
SPINK2	1.01501814	serine peptidase inhibitor. Kazal type 2 (acrosin-trypsin inhibitor)
CLGN	1.055267822	calmegin
SPARC	1.056359881	secreted protein. acidic. cysteine-rich (osteonectin)
CPE	1.06313884	carboxypeptidase E
TKTL1	1.085322825	transketolase-like 1
GJA1	1.114799484	gap junction protein. alpha 1. 43kDa
LPCAT2	1.155849895	lysophosphatidylcholine acyltransferase 2
EPS8	1.344465043	epidermal growth factor receptor pathway substrate 8

Table S3: Differentially expressed genes in the analysis of JJN3 anti-Gal-1 vs JJN3 scramble after hypoxic treatment. (Variation= ratio of the difference between the expression level of the two experiments on the mean value of the same two variables. The most significant differentially expressed transcripts have been selected as those exceeding the mean plus 3 standard deviation of all the ratio values.)

Gene.symbol	Variation	Gene name
LGALS1	-1.912404366	lectin. galactoside-binding. soluble. 1
TUBB2B	-0.87677153	tubulin. beta 2B
EML1	-0.821829014	echinoderm microtubule associated protein like 1
FSTL5	-0.790261763	follistatin-like 5
IRX4	-0.771851606	iroquois homeobox 4
NLRP7	-0.732498543	NLR family. pyrin domain containing 7
RAPGEF4	-0.681823695	Rap guanine nucleotide exchange factor (GEF) 4
CST7	-0.66960769	cystatin F (leukocystatin)
XK	-0.667585002	X-linked Kx blood group (McLeod syndrome)
PXDN	-0.667345519	peroxidasin homolog (Drosophila)
NOD2	-0.649656946	nucleotide-binding oligomerization domain containing 2
SCARNA17	-0.639625318	small Cajal body-specific RNA 17
ELOVL2	-0.637999672	elongation of very long chain fatty acids (FEN1/Elo2. SUR4/Elo3. yeast)-like 2
SLC46A3	-0.625672884	solute carrier family 46. member 3
ARRB1	-0.60381625	arrestin. beta 1
LOC286382	-0.584387082	hypothetical protein LOC286382
PPP1R9A	-0.58359001	protein phosphatase 1. regulatory (inhibitor) subunit 9A
CCL2	-0.581891364	chemokine (C-C motif) ligand 2
CCDC63	-0.57755151	coiled-coil domain containing 63
KCNT2	-0.565957269	potassium channel. subfamily T. member 2
GPX7	-0.557984837	glutathione peroxidase 7
CAT	-0.553904999	catalase
FRK	-0.548950532	fyn-related kinase
MEX3B	-0.5478356	mex-3 homolog B (C. elegans)
LOC200261	-0.545855119	hypothetical LOC200261
MGC15885	-0.545497679	hypothetical protein MGC15885
KCNK6	-0.539831643	potassium channel. subfamily K. member 6
TCL1A	-0.533568605	T-cell leukemia/lymphoma 1A
SMAD5OS	-0.530145999	SMAD family member 5 opposite strand
OMG	-0.525501635	oligodendrocyte myelin glycoprotein
SNORD116	-0.525074853	small nucleolar RNA. C/D box 116 cluster
KIAA0754	-0.513840407	hypothetical LOC643314
PSTPIP1	-0.512719697	proline-serine-threonine phosphatase interacting protein 1
ENSG00000234509	-0.50812017	
LRRC52	-0.504619525	leucine rich repeat containing 52

FOXS1	-0.503591405	forkhead box S1
ENSG00000220161	-0.501947898	
TTYH1	-0.499933602	tweety homolog 1 (Drosophila)
EFNA1	-0.498112579	ephrin-A1
ENSG00000233001	-0.496809344	
HHIPL1	-0.495270412	HHIP-like 1
LRP1B	-0.492399088	low density lipoprotein-related protein 1B (deleted in tumors)
IGDCC4	-0.490757291	immunoglobulin superfamily. DCC subclass. member 4
TSPAN2	-0.490446709	tetraspanin 2
NTAN1	-0.490245334	N-terminal asparagine amidase
HIST2H2BE	-0.485703757	histone cluster 2. H2be
HAPLN4	-0.485026309	hyaluronan and proteoglycan link protein 4
LOC150051	-0.479515385	hypothetical LOC150051
C14orf167	-0.475960853	chromosome 14 open reading frame 167
C5orf48	-0.475586708	chromosome 5 open reading frame 48
MCAM	-0.475391714	melanoma cell adhesion molecule
C15orf59	-0.473896474	chromosome 15 open reading frame 59
DRD4	-0.470656535	dopamine receptor D4
CPLX1	-0.470316859	complexin 1
ENSG00000236081	-0.46748272	
ENSG00000234283	-0.466461992	
UST	-0.466033695	uronyl-2-sulfotransferase
MMP9	-0.465310306	matrix metallopeptidase 9 (gelatinase B. 92kDa gelatinase. 92kDa type IV collagenase)
KAL1	-0.46482551	Kallmann syndrome 1 sequence
FLJ12120	-0.463710931	hypothetical LOC388439
CENPW	-0.461583163	
MGAM	-0.455800235	maltase-glucoamylase (alpha-glucosidase)
TDRD12	-0.455408318	tudor domain containing 12
C2orf58	-0.454264538	chromosome 2 open reading frame 58
ENSG00000234435	-0.452310792	
KCNJ11	-0.450861922	potassium inwardly-rectifying channel. subfamily J. member 11
LOC441268	-0.44774419	hypothetical LOC441268
MYO5C	-0.445032565	myosin VC
LOC145474	-0.441617631	hypothetical protein LOC145474
NLRP10	-0.44028069	NLR family. pyrin domain containing 10
ANG	-0.439161213	angiogenin. ribonuclease. RNase A family. 5
ZNF423	-0.438814164	zinc finger protein 423
LOC642776	-0.436570667	hypothetical protein LOC642776
HOXD8	-0.43475437	homeobox D8
TNIP3	-0.429892372	TNFAIP3 interacting protein 3
COMP	-0.429069706	cartilage oligomeric matrix protein
SPIC	-0.428238498	Spi-C transcription factor (Spi-1/PU.1 related)
IFNA2	-0.427458187	interferon. alpha 2
FAM55D	-0.427231181	family with sequence similarity 55. member D

OSCP1	-0.426119108	chromosome 1 open reading frame 102
KLF1	-0.424329795	Kruppel-like factor 1 (erythroid)
PRKAG3	-0.418852378	protein kinase. AMP-activated. gamma 3 non-catalytic subunit
LOC729635	-0.417710975	similar to high mobility group box 3
H2AFJ	-0.417223045	H2A histone family. member J
INSM1	-0.416929097	insulinoma-associated 1
ASB17	-0.416331596	ankyrin repeat and SOCS box-containing 17
ENSG00000224137	-0.415738071	
C6orf208	-0.415689566	chromosome 6 open reading frame 208
LOC285692	-0.413732921	hypothetical LOC285692
GPR18	-0.413055684	G protein-coupled receptor 18
MYEF2	-0.412975117	myelin expression factor 2
LOC441208	-0.412570599	zinc and ring finger 2 pseudogene
SASH3	-0.411003969	SAM and SH3 domain containing 3
NME7	-0.410169407	non-metastatic cells 7. protein expressed in (nucleoside-diphosphate kinase)
C6orf114	0.418113865	chromosome 6 open reading frame 114
FAM169A	0.418124011	family with sequence similarity 169. member A
GDAP1	0.419150139	ganglioside-induced differentiation-associated protein 1
CHMP4C	0.419207545	chromatin modifying protein 4C
ENSG00000232103	0.419341619	
HMCN1	0.42008718	hemicentin 1
CELA2A	0.420241394	chymotrypsin-like elastase family. member 2A
ELOVL7	0.420948069	ELOVL family member 7. elongation of long chain fatty acids (yeast)
PNPO	0.421000141	pyridoxamine 5'-phosphate oxidase
GABRB2	0.421142105	gamma-aminobutyric acid (GABA) A receptor. beta 2
LASS1	0.422191692	growth differentiation factor 1; LAG1 homolog. ceramide synthase 1
OR1C1	0.42293301	olfactory receptor. family 1. subfamily C. member 1
ASS1	0.423640039	argininosuccinate synthetase 1
PFN2	0.425410608	profilin 2
PPARGC1A	0.425681611	peroxisome proliferator-activated receptor gamma. coactivator 1 alpha
DHRS3	0.426089138	dehydrogenase/reductase (SDR family) member 3
DTX3L	0.427469717	deltex 3-like (Drosophila)
DNAJC5B	0.428350523	DnaJ (Hsp40) homolog. subfamily C. member 5 beta
MEIS3P1	0.428367568	Meis homeobox 3 pseudogene 1
TBX15	0.428545576	T-box 15
AIM2	0.429388314	absent in melanoma 2
ZSCAN1	0.431598694	zinc finger and SCAN domain containing 1
LOC284513	0.43242285	hypothetical protein LOC284513
LOC283682	0.432943943	hypothetical protein LOC283682

BEX5	0.433567473	brain expressed. X-linked 5
ENSG00000229522	0.433822206	
DDR1	0.434760069	discoidin domain receptor tyrosine kinase 1
ZSCAN5A	0.434805986	zinc finger and SCAN domain containing 5A
PKHD1L1	0.435350527	polycystic kidney and hepatic disease 1 (autosomal recessive)-like 1
GCNT2	0.436275527	glucosaminyl (N-acetyl) transferase 2. I-branching enzyme (I blood group)
ENSG00000230002	0.436468556	
MT2A	0.437149717	metallothionein 2A
VASH2	0.438084802	vasohibin 2
EFNA5	0.438807335	ephrin-A5
OR1F1	0.438911662	olfactory receptor. family 1. subfamily F. member 1
ENSG00000145063	0.438913597	
EPSTI1	0.4397357	epithelial stromal interaction 1 (breast)
CHST6	0.440603682	carbohydrate (N-acetylglucosamine 6-O) sulfotransferase 6
CCDC86	0.442743596	coiled-coil domain containing 86
DNAJB7	0.445293631	DnaJ (Hsp40) homolog. subfamily B. member 7
EOMES	0.446485498	eomesodermin homolog (Xenopus laevis)
S1PR1	0.446536198	sphingosine-1-phosphate receptor 1
PLAC8	0.447854901	placenta-specific 8
EGR1	0.448149133	early growth response 1
TGFBI	0.449482389	transforming growth factor. beta-induced. 68kDa
ENSG00000234859	0.450143252	
ENSG00000242615	0.45017703	
ABHD1	0.453970341	abhydrolase domain containing 1
SLC6A8	0.454149718	solute carrier family 6 (neurotransmitter transporter. creatine). member 8
SUSD5	0.456372223	sushi domain containing 5
HES1	0.458059914	hairy and enhancer of split 1. (Drosophila)
TIAM1	0.458686149	T-cell lymphoma invasion and metastasis 1
CST1	0.459935265	cystatin SN
IFNG	0.460599067	interferon. gamma
LAMP3	0.464968406	lysosomal-associated membrane protein 3
MIR17HG	0.466569534	microRNA host gene 1 (non-protein coding)
CXCL10	0.467996197	chemokine (C-X-C motif) ligand 10
SAMD12	0.468609131	sterile alpha motif domain containing 12
ATL1	0.469467443	atlastin GTPase 1
ENPP4	0.469574835	ectonucleotide pyrophosphatase/phosphodiesterase 4 (putative function)
LRRN1	0.469917909	leucine rich repeat neuronal 1
MACROD2	0.471040388	MACRO domain containing 2
TP73	0.473760901	tumor protein p73
TEC	0.476446532	tec protein tyrosine kinase

KIF12	0.478163361	kinesin family member 12
STRADB	0.478201346	STE20-related kinase adaptor beta
OR2M4	0.478405075	olfactory receptor. family 2. subfamily M. member 4
C3orf33	0.482407891	chromosome 3 open reading frame 33
IL8	0.482550272	interleukin 8
RGS13	0.484220997	regulator of G-protein signaling 13
GRIP1	0.486306789	glutamate receptor interacting protein 1
DPYSL3	0.488434482	dihydropyrimidinase-like 3
ABLIM1	0.488519669	actin binding LIM protein 1
WFDC5	0.48856119	WAP four-disulfide core domain 5
TMEM200A	0.489778899	transmembrane protein 200A
SLC25A18	0.489947303	solute carrier family 25 (mitochondrial carrier). member 18
WDFY3	0.492404935	WD repeat and FYVE domain containing 3
CAPN8	0.493990808	calpain 8
ACVR1C	0.494125712	activin A receptor. type IC
BLNK	0.49512922	B-cell linker
LOC642345	0.495761429	hCG1818123
PRKCH	0.496421408	protein kinase C. eta
ITK	0.497426931	IL2-inducible T-cell kinase
RGS16	0.49757565	regulator of G-protein signaling 16
VEGFC	0.499871042	vascular endothelial growth factor C
MAPK10	0.500755586	mitogen-activated protein kinase 10
CSTA	0.502000675	cystatin A (stefin A)
TMEM151A	0.505476915	transmembrane protein 151A
REEP3	0.506897542	receptor accessory protein 3
ENSG00000225794	0.50802657	
BTBD19	0.50868325	hypothetical protein LOC149478
EGR2	0.510405126	early growth response 2
DUSP6	0.514381863	dual specificity phosphatase 6
CCR7	0.515069909	chemokine (C-C motif) receptor 7
LRIG3	0.51539564	leucine-rich repeats and immunoglobulin-like domains 3
FKBP9	0.522243194	FK506 binding protein 9. 63 kDa
FAM129A	0.523836098	family with sequence similarity 129. member A
PTPLA	0.525247529	protein tyrosine phosphatase-like (proline instead of catalytic arginine). member A
SORL1	0.525352439	sortilin-related receptor. L(DLR class) A repeats-containing
CDHR1	0.525557064	protocadherin 21
SH3BGRL2	0.528145326	SH3 domain binding glutamic acid-rich protein like 2
C12orf54	0.534358536	chromosome 12 open reading frame 54
SGK1	0.537786808	serum/glucocorticoid regulated kinase 1
S100A8	0.539768948	S100 calcium binding protein A8
CD38	0.539941619	CD38 molecule
C3orf52	0.543298089	chromosome 3 open reading frame 52

NOG	0.545945957	noggin
GNAI1	0.552633947	guanine nucleotide binding protein (G protein). alpha inhibiting activity polypeptide 1
LOC348751	0.555475508	hypothetical protein LOC348751
PGF	0.560161331	placental growth factor
ENSG00000226966	0.563183249	
FAM95B1	0.569014315	family with sequence similarity 95. member B1
WARS	0.56944527	tryptophanyl-tRNA synthetase
PALLD	0.578059624	palladin. cytoskeletal associated protein
MGC14436	0.581679208	hypothetical LOC84983
GPR180	0.586132022	G protein-coupled receptor 180
CA2	0.591226437	carbonic anhydrase II
PARP9	0.594587909	poly (ADP-ribose) polymerase family. member 9
SEMA3A	0.598241322	sema domain. immunoglobulin domain (Ig). short basic domain. secreted. (semaphorin) 3A
PERP	0.599333404	PERP. TP53 apoptosis effector
AK7	0.600677765	adenylate kinase 7
TANC1	0.601570141	tetratricopeptide repeat. ankyrin repeat and coiled-coil containing 1
EGLN3	0.604322384	egl nine homolog 3 (C. elegans)
SI	0.604614101	sucrase-isomaltase (alpha-glucosidase)
CD109	0.605201353	CD109 molecule
LPAR1	0.608532813	lysophosphatidic acid receptor 1
IRF1	0.612573878	interferon regulatory factor 1
UCHL3	0.616135358	ubiquitin carboxyl-terminal esterase L3 (ubiquitin thiolesterase)
ENSG00000167912	0.619449597	
GBP2	0.620246122	guanylate binding protein 2. interferon-inducible
FSCN1	0.624029169	fascin homolog 1. actin-bundling protein (Strongylocentrotus purpuratus)
CLDN1	0.624709508	claudin 1
EDNRB	0.637959988	endothelin receptor type B
KBTBD11	0.643125252	kelch repeat and BTB (POZ) domain containing 11
PLK2	0.643191284	polo-like kinase 2 (Drosophila)
ENSG00000236239	0.656278014	
CCL5	0.660430338	chemokine (C-C motif) ligand 5
ZNF521	0.66544088	zinc finger protein 521
FAIM3	0.666242939	Fas apoptotic inhibitory molecule 3
UGT2B17	0.669317591	UDP glucuronosyltransferase 2 family. polypeptide B17
TWIST1	0.670321906	twist homolog 1 (Drosophila)
GBP5	0.672256111	guanylate binding protein 5
TUBB4Q	0.67316181	tubulin. beta polypeptide 4. member Q
BASP1	0.683274288	brain abundant. membrane attached signal protein 1
CTGF	0.685244833	connective tissue growth factor
CD6	0.686313544	CD6 molecule

SGK3	0.687437439	serum/glucocorticoid regulated kinase family. member 3
FAM19A2	0.690168539	family with sequence similarity 19 (chemokine (C-C motif)-like). member A2
CNTNAP4	0.710078993	contactin associated protein-like 4
AIG1	0.711260317	androgen-induced 1
CAV1	0.716144485	caveolin 1. caveolae protein. 22kDa
CBLN2	0.738610684	cerebellin 2 precursor
NAP1L3	0.747945449	nucleosome assembly protein 1-like 3
MGST2	0.753603368	microsomal glutathione S-transferase 2
IL21R	0.762459859	interleukin 21 receptor
LPCAT2	0.777843353	lysophosphatidylcholine acyltransferase 2
LHX2	0.780794233	LIM homeobox 2
GBP1	0.783027878	guanylate binding protein 1. interferon-inducible. 67kDa
LOC100289230	0.827185422	hypothetical protein LOC100289230
ENSG00000223786	0.828588963	
IGFBP2	0.846799255	insulin-like growth factor binding protein 2. 36kDa
ENSG00000230937	0.851177919	
HOOK1	0.859805198	hook homolog 1 (Drosophila)
MYOC	0.909513716	myocilin. trabecular meshwork inducible glucocorticoid response
BNC2	0.91007589	basonuclin 2
PPAP2B	0.919007258	phosphatidic acid phosphatase type 2B
SEPP1	0.934838696	selenoprotein P. plasma. 1
TKTL1	0.950430704	transketolase-like 1
C10orf99	0.976162881	chromosome 10 open reading frame 99
CLGN	0.990950923	calmegin
CA9	1.004654611	carbonic anhydrase IX
RASSF6	1.013904076	Ras association (RalGDS/AF-6) domain family member 6
GRIN2A	1.112688353	glutamate receptor. ionotropic. N-methyl D-aspartate 2A
DFNA5	1.123104329	deafness. autosomal dominant 5
PLEKHG1	1.148393582	pleckstrin homology domain containing. family G (with RhoGef domain) member 1
CPE	1.154893149	carboxypeptidase E
IL33	1.165487489	interleukin 33
SPARC	1.171835256	secreted protein. acidic. cysteine-rich (osteonectin)
BAMBI	1.173606617	hypothetical LOC729590; BMP and activin membrane-bound inhibitor homolog (Xenopus laevis)
PSD3	1.177791581	pleckstrin and Sec7 domain containing 3
MGC24103	1.186536696	hypothetical MGC24103
SPINK2	1.259934215	serine peptidase inhibitor. Kazal type 2 (acrosin-trypsin inhibitor)
CCL26	1.264326535	chemokine (C-C motif) ligand 26

GJA1	1.282997798	gap junction protein. alpha 1. 43kDa
EPS8	1.378865194	epidermal growth factor receptor pathway substrate 8

Table S4: Differentially expressed genes in the analysis of JJN3 anti-Gal-1 vs JJN3 scramble after re-oxygenation treatment. (Variation = ratio of the difference between the expression level of the two experiments on the mean value of the same two variables. The most significant differentially expressed transcripts have been selected as those exceeding the mean plus 3 standard deviation of all the ratio values.)

Gene.symbol	Variation	Gene Name
LGALS1	-1.929572472	lectin. galactoside-binding. soluble. 1
LOC100287482	-1.066450293	similar to hCG2038584
FOS	-1.049641012	v-fos FBJ murine osteosarcoma viral oncogene homolog
FSTL5	-0.900202861	follistatin-like 5
XK	-0.888379752	X-linked Kx blood group (McLeod syndrome)
RAPGEF4	-0.871993333	Rap guanine nucleotide exchange factor (GEF) 4
CCL2	-0.829178592	chemokine (C-C motif) ligand 2
EML1	-0.813524331	echinoderm microtubule associated protein like 1
HEPACAM2	-0.798934128	HEPACAM family member 2
HBBP1	-0.746057287	hemoglobin. beta pseudogene 1
PIRT	-0.729355752	phosphoinositide-interacting regulator of transient receptor potential channels
ANKLE1	-0.726714079	ankyrin repeat and LEM domain containing 1
IRX4	-0.706181282	iroquois homeobox 4
PTMS	-0.701066874	parathymosin
ZNF57	-0.696594613	zinc finger protein 57
PKIG	-0.65571674	protein kinase (cAMP-dependent. catalytic) inhibitor gamma
SLC46A3	-0.643094039	solute carrier family 46. member 3
PXDN	-0.640477692	peroxidasin homolog (Drosophila)
HMOX1	-0.636944948	heme oxygenase (decycling) 1
CNN3	-0.632122944	calponin 3. acidic
CXCL14	-0.627681388	chemokine (C-X-C motif) ligand 14
MCAM	-0.614392987	melanoma cell adhesion molecule
FOSB	-0.608095365	FBJ murine osteosarcoma viral oncogene homolog B
VCX2	-0.606394556	variable charge. X-linked 2
CYP2A13	-0.602443916	cytochrome P450. family 2. subfamily A. polypeptide 13
PLA1A	-0.594907856	phospholipase A1 member A
TCL1A	-0.594658563	T-cell leukemia/lymphoma 1A
CRYBA2	-0.593827176	crystallin. beta A2
ZNF257	-0.593346354	zinc finger protein 257
FOXC2	-0.591880106	forkhead box C2 (MFH-1. mesenchyme forkhead 1)
TUBB2B	-0.586408597	tubulin. beta 2B
FCRLB	-0.584625849	Fc receptor-like B

CENPW	-0.577144861	
ENSG00000236700	-0.571859459	
WNT5A	-0.56141944	wingless-type MMTV integration site family. member 5A
FLJ42418	-0.559040085	FLJ42418 protein
GPX7	-0.558253369	glutathione peroxidase 7
TTTY14	-0.554230751	testis-specific transcript. Y-linked 14
ITGA8	-0.55176749	integrin. alpha 8
CD300C	-0.548097991	CD300c molecule
DUSP1	-0.545196953	dual specificity phosphatase 1
NPDC1	-0.542844191	neural proliferation. differentiation and control. 1
PANK1	-0.541629673	pantothenate kinase 1
HDGFRP3	-0.541494938	hepatoma-derived growth factor. related protein 3
MAGEB6	-0.535303602	melanoma antigen family B. 6
FAM92A1	-0.533808779	family with sequence similarity 92. member A2; family with sequence similarity 92. member A1
CRISP3	-0.533696292	cysteine-rich secretory protein 3
GPM6B	-0.532187198	glycoprotein M6B
FAM24A	-0.531078138	family with sequence similarity 24. member A
C5orf49	-0.530465613	chromosome 5 open reading frame 49
COTL1	-0.529112727	coactosin-like 1 (Dictyostelium)
KCNJ2	-0.528157936	potassium inwardly-rectifying channel. subfamily J. member 2
NQO1	-0.527404237	NAD(P)H dehydrogenase. quinone 1
NPB	-0.52581857	neuropeptide B
ARRB1	-0.516379103	arrestin. beta 1
PHLDA2	-0.515193931	pleckstrin homology-like domain. family A. member 2
TEX15	-0.510712648	testis expressed 15
RAMP1	-0.508296817	receptor (G protein-coupled) activity modifying protein 1
ZNF43	-0.506777556	zinc finger protein 43
ENSG00000229048	-0.506138607	
SCCPDH	-0.497651415	saccharopine dehydrogenase (putative)
LOC729164	-0.49362486	hCG1732469
HEATR4	-0.491120826	HEAT repeat containing 4
ENSG00000242687	-0.490357539	
MMP9	-0.490307112	matrix metallopeptidase 9 (gelatinase B. 92kDa gelatinase. 92kDa type IV collagenase)
SLC25A43	-0.489078329	solute carrier family 25. member 43
CREB5	-0.485991298	cAMP responsive element binding protein 5
RERG	-0.485518836	RAS-like. estrogen-regulated. growth inhibitor
ANKRD30B	-0.484690711	ankyrin repeat domain 30B
PRSS35	-0.48280857	protease. serine. 35
PEG10	-0.481767687	paternally expressed 10

GBX2	-0.480278852	gastrulation brain homeobox 2
MEST	-0.478663869	mesoderm specific transcript homolog (mouse)
ZMYND15	-0.478338418	zinc finger. MYND-type containing 15
LOC146795	-0.477885877	hypothetical protein LOC146795
CD69	-0.475900567	CD69 molecule
CXCL13	-0.475497641	chemokine (C-X-C motif) ligand 13
PCOLCE2	-0.47526232	procollagen C-endopeptidase enhancer 2
KCNJ11	-0.470739053	potassium inwardly-rectifying channel. subfamily J. member 11
LAIR2	-0.467812508	leukocyte-associated immunoglobulin-like receptor 2
C21orf37	-0.464778482	immunoglobulin heavy variable (II)-20-1 pseudogene; chromosome 21 open reading frame 37
POU2F3	-0.464183243	POU class 2 homeobox 3
B3GALNT1	-0.463429116	beta-1.3-N-acetylgalactosaminyltransferase 1 (globoside blood group)
ENSG00000228735	-0.460573837	
LRP11	-0.458949401	low density lipoprotein receptor-related protein 11
CYBRD1	-0.458451857	cytochrome b reductase 1
MLLT10L	-0.45823587	myeloid/lymphoid or mixed-lineage leukemia (trithorax homolog. Drosophila); translocated to. 10-like
ENSG00000224405	-0.457229621	
NTAN1	-0.455515471	N-terminal asparagine amidase
ZNF69	0.456414676	zinc finger protein 69
RASGRP1	0.456617095	RAS guanyl releasing protein 1 (calcium and DAG-regulated)
SLC25A18	0.458483129	solute carrier family 25 (mitochondrial carrier). member 18
G0S2	0.45852332	G0/G1switch 2
DEFB4A	0.45867707	defensin. beta 4
CARS	0.461026219	cysteinyl-tRNA synthetase
TMTC1	0.461150787	transmembrane and tetratricopeptide repeat containing 1
ETV1	0.461893165	ets variant 1
MRPS11P1	0.462547263	mitochondrial ribosomal protein S11 pseudogene 1
LTF	0.463155175	lactotransferrin
NEAT1	0.464478153	non-protein coding RNA 84
PSG6	0.464835034	pregnancy specific beta-1-glycoprotein 6
ENSG00000224798	0.466859815	
ISL2	0.467380719	ISL LIM homeobox 2
CCL26	0.46874259	chemokine (C-C motif) ligand 26
C6	0.469240728	complement component 6
KIAA0485	0.470203991	hypothetical LOC57235

SLC7A5	0.470962462	solute carrier family 7 (cationic amino acid transporter. y+ system). member 5
MAFF	0.472863613	v-maf musculoaponeurotic fibrosarcoma oncogene homolog F (avian)
DPYSL3	0.473095246	dihydropyrimidinase-like 3
C10orf99	0.4733034	chromosome 10 open reading frame 99
SMAD7	0.473392335	SMAD family member 7
ABLIM1	0.474581568	actin binding LIM protein 1
TEX14	0.474796765	testis expressed 14
PMAIP1	0.47873083	phorbol-12-myristate-13-acetate-induced protein 1
TUBE1	0.478892939	tubulin. epsilon 1
C16orf74	0.480606953	chromosome 16 open reading frame 74
CD109	0.481875727	CD109 molecule
LOC728543	0.482442075	hypothetical protein LOC728543
ENPP4	0.484265673	ectonucleotide pyrophosphatase/phosphodiesterase 4 (putative function)
SORL1	0.487802653	sortilin-related receptor. L(DLR class) A repeats-containing
SPRY2	0.491484263	sprouty homolog 2 (Drosophila)
ALDH1L2	0.492863424	aldehyde dehydrogenase 1 family. member L2
GBP1	0.495866601	guanylate binding protein 1. interferon-inducible. 67kDa
ANK2	0.499654336	ankyrin 2. neuronal
FLJ40330	0.50003938	hypothetical LOC645784
ENSG00000239791	0.500338267	
LRRN1	0.500772574	leucine rich repeat neuronal 1
LOC100129917	0.502055819	hypothetical protein LOC100129917
LPAR1	0.502435776	lysophosphatidic acid receptor 1
APOLD1	0.502626936	apolipoprotein L domain containing 1
LCE1B	0.50512887	late cornified envelope 1B
PKHD1L1	0.505518133	polycystic kidney and hepatic disease 1 (autosomal recessive)-like 1
GCNT2	0.505847608	glucosaminyl (N-acetyl) transferase 2. I-branching enzyme (I blood group)
SLC7A11	0.50849037	solute carrier family 7. (cationic amino acid transporter. y+ system) member 11
OTUD1	0.50897749	OTU domain containing 1
KIAA0355	0.509261225	KIAA0355
TP73	0.513314588	tumor protein p73
LOC643072	0.515426016	hypothetical LOC643072
PRICKLE2	0.518524846	prickle homolog 2 (Drosophila)
APOL6	0.519473004	apolipoprotein L. 6
DHRS3	0.52006394	dehydrogenase/reductase (SDR family) member 3
CCL20	0.528008759	chemokine (C-C motif) ligand 20

FAM107B	0.529380325	family with sequence similarity 107. member B
GPT2	0.529948545	glutamic pyruvate transaminase (alanine aminotransferase) 2
FRMD6	0.531345742	FERM domain containing 6
ZNF695	0.531744194	zinc finger protein 695
LOC151438	0.534135594	hypothetical protein LOC151438
LOC400684	0.535651784	hypothetical gene supported by BC000922
GAB2	0.536837211	GRB2-associated binding protein 2
SOX21	0.538838907	SRY (sex determining region Y)-box 21
LOC339505	0.539011905	hypothetical protein LOC339505
KREMEN1	0.541405167	kringle containing transmembrane protein 1
ZNF521	0.542713064	zinc finger protein 521
CTGF	0.542816008	connective tissue growth factor
C5orf41	0.543102385	chromosome 5 open reading frame 41
ZBTB20	0.54580297	zinc finger and BTB domain containing 20
BTBD3	0.546357546	BTB (POZ) domain containing 3
RORB	0.54715603	RAR-related orphan receptor B
SUMO1P2	0.550695996	SUMO1 pseudogene 2
CRISPLD1	0.551134139	cysteine-rich secretory protein LCCL domain containing 1
S100A8	0.552235066	S100 calcium binding protein A8
TIAM1	0.554871375	T-cell lymphoma invasion and metastasis 1
SEMA3A	0.555014597	sema domain. immunoglobulin domain (Ig). short basic domain. secreted. (semaphorin) 3A
FAM129A	0.5561127	family with sequence similarity 129. member A
MGC12488	0.560458045	hypothetical protein MGC12488
SCARNA2	0.561813657	small Cajal body-specific RNA 2
CLC	0.562508901	Charcot-Leyden crystal protein
ALDH8A1	0.562520076	aldehyde dehydrogenase 8 family. member A1
NAP1L3	0.565707212	nucleosome assembly protein 1-like 3
NUAK2	0.567163504	NUAK family. SNF1-like kinase. 2
CCL4	0.567194474	chemokine (C-C motif) ligand 4
KLF2	0.568758217	Kruppel-like factor 2 (lung)
LOC100132356	0.568983165	hypothetical protein LOC100132356
FAIM3	0.570810225	Fas apoptotic inhibitory molecule 3
HAL	0.574839511	histidine ammonia-lyase
ENSG00000167912	0.57627076	
C15orf48	0.576644252	chromosome 15 open reading frame 48
FERMT2	0.586605741	fermitin family homolog 2 (Drosophila)
ANKRD30A	0.589320865	ankyrin repeat domain 30A
PPAP2B	0.594125476	phosphatidic acid phosphatase type 2B
MME	0.596746789	membrane metallo-endopeptidase
RAB38	0.598234861	RAB38. member RAS oncogene family
GABRB2	0.60041093	gamma-aminobutyric acid (GABA) A receptor. beta 2

VLDLR	0.605785	very low density lipoprotein receptor
ADAM21	0.605895486	ADAM metallopeptidase domain 21 pseudogene; ADAM metallopeptidase domain 21
ERMN	0.606025685	ermin. ERM-like protein
ENSG00000223786	0.606903506	
GEM	0.607924079	GTP binding protein overexpressed in skeletal muscle
TWIST1	0.613244939	twist homolog 1 (Drosophila)
DDIT3	0.614233138	DNA-damage-inducible transcript 3
LOC729986	0.618846008	hypothetical LOC729986
CD38	0.62586996	CD38 molecule
PLEK	0.628462709	pleckstrin
GUSBP1	0.62943108	glucuronidase. beta-like 2; glucuronidase. beta pseudogene
C21orf125	0.638320326	chromosome 21 open reading frame 125
MGST2	0.639590485	microsomal glutathione S-transferase 2
PCK2	0.644298697	phosphoenolpyruvate carboxykinase 2 (mitochondrial)
PLK2	0.64514017	polo-like kinase 2 (Drosophila)
TANC1	0.645649475	tetratricopeptide repeat. ankyrin repeat and coiled-coil containing 1
IL21R	0.658206833	interleukin 21 receptor
NOG	0.660043415	noggin
HIST1H3D	0.665178541	histone cluster 1. H3j; histone cluster 1. H3i; histone cluster 1. H3h; histone cluster 1. H3g; histone cluster 1. H3f; histone cluster 1. H3e; histone cluster 1. H3d; histone cluster 1. H3c; histone cluster 1. H3b; histone cluster 1. H3a; histone cluster 1. H2ad; histone cluster 2. H3a; histone cluster 2. H3c; histone cluster 2. H3d
CLDN1	0.667063088	claudin 1
FAM65B	0.668817424	family with sequence similarity 65. member B
CBLN2	0.67315889	cerebellin 2 precursor
FBXO32	0.68205803	F-box protein 32
MYOC	0.688801612	myocilin. trabecular meshwork inducible glucocorticoid response
SHROOM2	0.689813378	shroom family member 2
CAV1	0.690101248	caveolin 1. caveolae protein. 22kDa
KRTAP19-1	0.693992762	keratin associated protein 19-1
ENSG00000244210	0.697124173	
ENSG00000235687	0.699490738	
FKBP9	0.699940938	FK506 binding protein 9. 63 kDa
LHX8	0.70022331	LIM homeobox 8
TGFBI	0.701863913	transforming growth factor. beta-induced. 68kDa
EREG	0.70818998	epiregulin
KIF21B	0.709221421	kinesin family member 21B
AIG1	0.709874418	androgen-induced 1

CTH	0.711247308	cystathionase (cystathionine gamma-lyase)
MACROD2	0.713681771	MACRO domain containing 2
PPARGC1A	0.713971247	peroxisome proliferator-activated receptor gamma. coactivator 1 alpha
TRIB2	0.714436438	tribbles homolog 2 (Drosophila)
MAPK10	0.717010683	mitogen-activated protein kinase 10
PSAT1	0.719906299	chromosome 8 open reading frame 62; phosphoserine aminotransferase 1
C3orf52	0.722400559	chromosome 3 open reading frame 52
FSCN1	0.725365379	fascin homolog 1. actin-bundling protein (Strongylocentrotus purpuratus)
GRIP1	0.72598199	glutamate receptor interacting protein 1
FBXL2	0.726932063	F-box and leucine-rich repeat protein 2
DDIT4	0.73416391	DNA-damage-inducible transcript 4
ENSG00000231249	0.735407802	
ASNS	0.747212667	asparagine synthetase
DFNA5	0.748296166	deafness. autosomal dominant 5
S1PR1	0.750137553	sphingosine-1-phosphate receptor 1
KBTBD11	0.770717081	kelch repeat and BTB (POZ) domain containing 11
CAPN8	0.790814075	calpain 8
LHX2	0.791145908	LIM homeobox 2
ACPP	0.792759432	acid phosphatase. prostate
CNTNAP4	0.797395726	contactin associated protein-like 4
ENSG00000230937	0.79822366	
CDH17	0.815188752	cadherin 17. LI cadherin (liver-intestine)
GNAI1	0.817856209	guanine nucleotide binding protein (G protein). alpha inhibiting activity polypeptide 1
LRIG3	0.818798792	leucine-rich repeats and immunoglobulin-like domains 3
MAP1B	0.822039211	microtubule-associated protein 1B
BAI3	0.825415132	brain-specific angiogenesis inhibitor 3
PALLD	0.836603086	palladin. cytoskeletal associated protein
RASSF6	0.845200654	Ras association (RalGDS/AF-6) domain family member 6
FAM19A2	0.847420836	family with sequence similarity 19 (chemokine (C-C motif)-like). member A2
HOOK1	0.850635162	hook homolog 1 (Drosophila)
PRKCH	0.854211766	protein kinase C. eta
SESN2	0.856096661	sestrin 2
ENSG00000228288	0.868932653	
BASP1	0.869066544	brain abundant. membrane attached signal protein 1
PERP	0.875863256	PERP. TP53 apoptosis effector
FAM49A	0.880247758	family with sequence similarity 49. member A
NXN	0.882793363	nucleoredoxin
LOC286184	0.901886951	hypothetical protein LOC286184
PHGDH	0.906027468	phosphoglycerate dehydrogenase

BLNK	0.907365311	B-cell linker
PLEKHG1	0.911066829	pleckstrin homology domain containing. family G (with RhoGef domain) member 1
LPCAT2	0.931688722	lysophosphatidylcholine acyltransferase 2
HMCN1	0.95045637	hemicentin 1
BNC2	0.95667367	basonuclin 2
CHAC1	0.960956993	ChaC. cation transport regulator homolog 1 (E. coli)
FEZ1	0.962157592	fasciculation and elongation protein zeta 1 (zygin I)
ASS1	0.988178025	argininosuccinate synthetase 1
GRIN2A	1.007845115	glutamate receptor. ionotropic. N-methyl D-aspartate 2A
CPE	1.047134955	carboxypeptidase E
EPS8	1.06442377	epidermal growth factor receptor pathway substrate 8
ASB17	1.064535486	ankyrin repeat and SOCS box-containing 17
BAMBI	1.070133438	hypothetical LOC729590; BMP and activin membrane-bound inhibitor homolog (Xenopus laevis)
TKTL1	1.082835023	transketolase-like 1
SPARC	1.089607154	secreted protein. acidic. cysteine-rich (osteonectin)
SGK1	1.172444767	serum/glucocorticoid regulated kinase 1
GJA1	1.197986819	gap junction protein. alpha 1. 43kDa
MGC24103	1.212745282	hypothetical MGC24103
PSD3	1.220752904	pleckstrin and Sec7 domain containing 3
SPINK2	1.254115179	serine peptidase inhibitor. Kazal type 2 (acrosin-trypsin inhibitor)
CLGN	1.36834692	calmegin
INHBE	1.504863162	inhibin. beta E

Table S5: Differentially expressed genes in the analysis of JJN3 anti-Gal-1 vs JJN3 scramble specific for normoxia. (Variation= ratio of the difference between the expression level of the two experiments on the mean value of the same two variables. The most significant differentially expressed transcripts have been selected as those exceeding the mean plus 3 standard deviation of all the ratio values.)

Gene.symbol	Variation	Gene name
ENSG00000237940	-0.742918596	
FBXW10	-0.731076108	F-box and WD repeat domain containing 10; similar to FBXW10 protein
ENSG00000240207	-0.724072714	
C3orf79	-0.678776406	hypothetical protein LOC152118
LOC100134937	-0.666634183	hypothetical LOC100134937
LOC284898	-0.639633783	hypothetical protein LOC284898
CDKN1C	-0.638870953	cyclin-dependent kinase inhibitor 1C (p57. Kip2)
LOC100127972	-0.619592303	hypothetical LOC100127972
NCRNA00182	-0.619232115	
ENSG00000240405	-0.602508922	
ENSG00000145965	-0.592024723	
ACRC	-0.589474207	acidic repeat containing
TMEM51	-0.575392698	transmembrane protein 51
CUX2	-0.563868641	cut-like homeobox 2
ENSG00000238217	-0.555715651	
ENSG00000222017	-0.553635776	
HIST1H2BC	-0.547363692	histone cluster 1. H2bi; histone cluster 1. H2bg; histone cluster 1. H2be; histone cluster 1. H2bf; histone cluster 1. H2bc
ENSG00000237512	-0.547052253	
GPR20	-0.544671111	G protein-coupled receptor 20
PCP4L1	-0.540770892	Purkinje cell protein 4 like 1
ENSG00000222044	-0.537298033	
APOBEC3A	-0.536634271	apolipoprotein B mRNA editing enzyme. catalytic polypeptide-like 3A
C1orf104	-0.530258026	chromosome 1 open reading frame 104
PTP4A3	-0.52885229	protein tyrosine phosphatase type IVA. member 3
LOC375295	-0.525181452	hypothetical protein LOC375295
ENSG00000223750	-0.525017154	
C1orf38	-0.518513274	chromosome 1 open reading frame 38
KRTAP9-2	-0.518079867	keratin associated protein 9-9; keratin associated protein 9-2
MAML2	-0.510626931	mastermind-like 2 (Drosophila)
LOC400965	-0.50696023	hypothetical LOC400965
ADAM19	-0.501676621	ADAM metallopeptidase domain 19 (meltrin beta)
ENSG00000237101	-0.487594433	
FLJ37786	-0.482272974	hypothetical LOC100133086; hypothetical LOC642691

RIN2	-0.479999321	Ras and Rab interactor 2
STEAP1	-0.475103542	six transmembrane epithelial antigen of the prostate 1
LOC144481	-0.47450745	hypothetical protein LOC144481
LOC285033	-0.469010875	hypothetical protein LOC285033
ENSG00000234264	-0.466840168	
ENSG00000228372	-0.465756469	
RAB39B	-0.465293153	RAB39B. member RAS oncogene family
OR2K2	-0.465054236	olfactory receptor. family 2. subfamily K. member 2
LOC100129845	-0.462329945	hypothetical LOC100129845
GABARAPL3	-0.461384738	GABA(A) receptors associated protein like 3 (pseudogene); GABA(A) receptor-associated protein like 1
SPIB	-0.457788016	Spi-B transcription factor (Spi-1/PU.1 related)
LOC285281	-0.452989668	hypothetical protein LOC285281
ORM1	-0.447307982	orosomucoid 1
IRF8	-0.445972726	interferon regulatory factor 8
POU3F4	-0.445338379	POU class 3 homeobox 4
OR1A1	-0.444838725	olfactory receptor. family 1. subfamily A. member 1
ENSG00000238184	-0.444243589	
RIC3	-0.443180725	resistance to inhibitors of cholinesterase 3 homolog (C. elegans)
MEFV	-0.437120833	Mediterranean fever
GPR160	-0.436597073	G protein-coupled receptor 160
SLIT1	-0.435783441	slit homolog 1 (Drosophila)
NRTN	-0.431173751	neurturin
LOC100132815	-0.430097696	hypothetical protein LOC100132815
PRKACG	-0.428205281	protein kinase. cAMP-dependent. catalytic. gamma
MEP1B	-0.427040264	meprin A. beta
SLC41A2	-0.425061039	solute carrier family 41. member 2
C5orf20	-0.42349135	TRAF-interacting protein with forkhead-associated domain. family member B; chromosome 5 open reading frame 20
ENSG00000234350	-0.420386309	
TIMD4	-0.420272208	T-cell immunoglobulin and mucin domain containing 4
DOC2B	-0.420023931	double C2-like domains. beta
MGC2889	-0.419750448	hypothetical protein MGC2889
C1orf192	-0.417702973	chromosome 1 open reading frame 192
ENSG00000232533	-0.416863725	
HS3ST5	-0.416635492	heparan sulfate (glucosamine) 3-O-sulfotransferase 5
LRRC55	-0.415811079	leucine rich repeat containing 55
ENSG00000236714	-0.413973681	
JAKMIP2	0.405058761	Janus kinase and microtubule interacting protein 2

IRS4	0.406333396	insulin receptor substrate 4
ENSG00000226363	0.409154289	
TSSK4	0.410245338	testis-specific serine kinase 4
ENSG00000234352	0.410343998	
NKX6-3	0.412314733	NK6 homeobox 3
TNFSF4	0.412792412	tumor necrosis factor (ligand) superfamily. member 4
ENSG00000227290	0.413248111	
ENC1	0.413615985	ectodermal-neural cortex (with BTB-like domain)
LOC285423	0.414614334	hypothetical LOC285423
ENSG00000203691	0.415418644	
PENK	0.416115361	proenkephalin
LOC285547	0.416429206	hypothetical protein LOC285547
SPINT2	0.41707633	serine peptidase inhibitor. Kunitz type. 2
HTR2C	0.418981126	5-hydroxytryptamine (serotonin) receptor 2C
ENSG00000224189	0.419448943	
LOC503519	0.420109684	hypothetical LOC503519
PON3	0.420205465	paraoxonase 3
IL29	0.422023578	interleukin 29 (interferon. lambda 1)
LOC653160	0.428251141	Hypothetical protein LOC653160
C6orf147	0.428604833	chromosome 6 open reading frame 147
ENSG00000230606	0.428816735	
ENSG00000232058	0.429132071	
LOC285000	0.429541559	hypothetical protein LOC285000
ANKRD22	0.429563463	ankyrin repeat domain 22
FOXB1	0.430413582	forkhead box B1
NPTXR	0.430470752	neuronal pentraxin receptor
TSPAN10	0.431432276	tetraspanin 10
ENSG00000227877	0.432988357	
KIF24	0.433898455	kinesin family member 24
CHRM5	0.434656416	cholinergic receptor. muscarinic 5
C21orf117	0.436652469	chromosome 21 open reading frame 117
LRP4	0.436982343	low density lipoprotein receptor-related protein 4
BASE	0.439507267	breast cancer and salivary gland expression gene
TRDV2	0.440900937	T cell receptor alpha constant; T cell receptor alpha locus; T cell receptor alpha variable 20; T cell receptor delta locus; T cell receptor delta variable 2
PLXDC2	0.443047662	plexin domain containing 2
ENSG00000232655	0.443822416	
OR51B5	0.444268553	olfactory receptor. family 51. subfamily B. member 5
ENSG00000206552	0.447753282	
LOC100170939	0.448229792	glucuronidase. beta pseudogene
ENSG00000233061	0.449863329	
LOC441086	0.452747573	hypothetical protein LOC441086
C20orf197	0.455369695	chromosome 20 open reading frame 197
MAP3K9	0.455801573	mitogen-activated protein kinase kinase kinase 9

ENSG00000236094	0.465187277	
C9orf66	0.467292618	chromosome 9 open reading frame 66
LOC727944	0.472325604	similar to hCG2042412
KDR	0.472763161	kinase insert domain receptor (a type III receptor tyrosine kinase)
GRIA4	0.482743507	glutamate receptor. ionotrophic. AMPA 4
ANXA13	0.483858162	annexin A13
LOC283270	0.490920034	hypothetical protein LOC283270
PCDHB4	0.495888919	protocadherin beta 4
IGSF5	0.498732806	immunoglobulin superfamily. member 5
ENSG00000224397	0.503965129	
ULBP2	0.509587279	UL16 binding protein 2
ENSG00000237807	0.509696432	
MUC8	0.516289563	mucin 8
GPR37	0.520039677	G protein-coupled receptor 37 (endothelin receptor type B-like)
ENSG00000226383	0.528011306	
C11orf84	0.536901261	chromosome 11 open reading frame 84
ENSG00000229051	0.540419522	
TSPY1	0.545501753	testis specific protein. Y-linked 3; testis specific protein. Y-linked 2; testis specific protein. Y-linked 1; testis specific protein. Y-linked pseudogene 7
ENSG00000229689	0.546299559	
LOC100128554	0.550344944	hypothetical protein LOC100128554
NPAS4	0.591502459	neuronal PAS domain protein 4
GSTA1	0.605678444	glutathione S-transferase alpha 1
ABCA12	0.609389114	ATP-binding cassette. sub-family A (ABC1). member 12
LOC283914	0.617863604	hypothetical protein LOC283914
LOC646241	0.621453798	hypothetical protein LOC646241
SLC22A24	0.650800121	solute carrier family 22. member 24
ENSG00000230627	0.708327529	

Table S6: Differentially expressed genes in the analysis of JJN3 anti-Gal-1 vs JJN3 scramble specific after hypoxic treatment. (Variation= ratio of the difference between the expression level of the two experiments on the mean value of the same two variables. The most significant differentially expressed transcripts have been selected as those exceeding the mean plus 3 standard deviation of all the ratio values.)

Gene.symbol	Variation	Gene name
LGALS1	-1.912404366	lectin. galactoside-binding. soluble. 1
TUBB2B	-0.87677153	tubulin. beta 2B
EML1	-0.821829014	echinoderm microtubule associated protein like 1
FSTL5	-0.790261763	follistatin-like 5
IRX4	-0.771851606	iroquois homeobox 4
NLRP7	-0.732498543	NLR family. pyrin domain containing 7
RAPGEF4	-0.681823695	Rap guanine nucleotide exchange factor (GEF) 4
CST7	-0.66960769	cystatin F (leukocystatin)
XK	-0.667585002	X-linked Kx blood group (McLeod syndrome)
PXDN	-0.667345519	peroxidasin homolog (Drosophila)
NOD2	-0.649656946	nucleotide-binding oligomerization domain containing 2
SCARNA17	-0.639625318	small Cajal body-specific RNA 17
ELOVL2	-0.637999672	elongation of very long chain fatty acids (FEN1/Elo2. SUR4/Elo3. yeast)-like 2
SLC46A3	-0.625672884	solute carrier family 46. member 3
ARRB1	-0.60381625	arrestin. beta 1
LOC286382	-0.584387082	hypothetical protein LOC286382
PPP1R9A	-0.58359001	protein phosphatase 1. regulatory (inhibitor) subunit 9A
CCL2	-0.581891364	chemokine (C-C motif) ligand 2
CCDC63	-0.57755151	coiled-coil domain containing 63
KCNT2	-0.565957269	potassium channel. subfamily T. member 2
GPX7	-0.557984837	glutathione peroxidase 7
CAT	-0.553904999	catalase
FRK	-0.548950532	fyn-related kinase
MEX3B	-0.5478356	mex-3 homolog B (C. elegans)
LOC200261	-0.545855119	hypothetical LOC200261
MGC15885	-0.545497679	hypothetical protein MGC15885
KCNK6	-0.539831643	potassium channel. subfamily K. member 6
TCL1A	-0.533568605	T-cell leukemia/lymphoma 1A
SMAD5OS	-0.530145999	SMAD family member 5 opposite strand
OMG	-0.525501635	oligodendrocyte myelin glycoprotein
SNORD116	-0.525074853	small nucleolar RNA. C/D box 116 cluster
KIAA0754	-0.513840407	hypothetical LOC643314
PSTPIP1	-0.512719697	proline-serine-threonine phosphatase interacting protein 1
ENSG00000234509	-0.50812017	

LRRC52	-0.504619525	leucine rich repeat containing 52
FOXS1	-0.503591405	forkhead box S1
ENSG00000220161	-0.501947898	
TTYH1	-0.499933602	tweety homolog 1 (Drosophila)
EFNA1	-0.498112579	ephrin-A1
ENSG00000233001	-0.496809344	
HHIPL1	-0.495270412	HHIP-like 1
LRP1B	-0.492399088	low density lipoprotein-related protein 1B (deleted in tumors)
IGDCC4	-0.490757291	immunoglobulin superfamily. DCC subclass. member 4
TSPAN2	-0.490446709	tetraspanin 2
NTAN1	-0.490245334	N-terminal asparagine amidase
HIST2H2BE	-0.485703757	histone cluster 2. H2be
HAPLN4	-0.485026309	hyaluronan and proteoglycan link protein 4
LOC150051	-0.479515385	hypothetical LOC150051
C14orf167	-0.475960853	chromosome 14 open reading frame 167
C5orf48	-0.475586708	chromosome 5 open reading frame 48
MCAM	-0.475391714	melanoma cell adhesion molecule
C15orf59	-0.473896474	chromosome 15 open reading frame 59
DRD4	-0.470656535	dopamine receptor D4
CPLX1	-0.470316859	complexin 1
ENSG00000236081	-0.46748272	
ENSG00000234283	-0.466461992	
UST	-0.466033695	uronyl-2-sulfotransferase
MMP9	-0.465310306	matrix metallopeptidase 9 (gelatinase B. 92kDa gelatinase. 92kDa type IV collagenase)
KAL1	-0.46482551	Kallmann syndrome 1 sequence
FLJ12120	-0.463710931	hypothetical LOC388439
CENPW	-0.461583163	
MGAM	-0.455800235	maltase-glucoamylase (alpha-glucosidase)
TDRD12	-0.455408318	tudor domain containing 12
C2orf58	-0.454264538	chromosome 2 open reading frame 58
ENSG00000234435	-0.452310792	
KCNJ11	-0.450861922	potassium inwardly-rectifying channel. subfamily J. member 11
LOC441268	-0.44774419	hypothetical LOC441268
MYO5C	-0.445032565	myosin VC
LOC145474	-0.441617631	hypothetical protein LOC145474
NLRP10	-0.44028069	NLR family. pyrin domain containing 10
ANG	-0.439161213	angiogenin. ribonuclease. RNase A family. 5
ZNF423	-0.438814164	zinc finger protein 423
LOC642776	-0.436570667	hypothetical protein LOC642776
HOXD8	-0.43475437	homeobox D8
TNIP3	-0.429892372	TNFAIP3 interacting protein 3
COMP	-0.429069706	cartilage oligomeric matrix protein
SPIC	-0.428238498	Spi-C transcription factor (Spi-1/PU.1 related)
IFNA2	-0.427458187	interferon. alpha 2

FAM55D	-0.427231181	family with sequence similarity 55. member D
OSCP1	-0.426119108	chromosome 1 open reading frame 102
KLF1	-0.424329795	Kruppel-like factor 1 (erythroid)
PRKAG3	-0.418852378	protein kinase. AMP-activated. gamma 3 non-catalytic subunit
LOC729635	-0.417710975	similar to high mobility group box 3
H2AFJ	-0.417223045	H2A histone family. member J
INSM1	-0.416929097	insulinoma-associated 1
ASB17	-0.416331596	ankyrin repeat and SOCS box-containing 17
ENSG00000224137	-0.415738071	
C6orf208	-0.415689566	chromosome 6 open reading frame 208
LOC285692	-0.413732921	hypothetical LOC285692
GPR18	-0.413055684	G protein-coupled receptor 18
MYEF2	-0.412975117	myelin expression factor 2
LOC441208	-0.412570599	zinc and ring finger 2 pseudogene
SASH3	-0.411003969	SAM and SH3 domain containing 3
NME7	-0.410169407	non-metastatic cells 7. protein expressed in (nucleoside-diphosphate kinase)
C6orf114	0.418113865	chromosome 6 open reading frame 114
FAM169A	0.418124011	family with sequence similarity 169. member A
GDAP1	0.419150139	ganglioside-induced differentiation-associated protein 1
CHMP4C	0.419207545	chromatin modifying protein 4C
ENSG00000232103	0.419341619	
HMCN1	0.42008718	hemicentin 1
CELA2A	0.420241394	chymotrypsin-like elastase family. member 2A
ELOVL7	0.420948069	ELOVL family member 7. elongation of long chain fatty acids (yeast)
PNPO	0.421000141	pyridoxamine 5'-phosphate oxidase
GABRB2	0.421142105	gamma-aminobutyric acid (GABA) A receptor. beta 2
LASS1	0.422191692	growth differentiation factor 1; LAG1 homolog. ceramide synthase 1
OR1C1	0.42293301	olfactory receptor. family 1. subfamily C. member 1
ASS1	0.423640039	argininosuccinate synthetase 1
PFN2	0.425410608	profilin 2
PPARGC1A	0.425681611	peroxisome proliferator-activated receptor gamma. coactivator 1 alpha
DHRS3	0.426089138	dehydrogenase/reductase (SDR family) member 3
DTX3L	0.427469717	deltex 3-like (Drosophila)
DNAJC5B	0.428350523	DnaJ (Hsp40) homolog. subfamily C. member 5 beta
MEIS3P1	0.428367568	Meis homeobox 3 pseudogene 1
TBX15	0.428545576	T-box 15
AIM2	0.429388314	absent in melanoma 2
ZSCAN1	0.431598694	zinc finger and SCAN domain containing 1
LOC284513	0.43242285	hypothetical protein LOC284513

LOC283682	0.432943943	hypothetical protein LOC283682
BEX5	0.433567473	brain expressed. X-linked 5
ENSG00000229522	0.433822206	
DDR1	0.434760069	discoidin domain receptor tyrosine kinase 1
ZSCAN5A	0.434805986	zinc finger and SCAN domain containing 5A
PKHD1L1	0.435350527	polycystic kidney and hepatic disease 1 (autosomal recessive)-like 1
GCNT2	0.436275527	glucosaminyl (N-acetyl) transferase 2. I-branching enzyme (I blood group)
ENSG00000230002	0.436468556	
MT2A	0.437149717	metallothionein 2A
VASH2	0.438084802	vasohibin 2
EFNA5	0.438807335	ephrin-A5
OR1F1	0.438911662	olfactory receptor. family 1. subfamily F. member 1
ENSG00000145063	0.438913597	
EPSTI1	0.4397357	epithelial stromal interaction 1 (breast)
CHST6	0.440603682	carbohydrate (N-acetylglucosamine 6-O) sulfotransferase 6
CCDC86	0.442743596	coiled-coil domain containing 86
DNAJB7	0.445293631	DnaJ (Hsp40) homolog. subfamily B. member 7
EOMES	0.446485498	eomesodermin homolog (Xenopus laevis)
S1PR1	0.446536198	sphingosine-1-phosphate receptor 1
PLAC8	0.447854901	placenta-specific 8
EGR1	0.448149133	early growth response 1
TGFBI	0.449482389	transforming growth factor. beta-induced. 68kDa
ENSG00000234859	0.450143252	
ENSG00000242615	0.45017703	
ABHD1	0.453970341	abhydrolase domain containing 1
SLC6A8	0.454149718	solute carrier family 6 (neurotransmitter transporter. creatine). member 8
SUSD5	0.456372223	sushi domain containing 5
HES1	0.458059914	hairy and enhancer of split 1. (Drosophila)
TIAM1	0.458686149	T-cell lymphoma invasion and metastasis 1
CST1	0.459935265	cystatin SN
IFNG	0.460599067	interferon. gamma
LAMP3	0.464968406	lysosomal-associated membrane protein 3
MIR17HG	0.466569534	microRNA host gene 1 (non-protein coding)
CXCL10	0.467996197	chemokine (C-X-C motif) ligand 10
SAMD12	0.468609131	sterile alpha motif domain containing 12
ATL1	0.469467443	atlastin GTPase 1
ENPP4	0.469574835	ectonucleotide pyrophosphatase/phosphodiesterase 4 (putative function)
LRRN1	0.469917909	leucine rich repeat neuronal 1
MACROD2	0.471040388	MACRO domain containing 2
TP73	0.473760901	tumor protein p73

TEC	0.476446532	tec protein tyrosine kinase
KIF12	0.478163361	kinesin family member 12
STRADB	0.478201346	STE20-related kinase adaptor beta
OR2M4	0.478405075	olfactory receptor. family 2. subfamily M. member 4
C3orf33	0.482407891	chromosome 3 open reading frame 33
IL8	0.482550272	interleukin 8
RGS13	0.484220997	regulator of G-protein signaling 13
GRIP1	0.486306789	glutamate receptor interacting protein 1
DPYSL3	0.488434482	dihydropyrimidinase-like 3
ABLIM1	0.488519669	actin binding LIM protein 1
WFDC5	0.48856119	WAP four-disulfide core domain 5
TMEM200A	0.489778899	transmembrane protein 200A
SLC25A18	0.489947303	solute carrier family 25 (mitochondrial carrier). member 18
WDFY3	0.492404935	WD repeat and FYVE domain containing 3
CAPN8	0.493990808	calpain 8
ACVR1C	0.494125712	activin A receptor. type IC
BLNK	0.49512922	B-cell linker
LOC642345	0.495761429	hCG1818123
PRKCH	0.496421408	protein kinase C. eta
ITK	0.497426931	IL2-inducible T-cell kinase
RGS16	0.49757565	regulator of G-protein signaling 16
VEGFC	0.499871042	vascular endothelial growth factor C
MAPK10	0.500755586	mitogen-activated protein kinase 10
CSTA	0.502000675	cystatin A (stefin A)
TMEM151A	0.505476915	transmembrane protein 151A
REEP3	0.506897542	receptor accessory protein 3
ENSG00000225794	0.50802657	
BTBD19	0.50868325	hypothetical protein LOC149478
EGR2	0.510405126	early growth response 2
DUSP6	0.514381863	dual specificity phosphatase 6
CCR7	0.515069909	chemokine (C-C motif) receptor 7
LRIG3	0.51539564	leucine-rich repeats and immunoglobulin-like domains 3
FKBP9	0.522243194	FK506 binding protein 9. 63 kDa
FAM129A	0.523836098	family with sequence similarity 129. member A
PTPLA	0.525247529	protein tyrosine phosphatase-like (proline instead of catalytic arginine). member A
SORL1	0.525352439	sortilin-related receptor. L(DLR class) A repeats-containing
CDHR1	0.525557064	protocadherin 21
SH3BGRL2	0.528145326	SH3 domain binding glutamic acid-rich protein like 2
C12orf54	0.534358536	chromosome 12 open reading frame 54
SGK1	0.537786808	serum/glucocorticoid regulated kinase 1
S100A8	0.539768948	S100 calcium binding protein A8
CD38	0.539941619	CD38 molecule

C3orf52	0.543298089	chromosome 3 open reading frame 52
NOG	0.545945957	noggin
GNAI1	0.552633947	guanine nucleotide binding protein (G protein). alpha inhibiting activity polypeptide 1
LOC348751	0.555475508	hypothetical protein LOC348751
PGF	0.560161331	placental growth factor
ENSG00000226966	0.563183249	
FAM95B1	0.569014315	family with sequence similarity 95. member B1
WARS	0.56944527	tryptophanyl-tRNA synthetase
PALLD	0.578059624	palladin. cytoskeletal associated protein
MGC14436	0.581679208	hypothetical LOC84983
GPR180	0.586132022	G protein-coupled receptor 180
CA2	0.591226437	carbonic anhydrase II
PARP9	0.594587909	poly (ADP-ribose) polymerase family. member 9
SEMA3A	0.598241322	sema domain. immunoglobulin domain (Ig). short basic domain. secreted. (semaphorin) 3A
PERP	0.599333404	PERP. TP53 apoptosis effector
AK7	0.600677765	adenylate kinase 7
TANC1	0.601570141	tetratricopeptide repeat. ankyrin repeat and coiled-coil containing 1
EGLN3	0.604322384	egl nine homolog 3 (C. elegans)
SI	0.604614101	sucrase-isomaltase (alpha-glucosidase)
CD109	0.605201353	CD109 molecule
LPAR1	0.608532813	lysophosphatidic acid receptor 1
IRF1	0.612573878	interferon regulatory factor 1
UCHL3	0.616135358	ubiquitin carboxyl-terminal esterase L3 (ubiquitin thiolesterase)
ENSG00000167912	0.619449597	
GBP2	0.620246122	guanylate binding protein 2. interferon-inducible
FSCN1	0.624029169	fascin homolog 1. actin-bundling protein (Strongylocentrotus purpuratus)
CLDN1	0.624709508	claudin 1
EDNRB	0.637959988	endothelin receptor type B
KBTBD11	0.643125252	kelch repeat and BTB (POZ) domain containing 11
PLK2	0.643191284	polo-like kinase 2 (Drosophila)
ENSG00000236239	0.656278014	
CCL5	0.660430338	chemokine (C-C motif) ligand 5
ZNF521	0.66544088	zinc finger protein 521
FAIM3	0.666242939	Fas apoptotic inhibitory molecule 3
UGT2B17	0.669317591	UDP glucuronosyltransferase 2 family. polypeptide B17
TWIST1	0.670321906	twist homolog 1 (Drosophila)
GBP5	0.672256111	guanylate binding protein 5
TUBB4Q	0.67316181	tubulin. beta polypeptide 4. member Q
BASP1	0.683274288	brain abundant. membrane attached signal protein 1
CTGF	0.685244833	connective tissue growth factor

CD6	0.686313544	CD6 molecule
SGK3	0.687437439	serum/glucocorticoid regulated kinase family. member 3
FAM19A2	0.690168539	family with sequence similarity 19 (chemokine (C-C motif)-like). member A2
CNTNAP4	0.710078993	contactin associated protein-like 4
AIG1	0.711260317	androgen-induced 1
CAV1	0.716144485	caveolin 1. caveolae protein. 22kDa
CBLN2	0.738610684	cerebellin 2 precursor
NAP1L3	0.747945449	nucleosome assembly protein 1-like 3
MGST2	0.753603368	microsomal glutathione S-transferase 2
IL21R	0.762459859	interleukin 21 receptor
LPCAT2	0.777843353	lysophosphatidylcholine acyltransferase 2
LHX2	0.780794233	LIM homeobox 2
GBP1	0.783027878	guanylate binding protein 1. interferon-inducible. 67kDa
LOC100289230	0.827185422	hypothetical protein LOC100289230
ENSG00000223786	0.828588963	
IGFBP2	0.846799255	insulin-like growth factor binding protein 2. 36kDa
ENSG00000230937	0.851177919	
HOOK1	0.859805198	hook homolog 1 (Drosophila)
MYOC	0.909513716	myocilin. trabecular meshwork inducible glucocorticoid response
BNC2	0.91007589	basonuclin 2
PPAP2B	0.919007258	phosphatidic acid phosphatase type 2B
SEPP1	0.934838696	selenoprotein P. plasma. 1
TKTL1	0.950430704	transketolase-like 1
C10orf99	0.976162881	chromosome 10 open reading frame 99
CLGN	0.990950923	calmegin
CA9	1.004654611	carbonic anhydrase IX
RASSF6	1.013904076	Ras association (RalGDS/AF-6) domain family member 6
GRIN2A	1.112688353	glutamate receptor. ionotropic. N-methyl D-aspartate 2A
DFNA5	1.123104329	deafness. autosomal dominant 5
PLEKHG1	1.148393582	pleckstrin homology domain containing. family G (with RhoGef domain) member 1
CPE	1.154893149	carboxypeptidase E
IL33	1.165487489	interleukin 33
SPARC	1.171835256	secreted protein. acidic. cysteine-rich (osteonectin)
BAMBI	1.173606617	hypothetical LOC729590; BMP and activin membrane-bound inhibitor homolog (Xenopus laevis)
PSD3	1.177791581	pleckstrin and Sec7 domain containing 3
MGC24103	1.186536696	hypothetical MGC24103
SPINK2	1.259934215	serine peptidase inhibitor. Kazal type 2 (acrosin-trypsin inhibitor)

CCL26	1.264326535	chemokine (C-C motif) ligand 26
GJA1	1.282997798	gap junction protein. alpha 1. 43kDa
EPS8	1.378865194	epidermal growth factor receptor pathway substrate 8

Table S7: Differentially expressed genes in the analysis of JJN3 anti-Gal-1 vs JJN3 scramble specific after re-oxygenation process. (Variation= ratio of the difference between the expression level of the two experiments on the mean value of the same two variables. The most significant differentially expressed transcripts have been selected as those exceeding the mean plus 3 standard deviation of all the ratio values.)

Gene.symbol	Variation	Gene Name
FOS	-1.049641012	v-fos FBJ murine osteosarcoma viral oncogene homolog
HEPACAM2	-0.798934128	HEPACAM family member 2
PIRT	-0.729355752	phosphoinositide-interacting regulator of transient receptor potential channels
ANKLE1	-0.726714079	ankyrin repeat and LEM domain containing 1
PKIG	-0.65571674	protein kinase (cAMP-dependent. catalytic) inhibitor gamma
HMOX1	-0.636944948	heme oxygenase (decycling) 1
CNN3	-0.632122944	calponin 3. acidic
CXCL14	-0.627681388	chemokine (C-X-C motif) ligand 14
FOSB	-0.608095365	FBJ murine osteosarcoma viral oncogene homolog B
VCX2	-0.606394556	variable charge. X-linked 2
CYP2A13	-0.602443916	cytochrome P450. family 2. subfamily A. polypeptide 13
PLA1A	-0.594907856	phospholipase A1 member A
CRYBA2	-0.593827176	crystallin. beta A2
FOXC2	-0.591880106	forkhead box C2 (MFH-1. mesenchyme forkhead 1)
FCRLB	-0.584625849	Fc receptor-like B
FLJ42418	-0.559040085	FLJ42418 protein
TTTY14	-0.554230751	testis-specific transcript. Y-linked 14
ITGA8	-0.55176749	integrin. alpha 8
CD300C	-0.548097991	CD300c molecule
DUSP1	-0.545196953	dual specificity phosphatase 1
NPDC1	-0.542844191	neural proliferation. differentiation and control. 1
PANK1	-0.541629673	pantothenate kinase 1
HDGFRP3	-0.541494938	hepatoma-derived growth factor. related protein 3
FAM92A1	-0.533808779	family with sequence similarity 92. member A2; family with sequence similarity 92. member A1
CRISP3	-0.533696292	cysteine-rich secretory protein 3
GPM6B	-0.532187198	glycoprotein M6B
FAM24A	-0.531078138	family with sequence similarity 24. member A
C5orf49	-0.530465613	chromosome 5 open reading frame 49
COTL1	-0.529112727	coactosin-like 1 (Dictyostelium)

NQO1	-0.527404237	NAD(P)H dehydrogenase. quinone 1
NPB	-0.52581857	neuropeptide B
PHLDA2	-0.515193931	pleckstrin homology-like domain. family A. member 2
TEX15	-0.510712648	testis expressed 15
ZNF43	-0.506777556	zinc finger protein 43
ENSG00000229048	-0.506138607	
SCCPDH	-0.497651415	saccharopine dehydrogenase (putative)
LOC729164	-0.49362486	hCG1732469
HEATR4	-0.491120826	HEAT repeat containing 4
ENSG00000242687	-0.490357539	
SLC25A43	-0.489078329	solute carrier family 25. member 43
CREB5	-0.485991298	cAMP responsive element binding protein 5
RERG	-0.485518836	RAS-like. estrogen-regulated. growth inhibitor
ANKRD30B	-0.484690711	ankyrin repeat domain 30B
PRSS35	-0.48280857	protease. serine. 35
PEG10	-0.481767687	paternally expressed 10
GBX2	-0.480278852	gastrulation brain homeobox 2
MEST	-0.478663869	mesoderm specific transcript homolog (mouse)
ZMYND15	-0.478338418	zinc finger. MYND-type containing 15
LOC146795	-0.477885877	hypothetical protein LOC146795
CD69	-0.475900567	CD69 molecule
CXCL13	-0.475497641	chemokine (C-X-C motif) ligand 13
PCOLCE2	-0.47526232	procollagen C-endopeptidase enhancer 2
LAIR2	-0.467812508	leukocyte-associated immunoglobulin-like receptor 2
C21orf37	-0.464778482	immunoglobulin heavy variable (II)-20-1 pseudogene; chromosome 21 open reading frame 37
POU2F3	-0.464183243	POU class 2 homeobox 3
B3GALNT1	-0.463429116	beta-1.3-N-acetylgalactosaminyltransferase 1 (globoside blood group)
ENSG00000228735	-0.460573837	
CYBRD1	-0.458451857	cytochrome b reductase 1
MLLT10L	-0.45823587	myeloid/lymphoid or mixed-lineage leukemia (trithorax homolog. Drosophila); translocated to. 10-like
ENSG00000224405	-0.457229621	
ZNF69	0.456414676	zinc finger protein 69
RASGRP1	0.456617095	RAS guanyl releasing protein 1 (calcium and DAG-regulated)
G0S2	0.45852332	G0/G1switch 2
DEFB4A	0.45867707	defensin. beta 4
CARS	0.461026219	cysteinyl-tRNA synthetase
TMTC1	0.461150787	transmembrane and tetratricopeptide repeat containing 1
ETV1	0.461893165	ets variant 1

MRPS11P1	0.462547263	mitochondrial ribosomal protein S11 pseudogene 1
LTF	0.463155175	lactotransferrin
NEAT1	0.464478153	non-protein coding RNA 84
PSG6	0.464835034	pregnancy specific beta-1-glycoprotein 6
ENSG00000224798	0.466859815	
ISL2	0.467380719	ISL LIM homeobox 2
C6	0.469240728	complement component 6
KIAA0485	0.470203991	hypothetical LOC57235
SLC7A5	0.470962462	solute carrier family 7 (cationic amino acid transporter. y+ system). member 5
MAFF	0.472863613	v-maf musculoaponeurotic fibrosarcoma oncogene homolog F (avian)
SMAD7	0.473392335	SMAD family member 7
TEX14	0.474796765	testis expressed 14
PMAIP1	0.47873083	phorbol-12-myristate-13-acetate-induced protein 1
TUBE1	0.478892939	tubulin. epsilon 1
C16orf74	0.480606953	chromosome 16 open reading frame 74
LOC728543	0.482442075	hypothetical protein LOC728543
SPRY2	0.491484263	sprouty homolog 2 (Drosophila)
ALDH1L2	0.492863424	aldehyde dehydrogenase 1 family. member L2
ANK2	0.499654336	ankyrin 2. neuronal
FLJ40330	0.50003938	hypothetical LOC645784
ENSG00000239791	0.500338267	
APOLD1	0.502626936	apolipoprotein L domain containing 1
LCE1B	0.50512887	late cornified envelope 1B
SLC7A11	0.50849037	solute carrier family 7. (cationic amino acid transporter. y+ system) member 11
OTUD1	0.50897749	OTU domain containing 1
KIAA0355	0.509261225	KIAA0355
LOC643072	0.515426016	hypothetical LOC643072
PRICKLE2	0.518524846	prickle homolog 2 (Drosophila)
APOL6	0.519473004	apolipoprotein L. 6
FAM107B	0.529380325	family with sequence similarity 107. member B
GPT2	0.529948545	glutamic pyruvate transaminase (alanine aminotransferase) 2
FRMD6	0.531345742	FERM domain containing 6
ZNF695	0.531744194	zinc finger protein 695
LOC151438	0.534135594	hypothetical protein LOC151438
LOC400684	0.535651784	hypothetical gene supported by BC000922
GAB2	0.536837211	GRB2-associated binding protein 2
LOC339505	0.539011905	hypothetical protein LOC339505
KREMEN1	0.541405167	kringle containing transmembrane protein 1
C5orf41	0.543102385	chromosome 5 open reading frame 41
ZBTB20	0.54580297	zinc finger and BTB domain containing 20

BTBD3	0.546357546	BTB (POZ) domain containing 3
SUMO1P2	0.550695996	SUMO1 pseudogene 2
CRISPLD1	0.551134139	cysteine-rich secretory protein LCCL domain containing 1
MGC12488	0.560458045	hypothetical protein MGC12488
SCARNA2	0.561813657	small Cajal body-specific RNA 2
CLC	0.562508901	Charcot-Leyden crystal protein
ALDH8A1	0.562520076	aldehyde dehydrogenase 8 family. member A1
NUAK2	0.567163504	NUAK family. SNF1-like kinase. 2
KLF2	0.568758217	Kruppel-like factor 2 (lung)
LOC100132356	0.568983165	hypothetical protein LOC100132356
HAL	0.574839511	histidine ammonia-lyase
FERMT2	0.586605741	fermitin family homolog 2 (Drosophila)
ANKRD30A	0.589320865	ankyrin repeat domain 30A
RAB38	0.598234861	RAB38. member RAS oncogene family
VLDLR	0.605785	very low density lipoprotein receptor
ADAM21	0.605895486	ADAM metallopeptidase domain 21 pseudogene; ADAM metallopeptidase domain 21
ERMN	0.606025685	ermin. ERM-like protein
GEM	0.607924079	GTP binding protein overexpressed in skeletal muscle
LOC729986	0.618846008	hypothetical LOC729986
PLEK	0.628462709	pleckstrin
GUSBP1	0.62943108	glucuronidase. beta-like 2; glucuronidase. beta pseudogene
C21orf125	0.638320326	chromosome 21 open reading frame 125
PCK2	0.644298697	phosphoenolpyruvate carboxykinase 2 (mitochondrial)
HIST1H3D	0.665178541	histone cluster 1. H3j; histone cluster 1. H3i; histone cluster 1. H3h; histone cluster 1. H3g; histone cluster 1. H3f; histone cluster 1. H3e; histone cluster 1. H3d; histone cluster 1. H3c; histone cluster 1. H3b; histone cluster 1. H3a; histone cluster 1. H2ad; histone cluster 2. H3a; histone cluster 2. H3c; histone cluster 2. H3d
FAM65B	0.668817424	family with sequence similarity 65. member B
FBXO32	0.68205803	F-box protein 32
SHROOM2	0.689813378	shroom family member 2
KRTAP19-1	0.693992762	keratin associated protein 19-1
ENSG00000235687	0.699490738	
LHX8	0.70022331	LIM homeobox 8
EREG	0.70818998	epiregulin
KIF21B	0.709221421	kinesin family member 21B
CTH	0.711247308	cystathionase (cystathionine gamma-lyase)
PSAT1	0.719906299	chromosome 8 open reading frame 62; phosphoserine aminotransferase 1
DDIT4	0.73416391	DNA-damage-inducible transcript 4

ENSG00000231249	0.735407802	
ASNS	0.747212667	asparagine synthetase
ACPP	0.792759432	acid phosphatase. prostate
CDH17	0.815188752	cadherin 17. LI cadherin (liver-intestine)
MAP1B	0.822039211	microtubule-associated protein 1B
SESN2	0.856096661	sestrin 2
ENSG00000228288	0.868932653	
PHGDH	0.906027468	phosphoglycerate dehydrogenase
CHAC1	0.960956993	ChaC. cation transport regulator homolog 1 (E. coli)
INHBE	1.504863162	inhibin. beta E

Table S8: Common differentially expressed genes in the analysis of JJN3 anti-Gal-1 vs JJN3 scramble in all the three conditions (normoxia. hypoxia and re-oxygenation). (Variation= ratio of the difference between the expression level of the two experiments on the mean value of the same two variables. The most significant differentially expressed transcripts have been selected as those exceeding the mean plus 3 standard deviation of all the ratio values.)

Gene Symbol	Variation Normoxia	Variation Hypoxia	Variation Re-oxygenation	Gene Name
LGALS1	-1.857917838	-1.9124	-1.92957	lectin. galactoside-binding. soluble. 1
FSTL5	-0.96383885	-0.79026	-0.9002	follistatin-like 5
PXDN	-0.766106873	-0.66735	-0.64048	peroxidasin homolog (Drosophila)
TUBB2B	-0.757299963	-0.87677	-0.58641	tubulin. beta 2B
XK	-0.701087712	-0.66759	-0.88838	X-linked Kx blood group (McLeod syndrome)
EML1	-0.667884045	-0.82183	-0.81352	echinoderm microtubule associated protein like 1
ARRB1	-0.599410162	-0.60382	-0.51638	arrestin. beta 1
MCAM	-0.585821502	-0.47539	-0.61439	melanoma cell adhesion molecule
RAPGEF4	-0.566548071	-0.68182	-0.87199	Rap guanine nucleotide exchange factor (GEF) 4
CCL2	-0.5144572	-0.58189	-0.82918	chemokine (C-C motif) ligand 2
GPX7	-0.467049667	-0.55798	-0.55825	glutathione peroxidase 7
IRX4	-0.459209872	-0.77185	-0.70618	iroquois homeobox 4
CENPW	-0.454033514	-0.46158	-0.57714	
CBLN2	0.405043279	0.738611	0.673159	cerebellin 2 precursor
ENPP4	0.41702068	0.469575	0.484266	ectonucleotide pyrophosphatase/phosphodiesterase 4 (putative function)
MAPK10	0.417145335	0.500756	0.717011	mitogen-activated protein kinase 10
CNTNAP4	0.445283251	0.710079	0.797396	contactin associated protein-like 4
TANC1	0.446364717	0.60157	0.645649	tetratricopeptide repeat. ankyrin repeat and coiled-coil containing 1
LPAR1	0.449695167	0.608533	0.502436	lysophosphatidic acid receptor 1
TP73	0.449942688	0.473761	0.513315	tumor protein p73
ABLIM1	0.46386719	0.48852	0.474582	actin binding LIM protein 1
TWIST1	0.483635886	0.670322	0.613245	twist homolog 1 (Drosophila)
FSCN1	0.49065447	0.624029	0.725365	fascin homolog 1. actin-bundling protein (Strongylocentrotus purpuratus)
PPARGC1A	0.499260711	0.425682	0.713971	peroxisome proliferator-activated receptor gamma. coactivator 1 alpha
IL21R	0.509949353	0.76246	0.658207	interleukin 21 receptor
C3orf52	0.513539094	0.543298	0.722401	chromosome 3 open reading frame 52
MGST2	0.519106699	0.753603	0.63959	microsomal glutathione S-transferase 2
CD109	0.523125273	0.605201	0.481876	CD109 molecule
ASB17	0.549903955	-0.41633	1.064535	ankyrin repeat and SOCS box-containing 17
LHX2	0.549938269	0.780794	0.791146	LIM homeobox 2
CAV1	0.555900419	0.716144	0.690101	caveolin 1. caveolae protein. 22kDa
ENSG00000223786	0.56593985	0.828589	0.606904	
GABRB2	0.567217633	0.421142	0.600411	gamma-aminobutyric acid (GABA) A receptor. beta 2

LRIG3	0.571966241	0.515396	0.818799	leucine-rich repeats and immunoglobulin-like domains 3
GRIP1	0.576616191	0.486307	0.725982	glutamate receptor interacting protein 1
BLNK	0.577390378	0.495129	0.907365	B-cell linker
ENSG00000230937	0.59046546	0.851178	0.798224	
GCNT2	0.602899875	0.436276	0.505848	glucosaminyl (N-acetyl) transferase 2. I-branching enzyme (I blood group)
PALLD	0.603643178	0.57806	0.836603	palladin. cytoskeletal associated protein
NAP1L3	0.613187619	0.747945	0.565707	nucleosome assembly protein 1-like 3
FKBP9	0.645384479	0.522243	0.699941	FK506 binding protein 9. 63 kDa
KBTBD11	0.660976204	0.643125	0.770717	kelch repeat and BTB (POZ) domain containing 11
FAM19A2	0.667001837	0.690169	0.847421	family with sequence similarity 19 (chemokine (C-C motif)-like). member A2
PRKCH	0.677402674	0.496421	0.854212	protein kinase C. eta
CCL26	0.683414497	1.264327	0.468743	chemokine (C-C motif) ligand 26
DFNA5	0.684272939	1.123104	0.748296	deafness. autosomal dominant 5
MACROD2	0.704190389	0.47104	0.713682	MACRO domain containing 2
BNC2	0.71678925	0.910076	0.956674	basonuclin 2
PPAP2B	0.727105134	0.919007	0.594125	phosphatidic acid phosphatase type 2B
PLK2	0.736693116	0.643191	0.64514	polo-like kinase 2 (Drosophila)
BASP1	0.750217513	0.683274	0.869067	brain abundant. membrane attached signal protein 1
MYOC	0.756187636	0.909514	0.688802	myocilin. trabecular meshwork inducible glucocorticoid response
PERP	0.763144003	0.599333	0.875863	PERP. TP53 apoptosis effector
RASSF6	0.815902846	1.013904	0.845201	Ras association (RalGDS/AF-6) domain family member 6
CTGF	0.819730653	0.685245	0.542816	connective tissue growth factor
PSD3	0.831606933	1.177792	1.220753	pleckstrin and Sec7 domain containing 3
BAMBI	0.842391188	1.173607	1.070133	hypothetical LOC729590; BMP and activin membrane-bound inhibitor homolog (Xenopus laevis)
AIG1	0.850346377	0.71126	0.709874	androgen-induced 1
ZNF521	0.862741547	0.665441	0.542713	zinc finger protein 521
HOOK1	0.895694667	0.859805	0.850635	hook homolog 1 (Drosophila)
GRIN2A	0.956550634	1.112688	1.007845	glutamate receptor. ionotropic. N-methyl D-aspartate 2A
CLDN1	0.979162003	0.62471	0.667063	claudin 1
PLEKHG1	1.006657943	1.148394	0.911067	pleckstrin homology domain containing. family G (with RhoGef domain) member 1
SPINK2	1.01501814	1.259934	1.254115	serine peptidase inhibitor. Kazal type 2 (acrosin-trypsin inhibitor)
CLGN	1.055267822	0.990951	1.368347	calmegin
SPARC	1.056359881	1.171835	1.089607	secreted protein. acidic. cysteine-rich (osteonectin)
CPE	1.06313884	1.154893	1.047135	carboxypeptidase E
TKTL1	1.085322825	0.950431	1.082835	transketolase-like 1
GJA1	1.114799484	1.282998	1.197987	gap junction protein. alpha 1. 43kDa
LPCAT2	1.155849895	0.777843	0.931689	lysophosphatidylcholine acyltransferase 2
EPS8	1.344465043	1.378865	1.064424	epidermal growth factor receptor pathway substrate 8

RINGRAZIAMENTI

Ringrazio la Professoressa Magda de Eguileor, il Professor Douglas Noonan, la Dottoressa Adriana Albini, il Professor Nicola Giuliani e il suo gruppo di ricerca per aver contribuito, durante questo corso di dottorato, ad accrescere le mie competenze teoriche e pratiche.